Electronic Supplementary Material (ESI) for RSC Advances.

Molecular design and synthesis of new dithiocarbazate complexes; crystal structure, bioactivities and nano studies

Zahra Yekke-ghasemi,[a] Reza Takjoo,*[a] Mohamad Ramezani,[b] and Joel T. Mague[c]

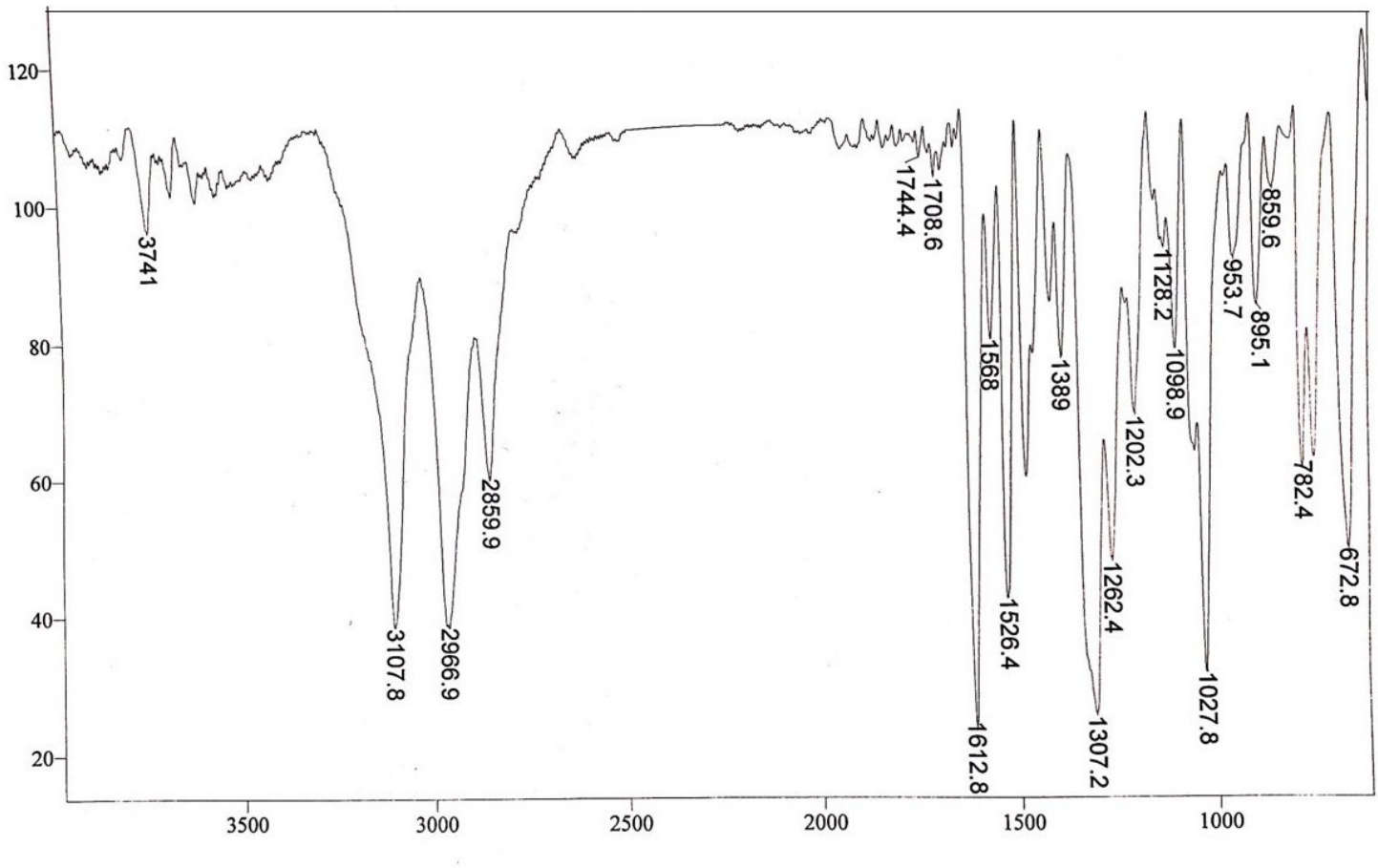

SI 1 a. IR spectrum of L.

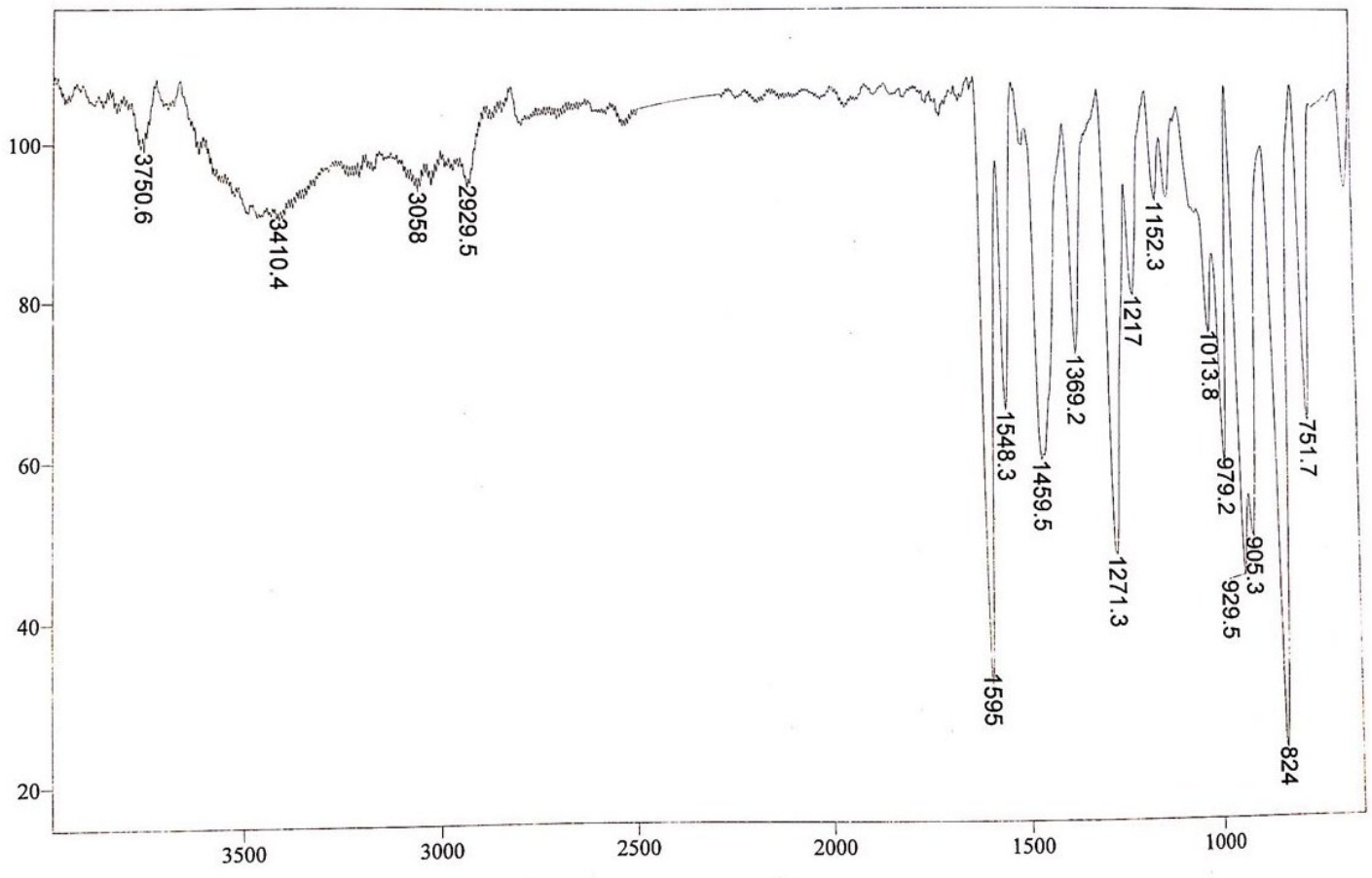

SI 1 b. IR spectrum of **1**.

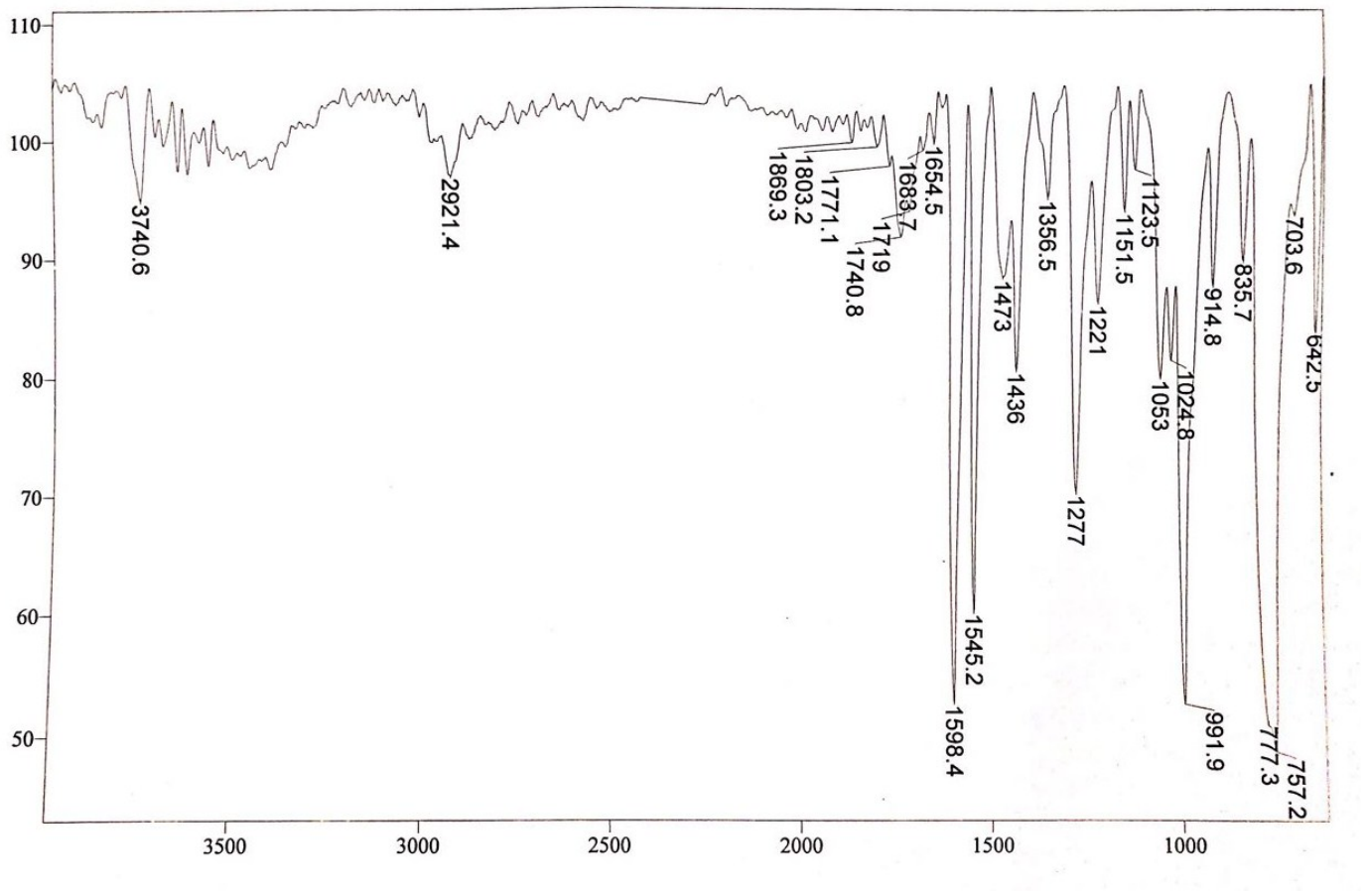

SI 1 c. IR spectrum of **2**.

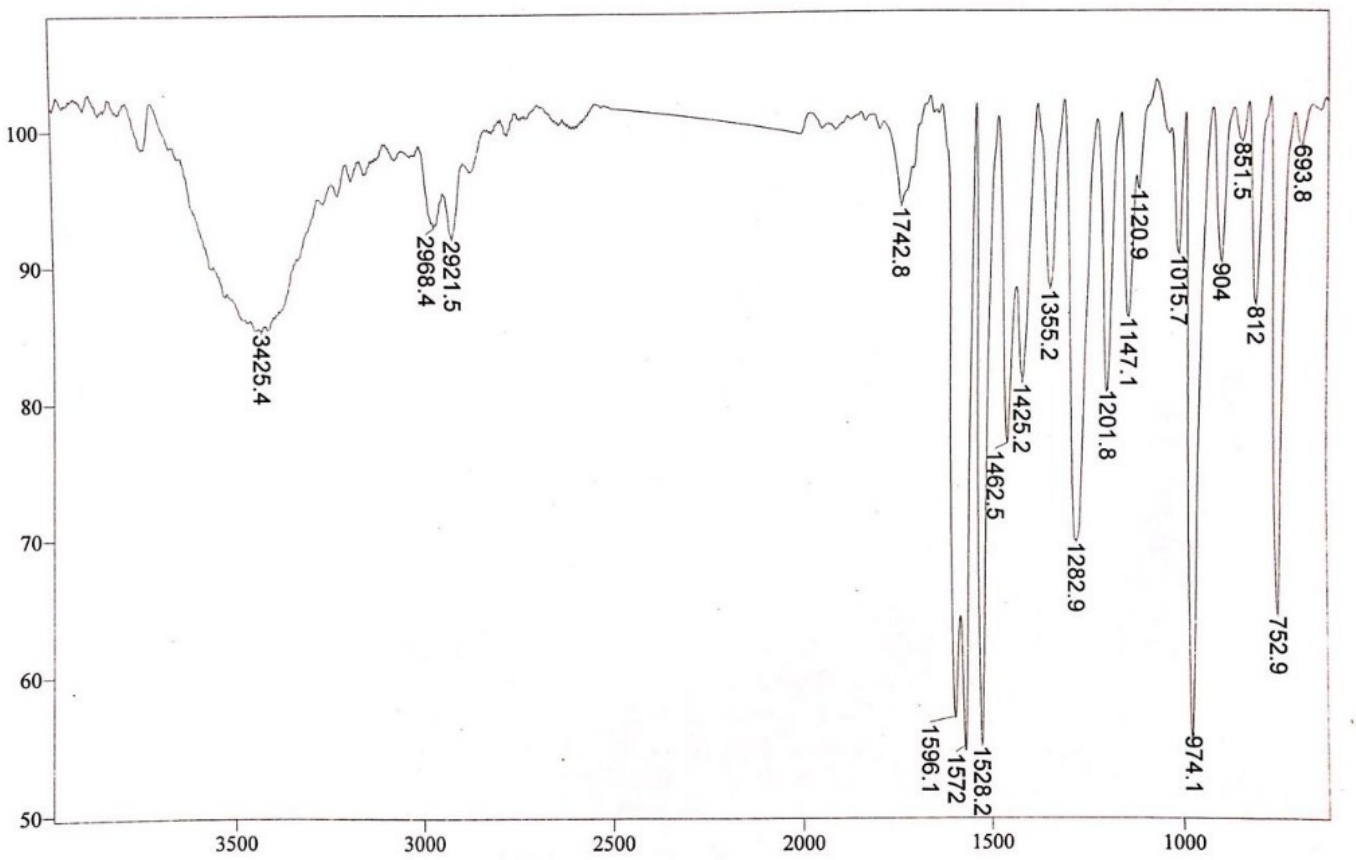

SI 1 d. IR spectrum of **3**.

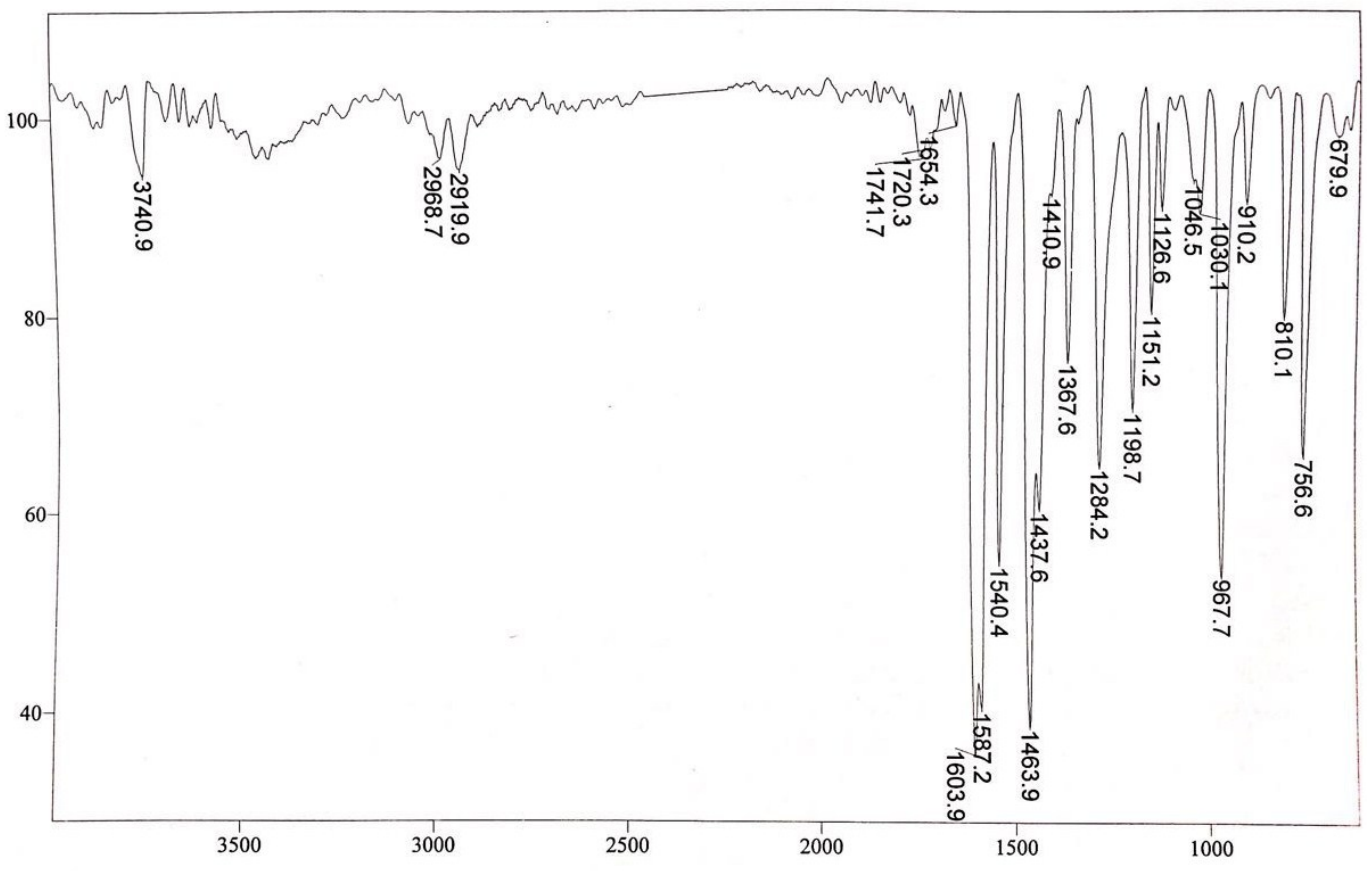

SI 1 e. IR spectrum of **4**.

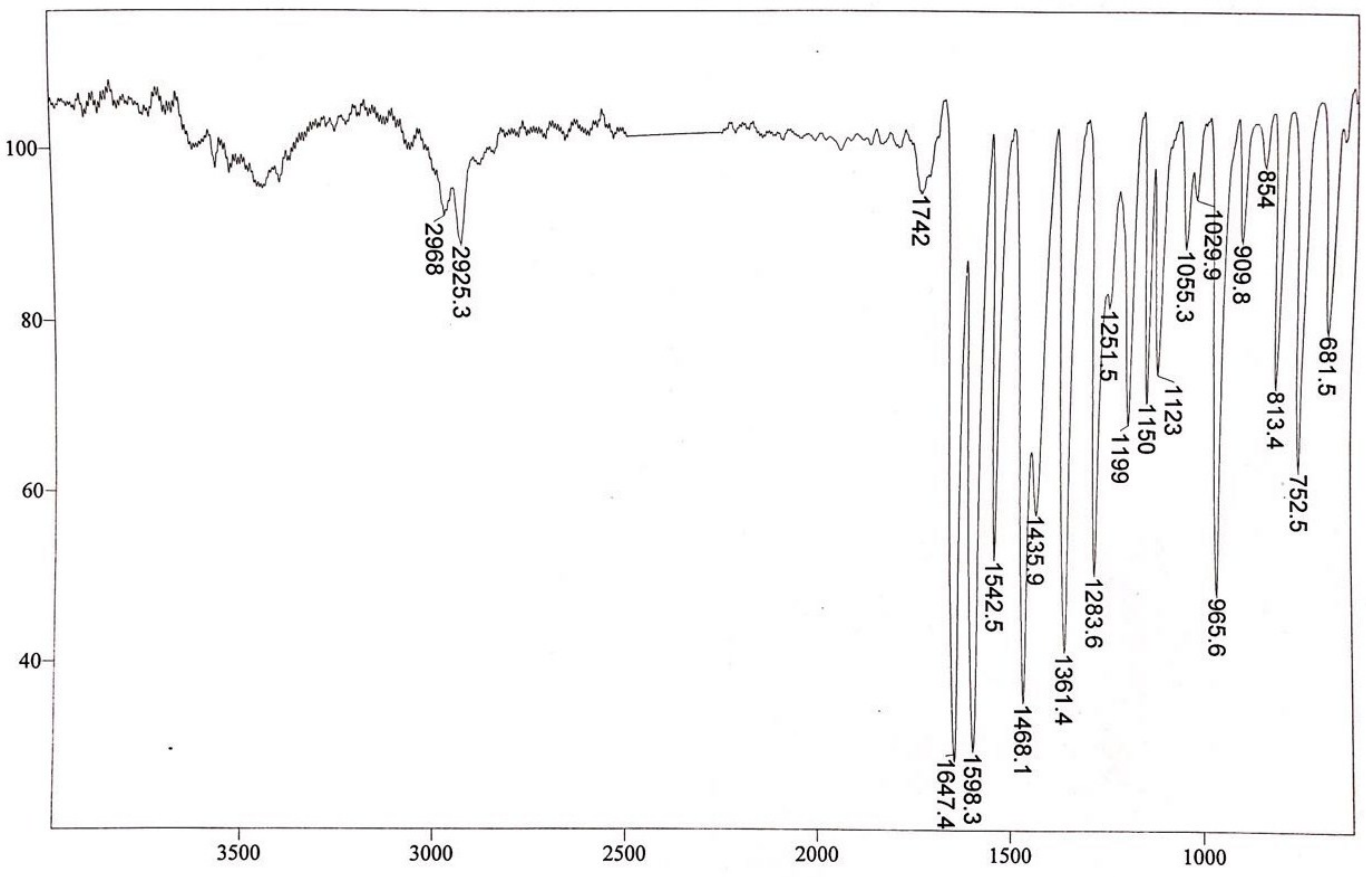

SI 1 f. IR spectrum of **5**.

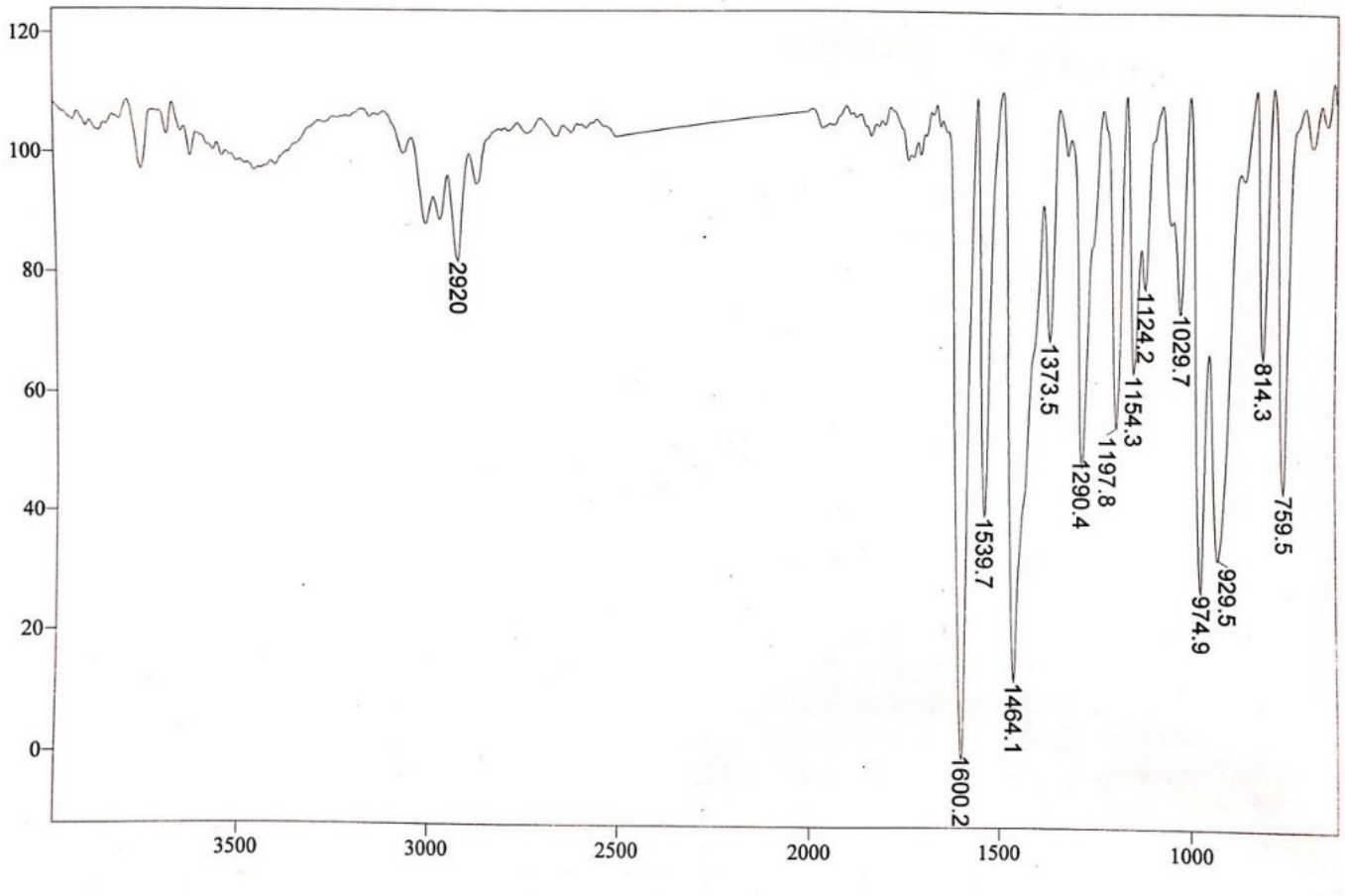

SI 1 g. IR spectrum of **6**.

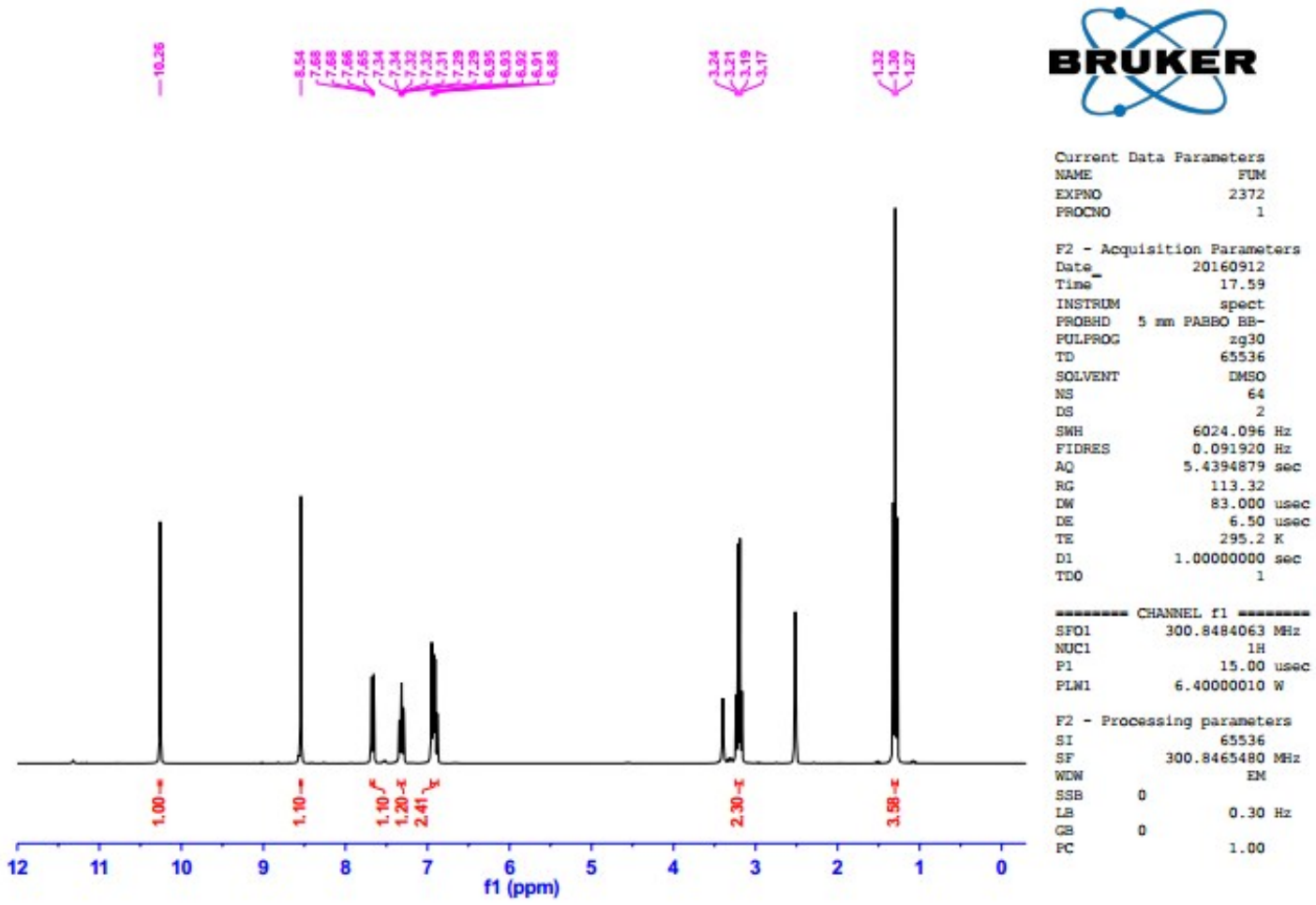

SI 2 a. ^{1}HNMR spectrum of L in DMSO-d_6.

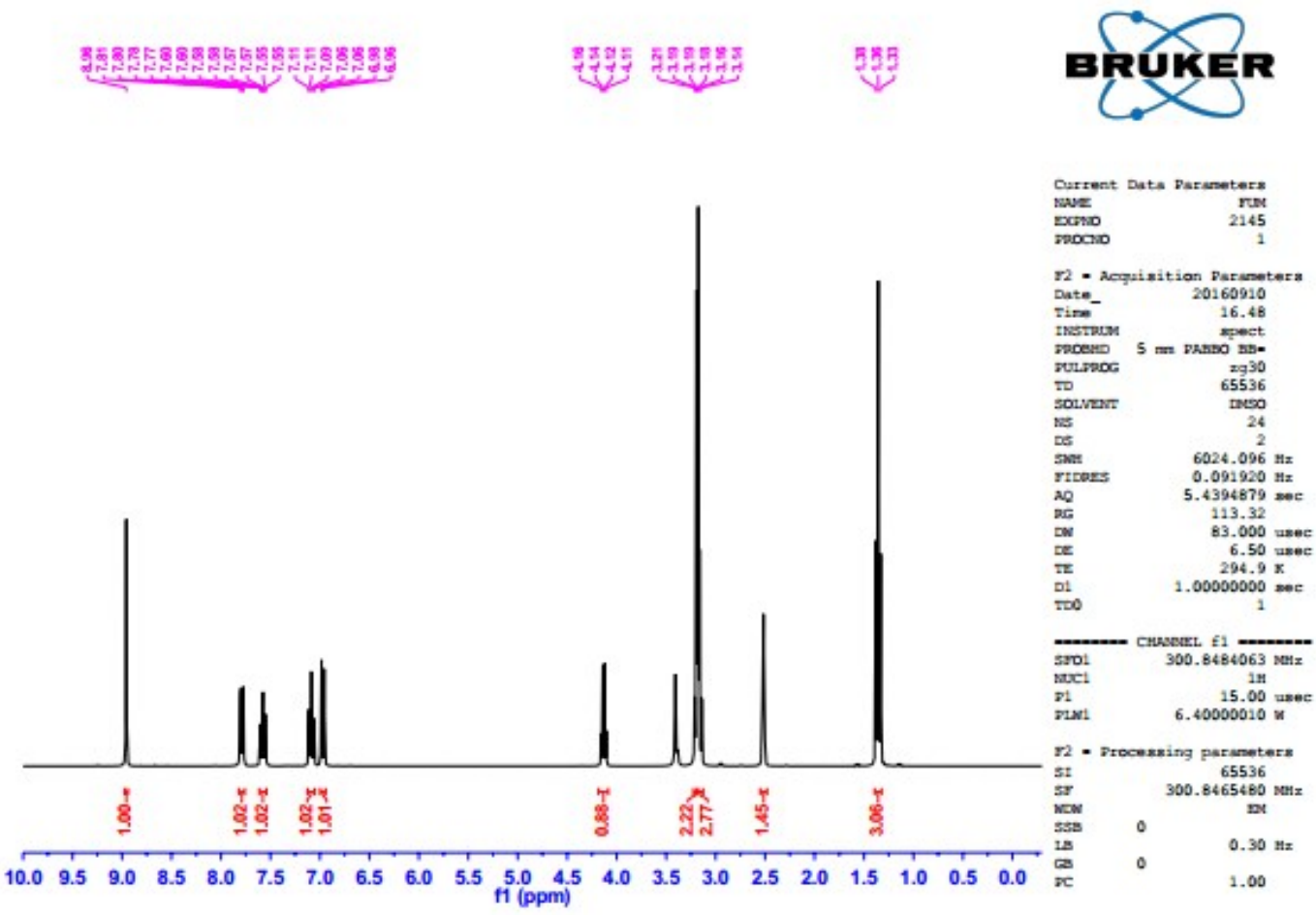

SI 2 b. [1]HNMR spectrum of **1** in DMSO-d_6.

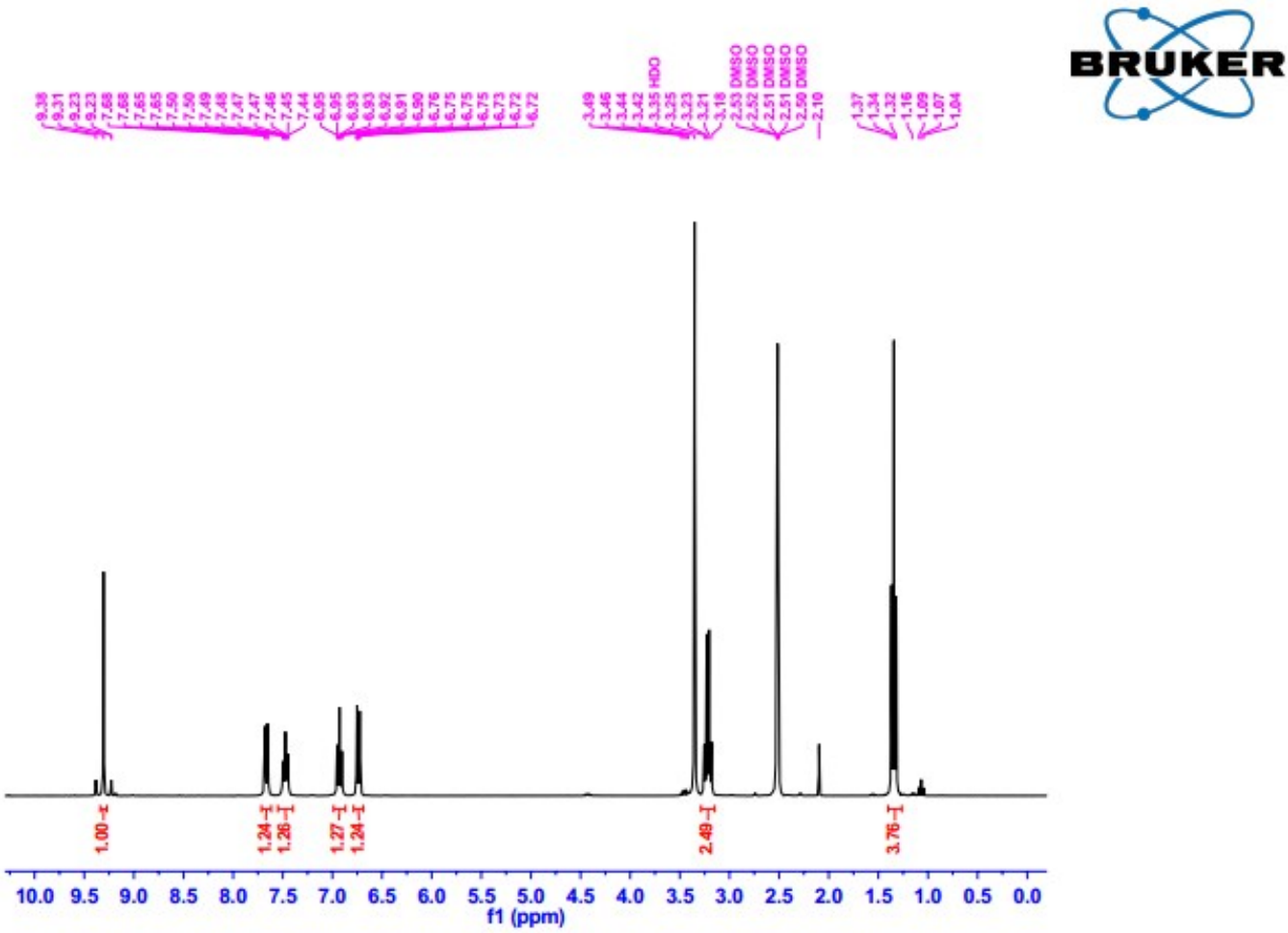

SI 2 c. [1]HNMR spectrum of **4** in DMSO-d_6.

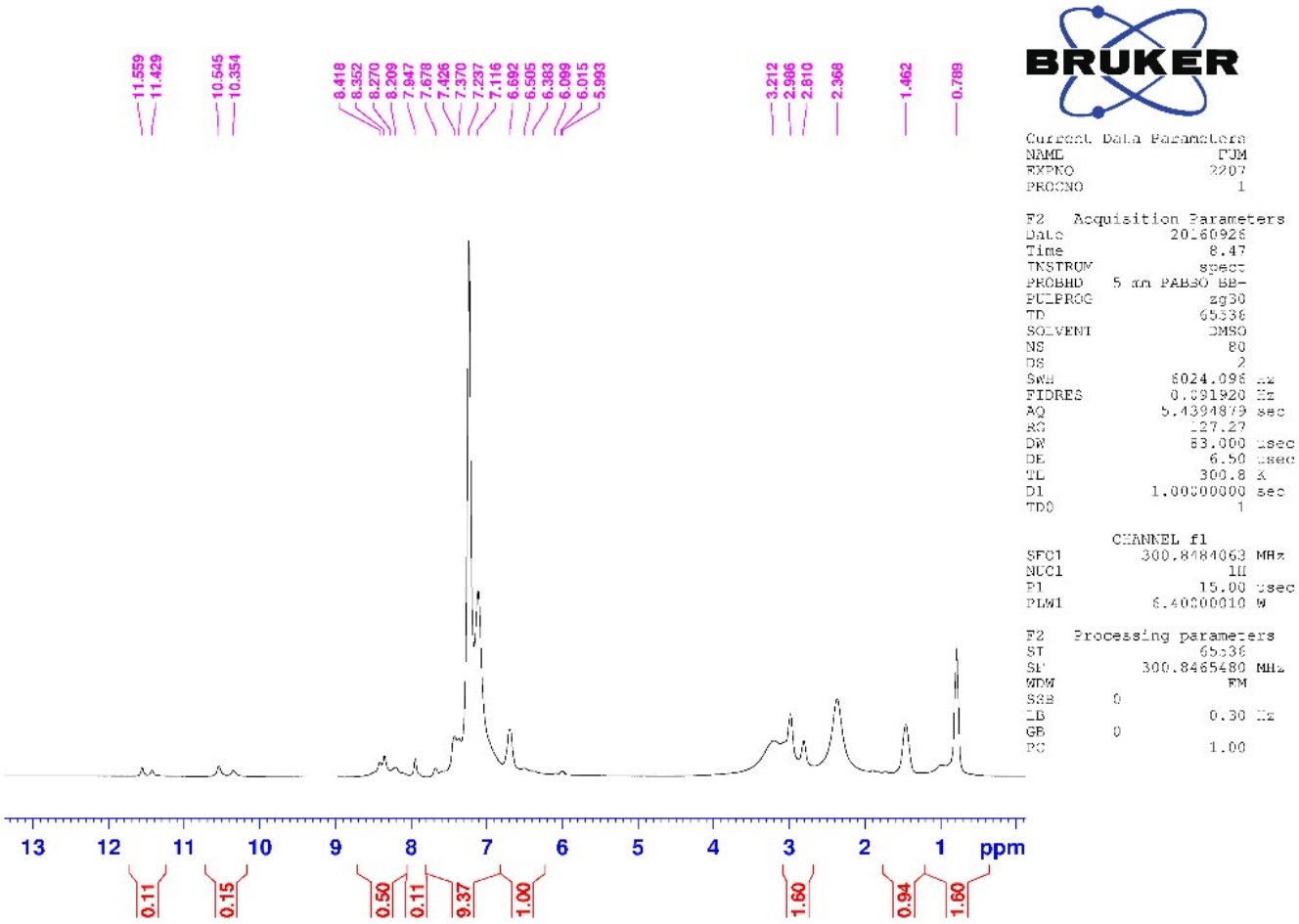

SI 2 d. [1]HNMR spectrum of **5** in DMSO-d_6.

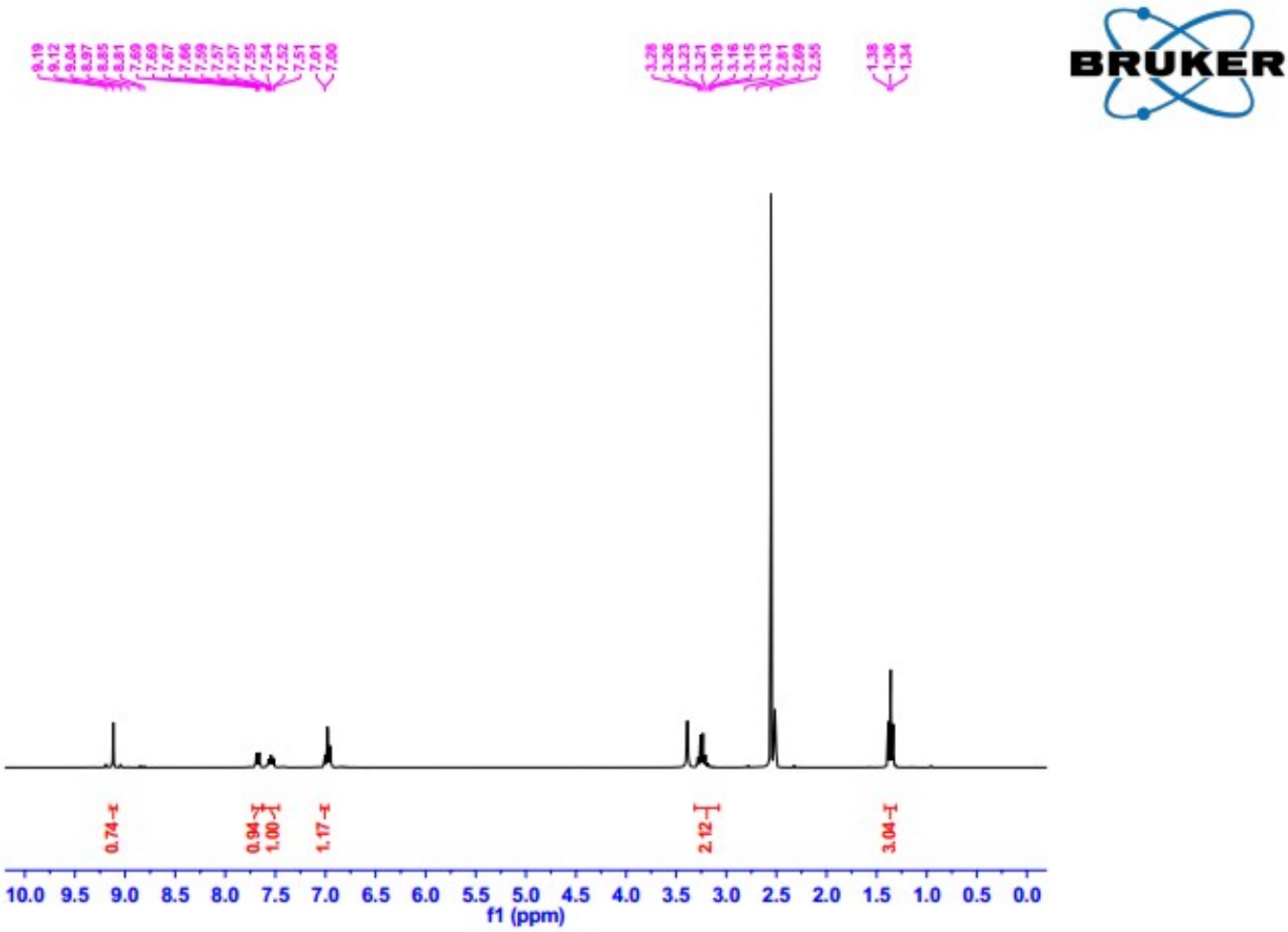

SI 2 e. ^{1}HNMR spectrum of **6** in DMSO-d_6.

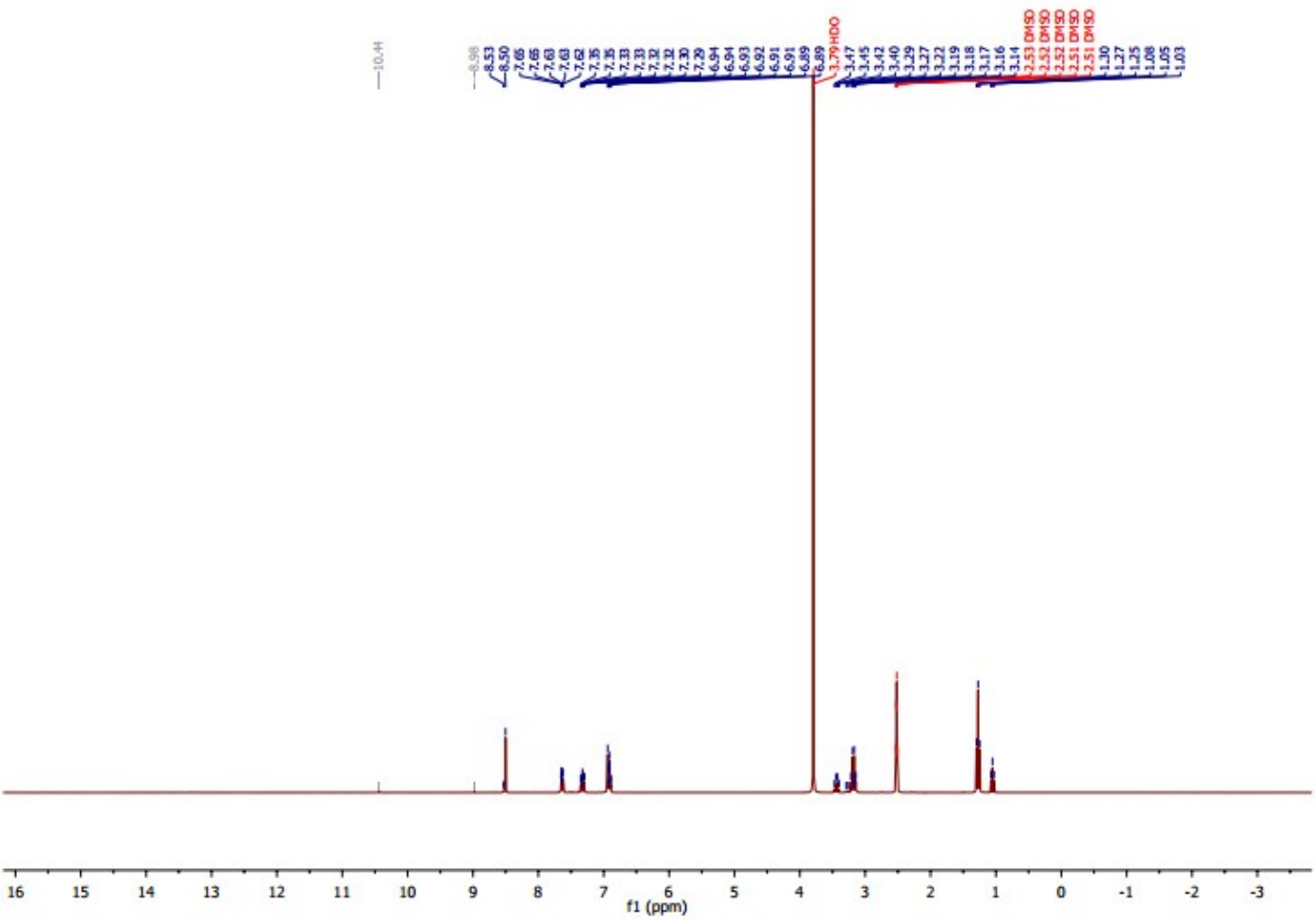

SI 2 f. ^{1}HNMR spectrum of L in DMSO-d_6 after D_2O addition.

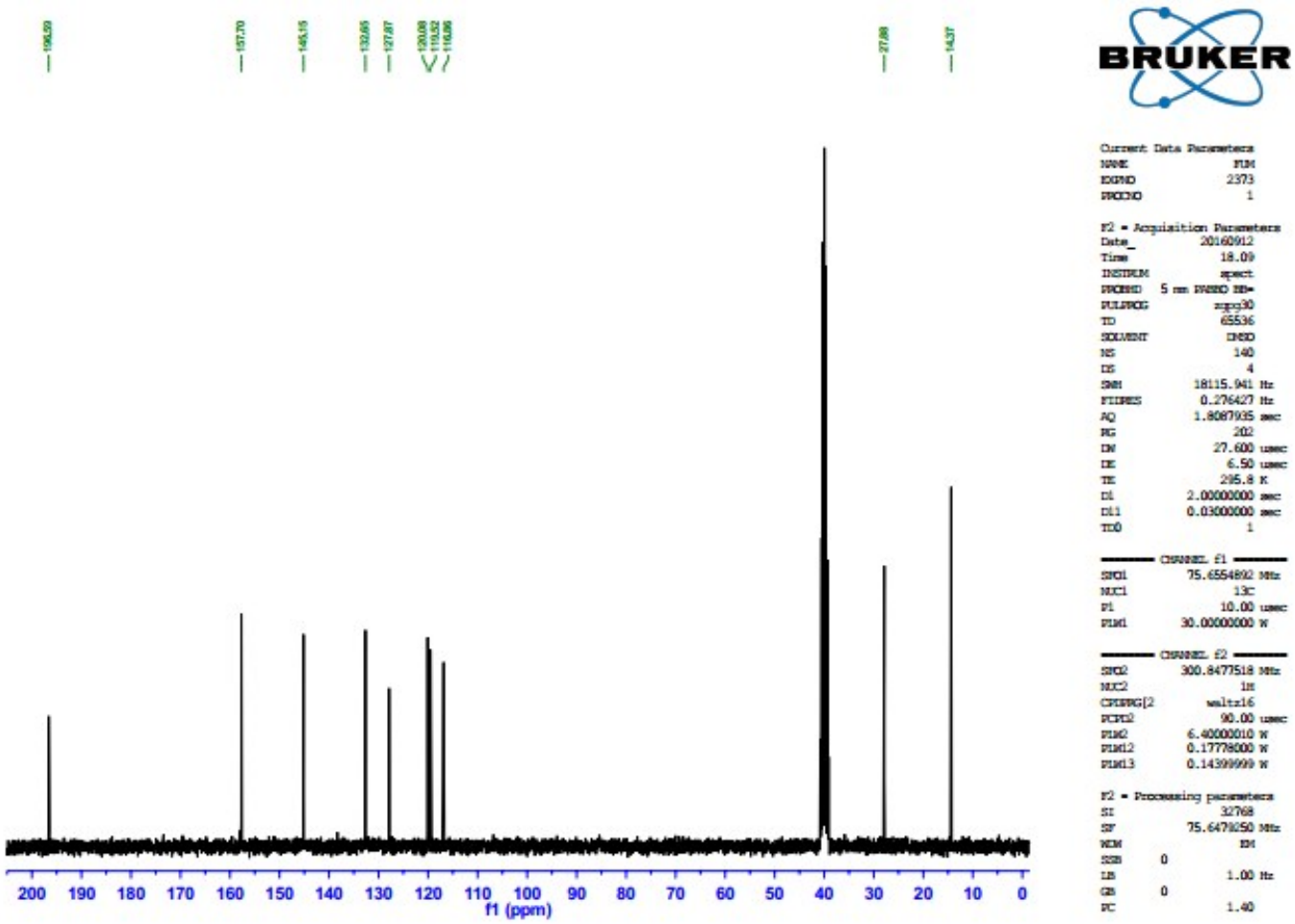

SI 3 a. ^{13}CNMR spectrum of L in DMSO-d_6.

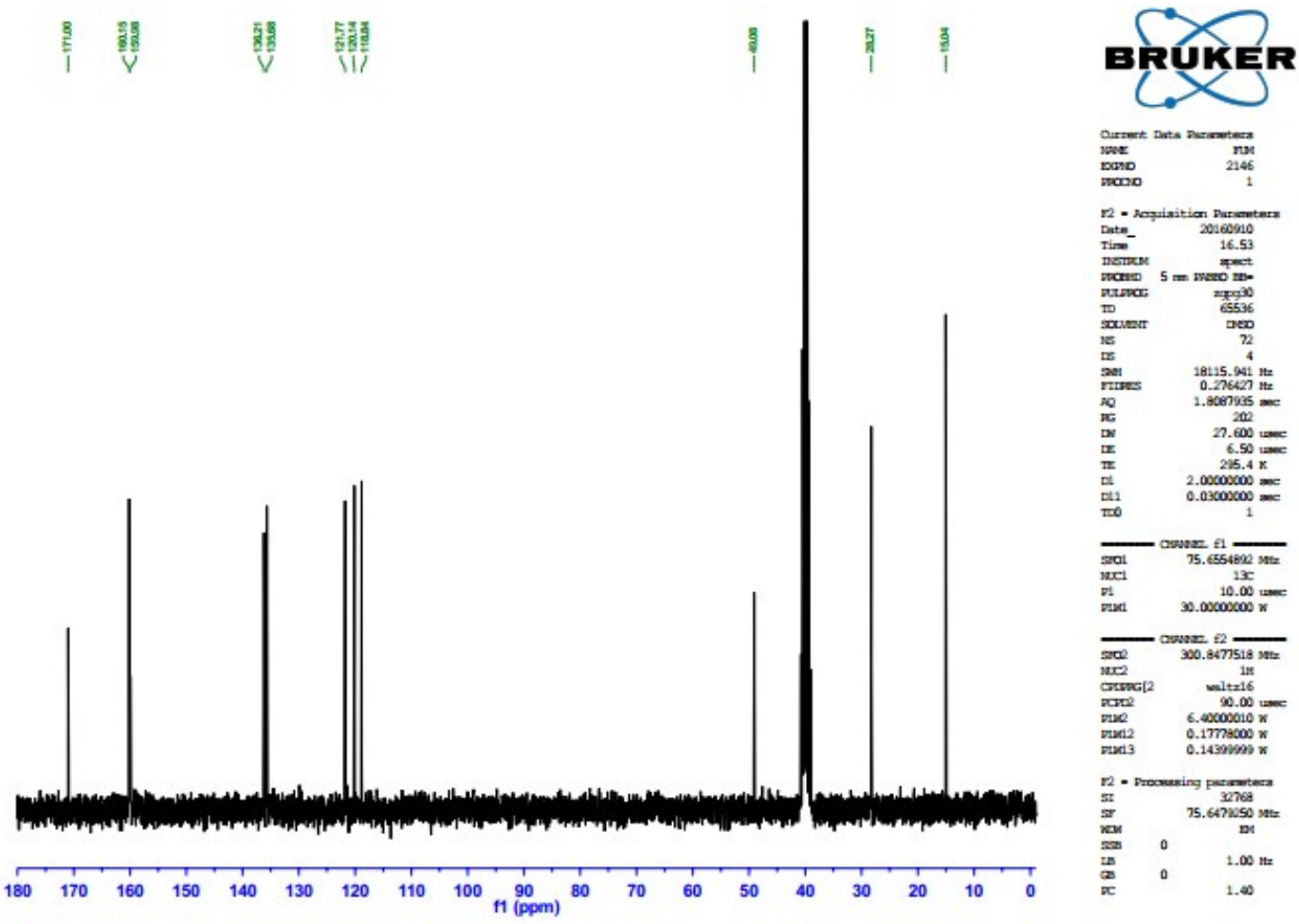

SI 3 b. ^{13}CNMR spectrum of **1** in DMSO-d_6.

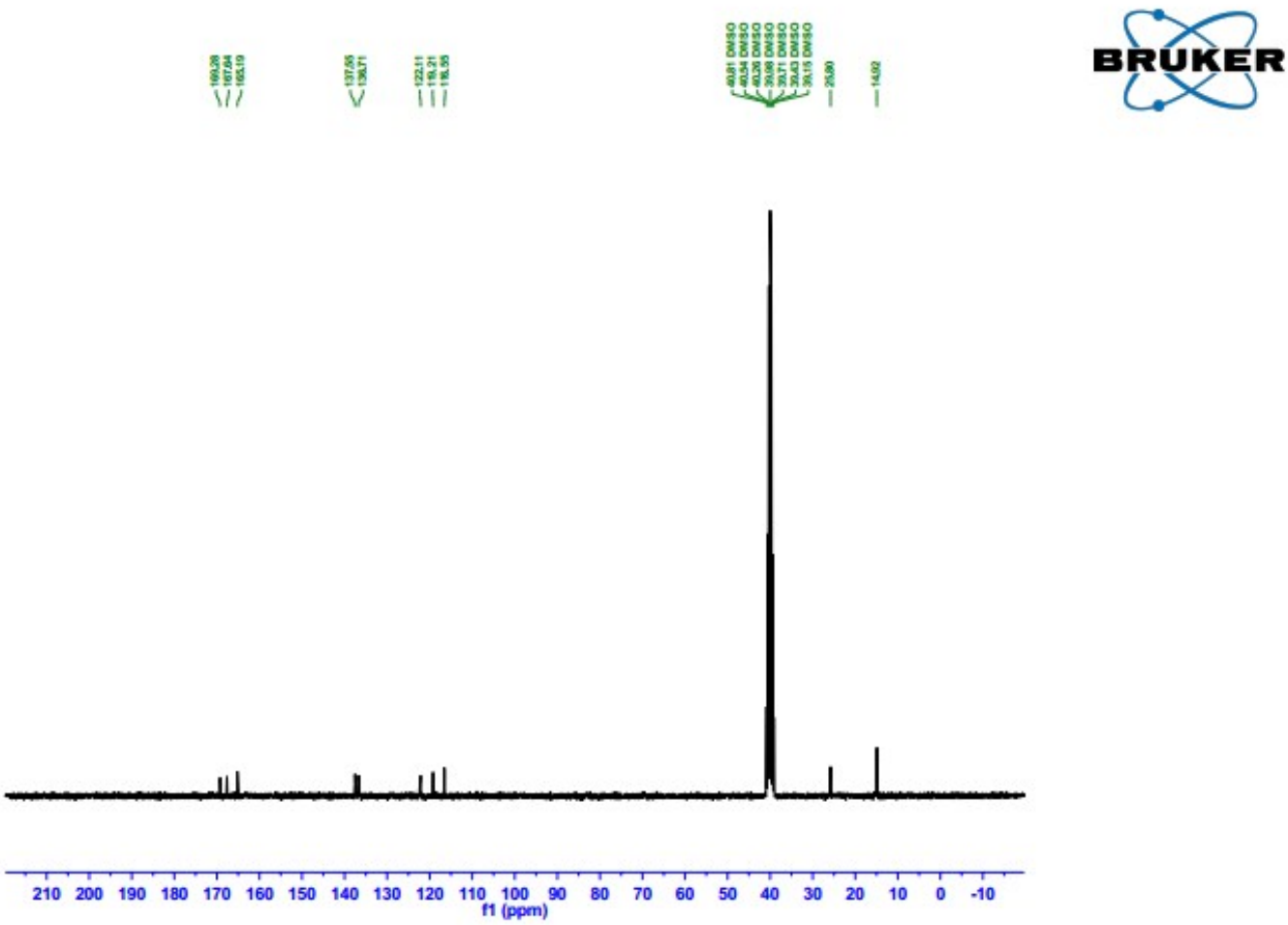

SI 3 c. ^{13}CNMR spectrum of **4** in DMSO-d_6.

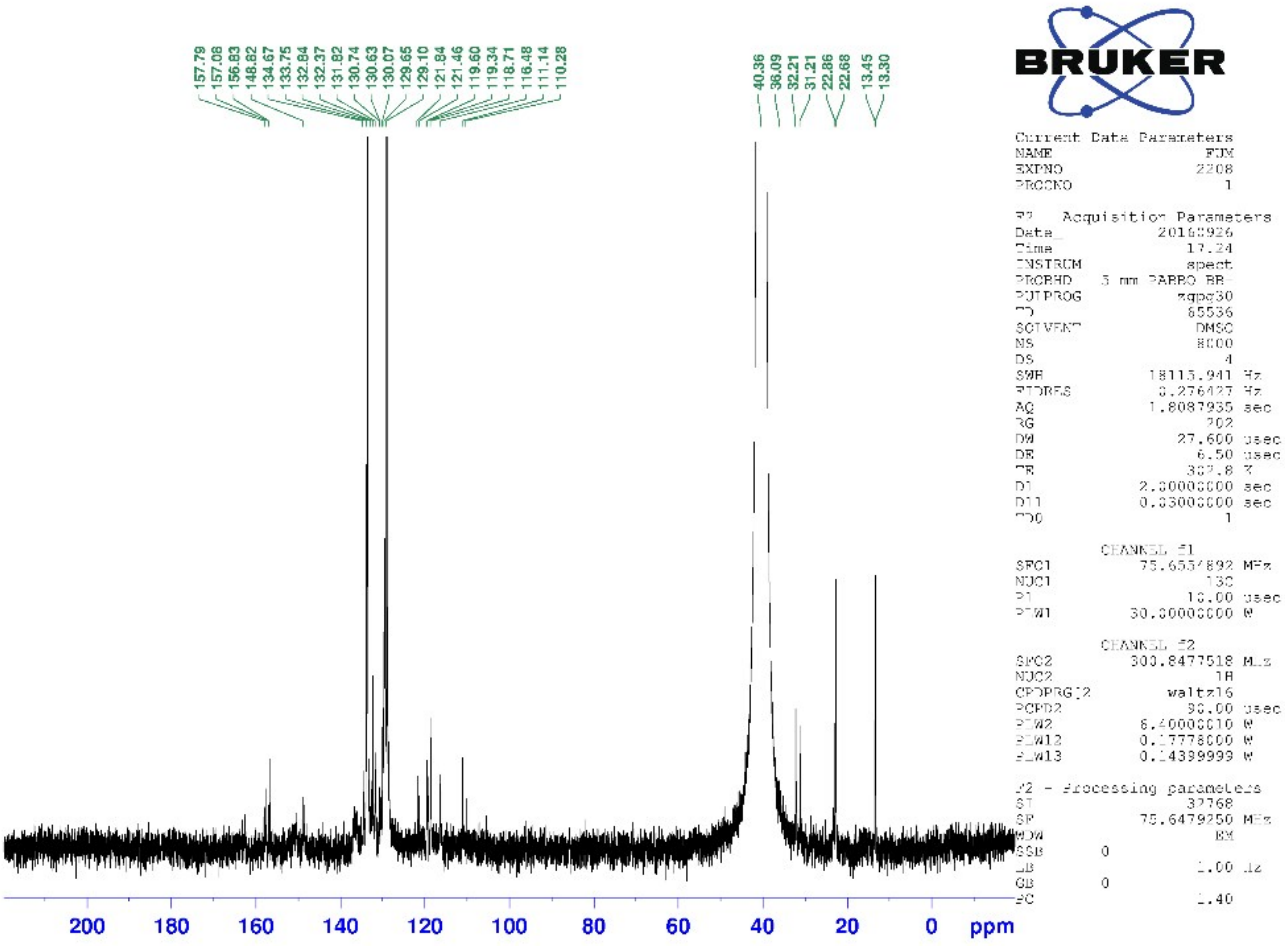

SI 3 d. ^{13}CNMR spectrum of **5** in DMSO-d_6.

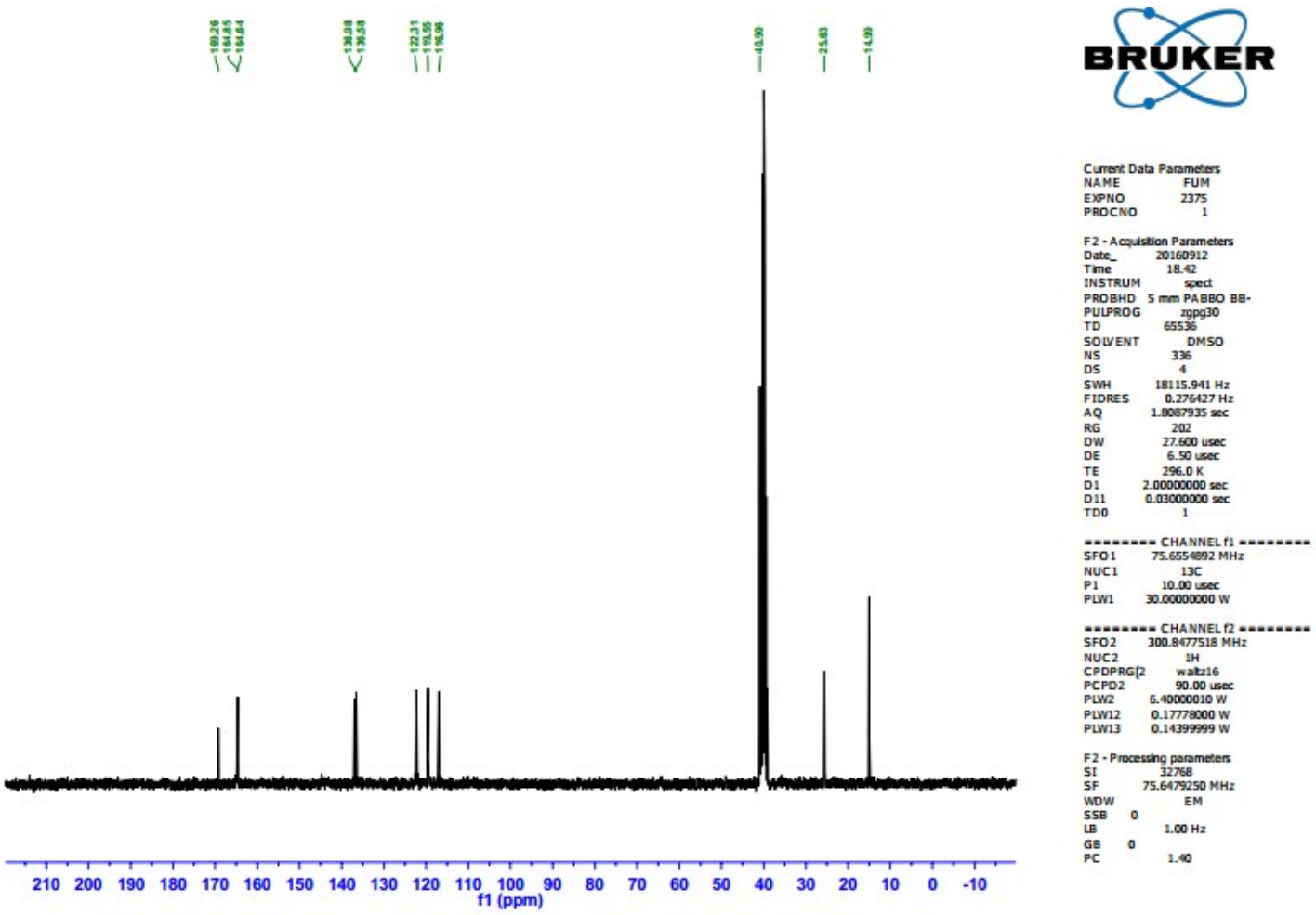

SI 3 e. ^{13}CNMR spectrum of **6** in DMSO-d_6.

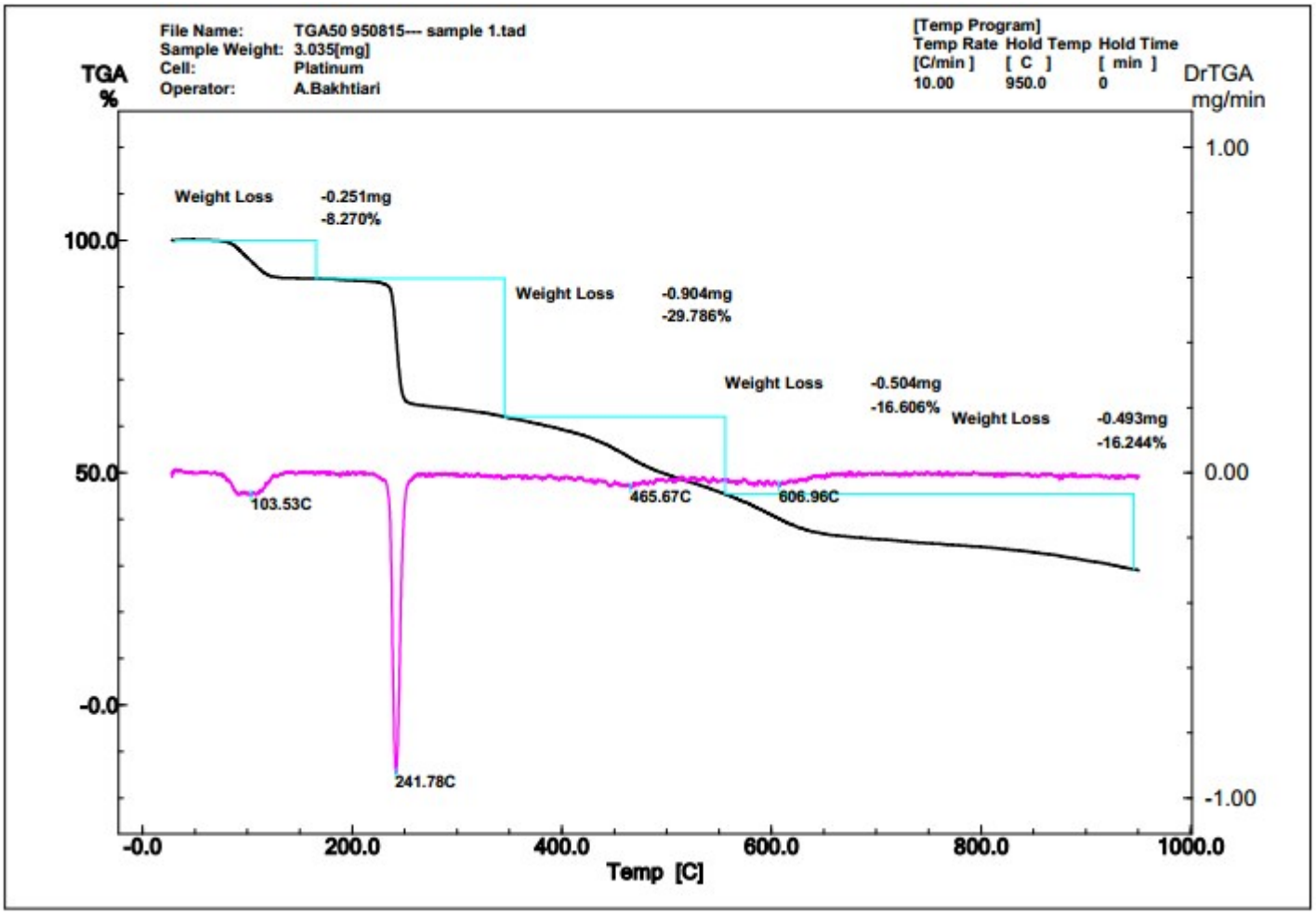

SI 4 a. TGA and DTG curves thermogram of **1**.

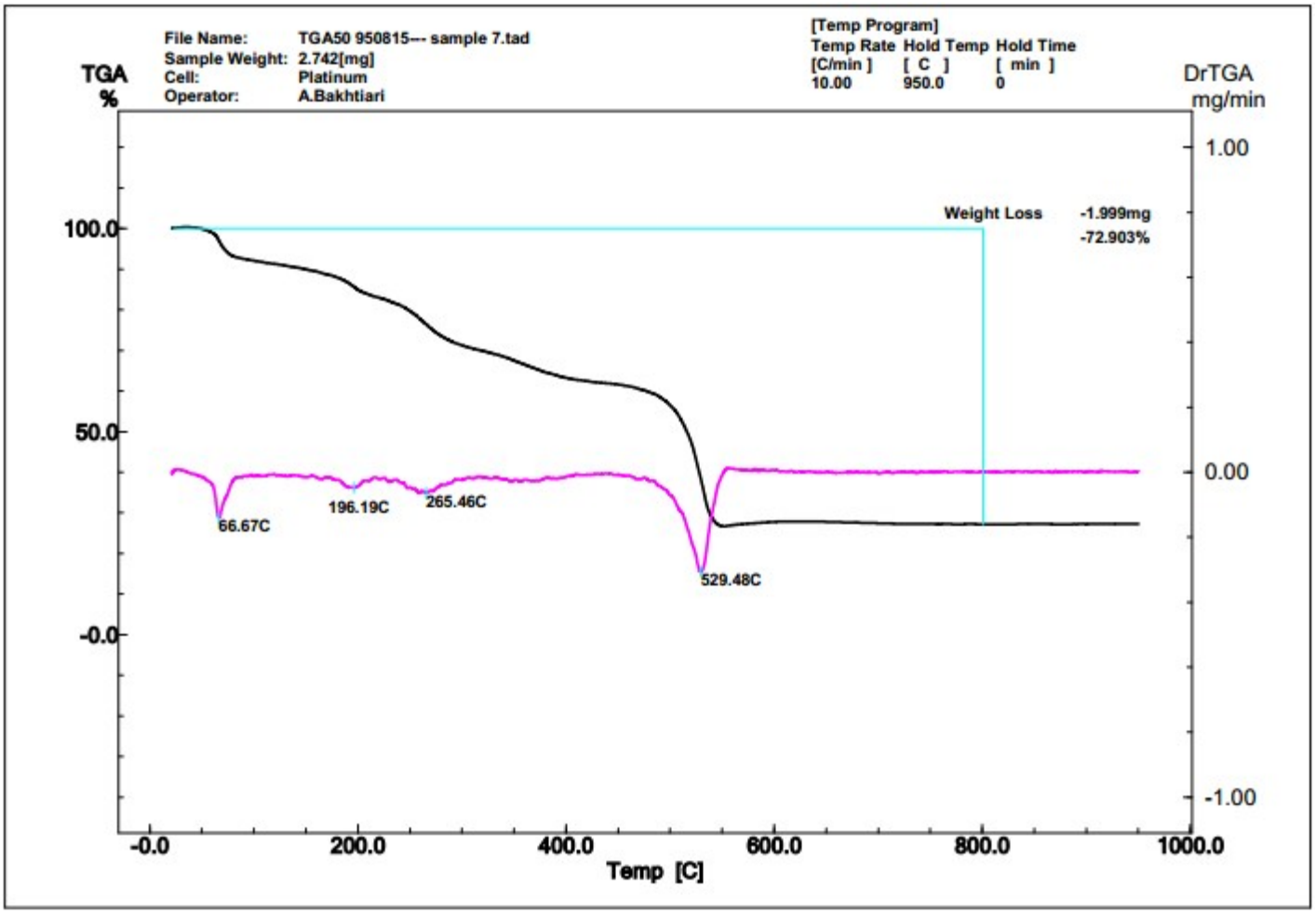

SI 4 b. TGA and DTG curves thermogram of **2**.

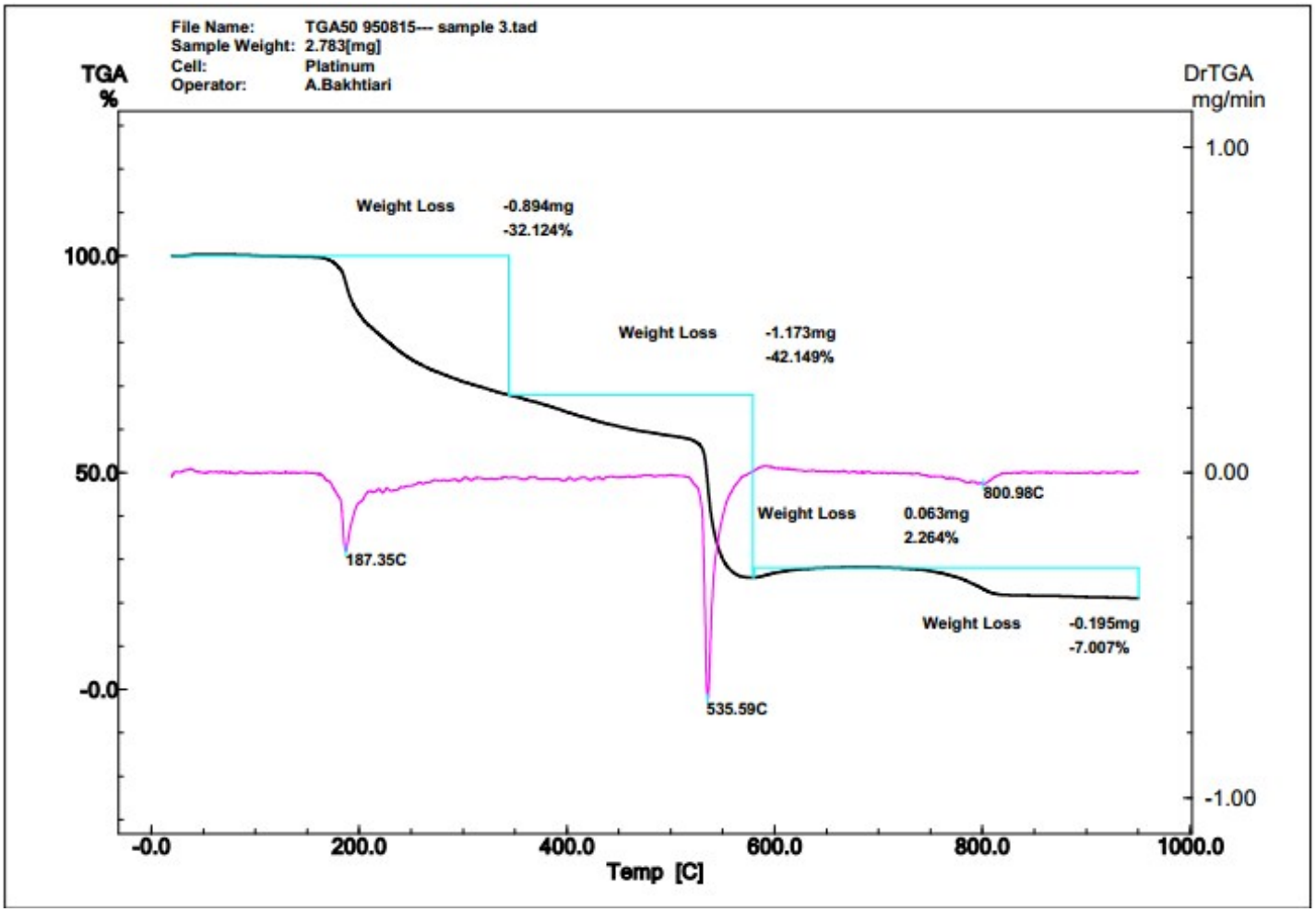

SI 4 c. TGA and DTG curves thermogram of **3**.

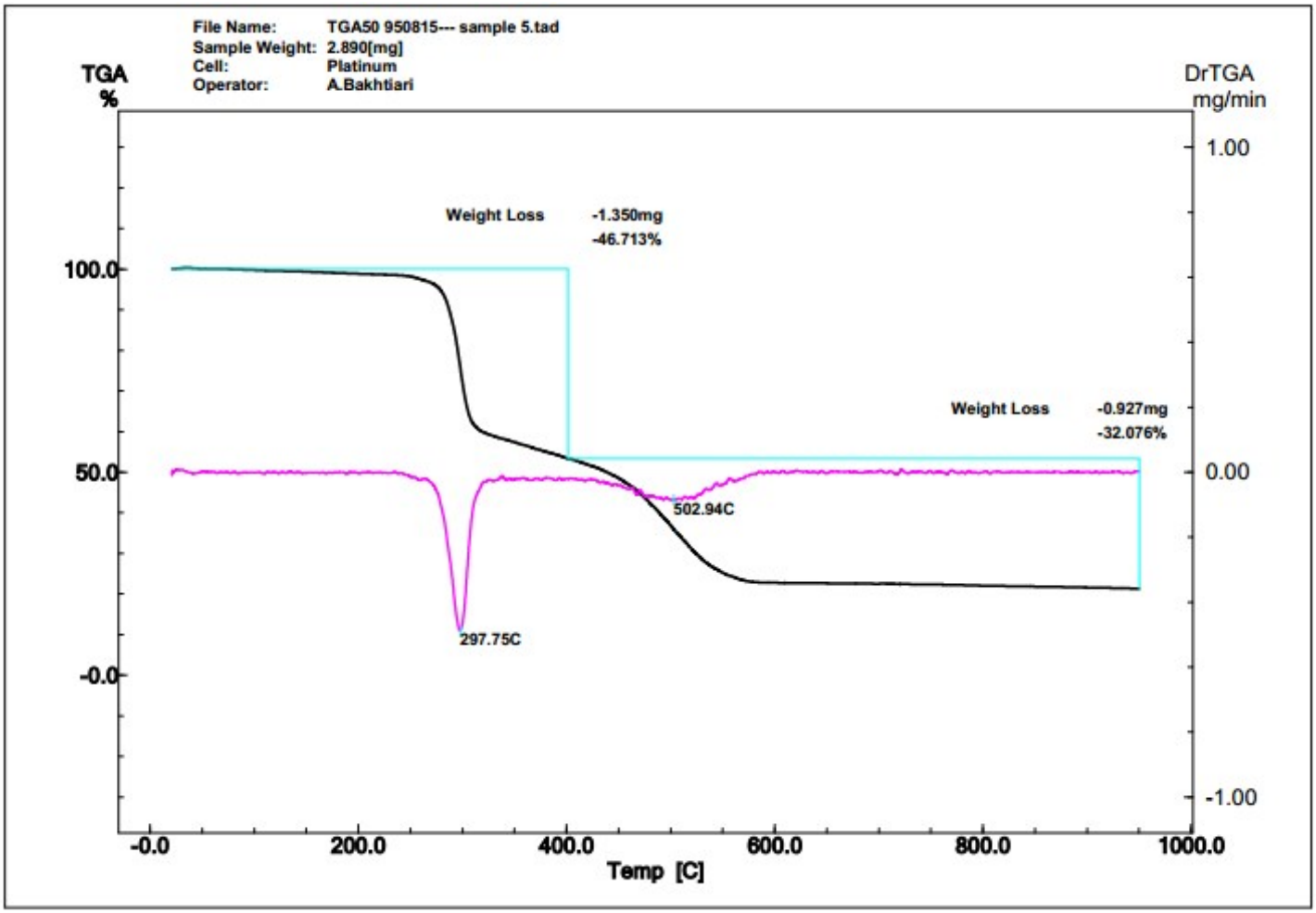

SI 4 d. TGA and DTG curves thermogram of **4**.

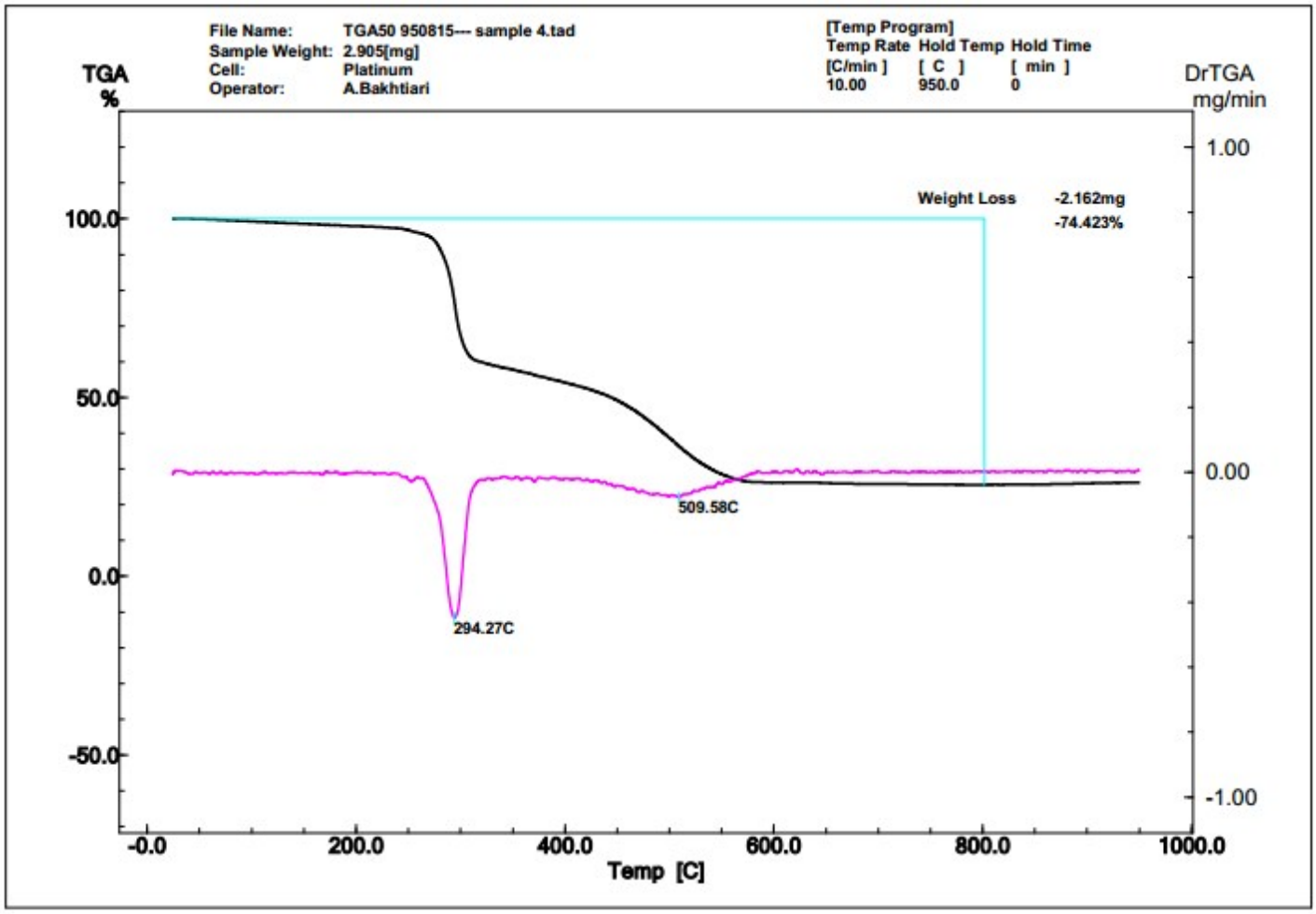

SI 4 e. TGA and DTG curves thermogram of **5**.

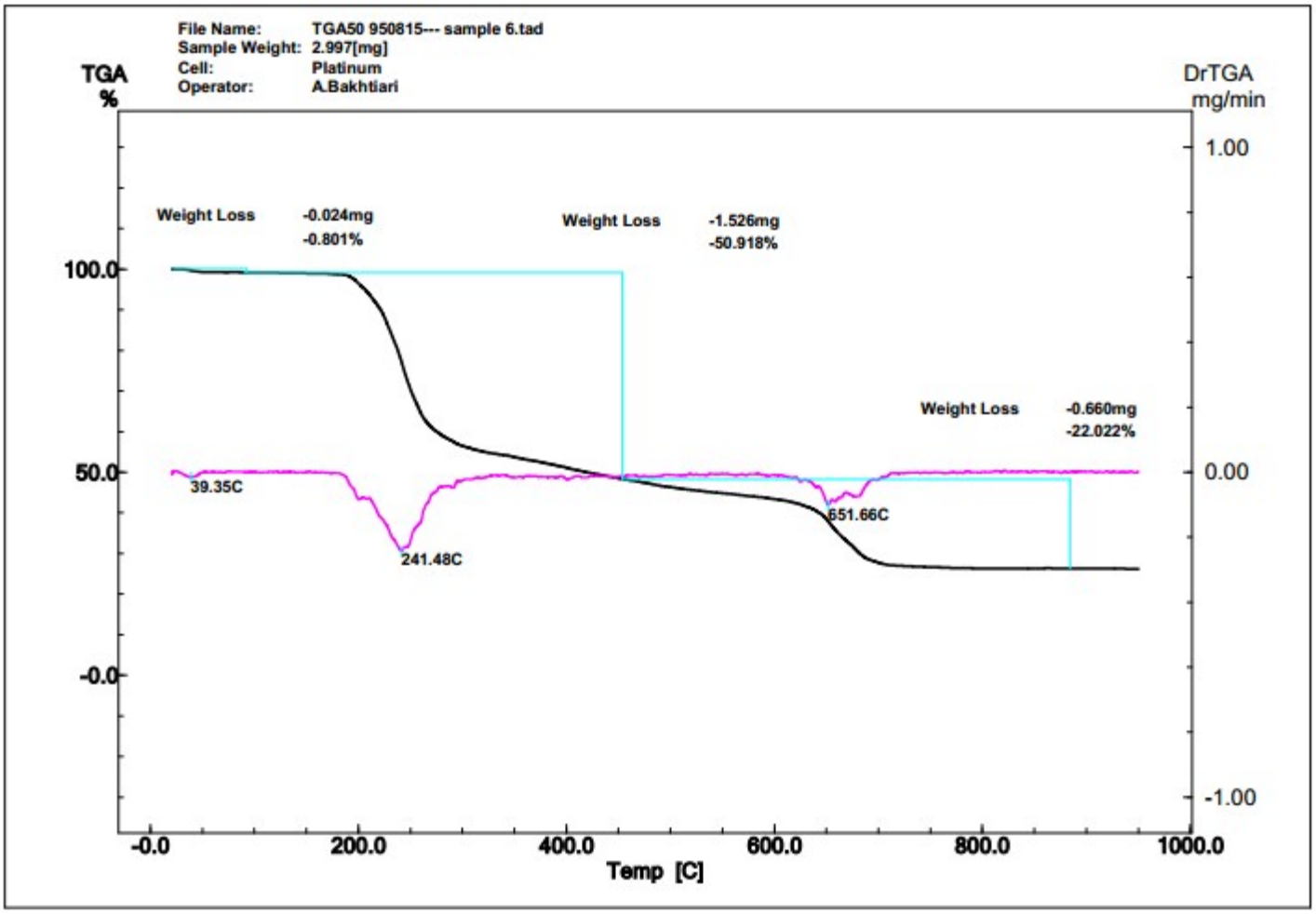

SI 4 f. TGA and DTG curves thermogram of **6**.

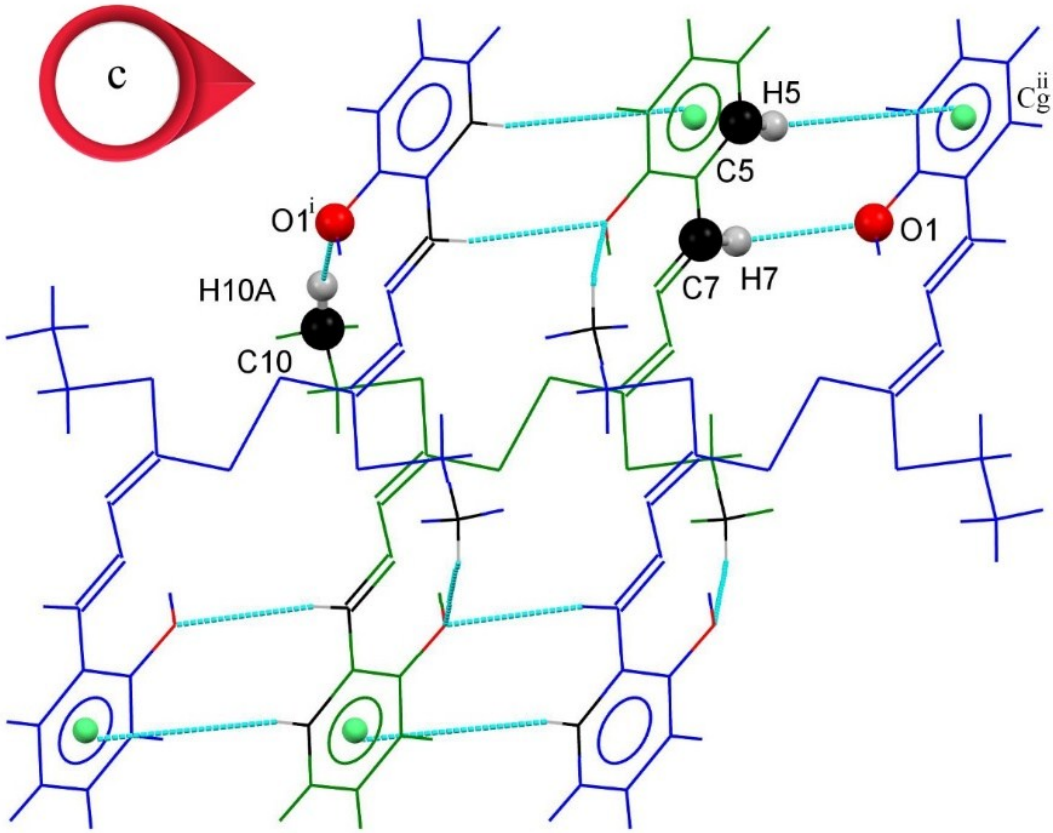

SI 5 a. C10—H10A···$O1^i$ (2.644 Å) (symm. code *i*: 1-*x*, 1-*y*, -*z*), C7—H7···O1 (2.692 Å) hydrogen bonds and C5—H5···C_g^{ii} (C_g: C1-C6) (3.715 Å) (symm. code *ii*: 1-*x*, 1-*y*, 1-*z*) interaction along the *c* axis.

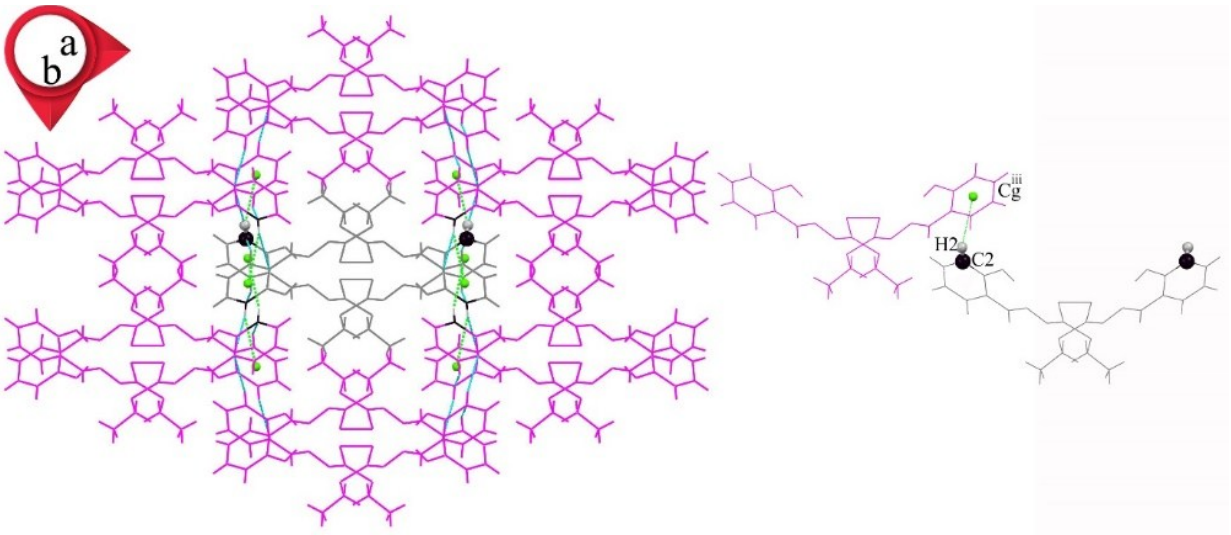

SI 5 b. Chains expand through C2—H2···C_g^{iii} (C_g: C1-C6) (2.865 Å) (symm. code *iii*: 1-*x*, 1-*y*, 1-*z*) interaction in the *bc* plane.

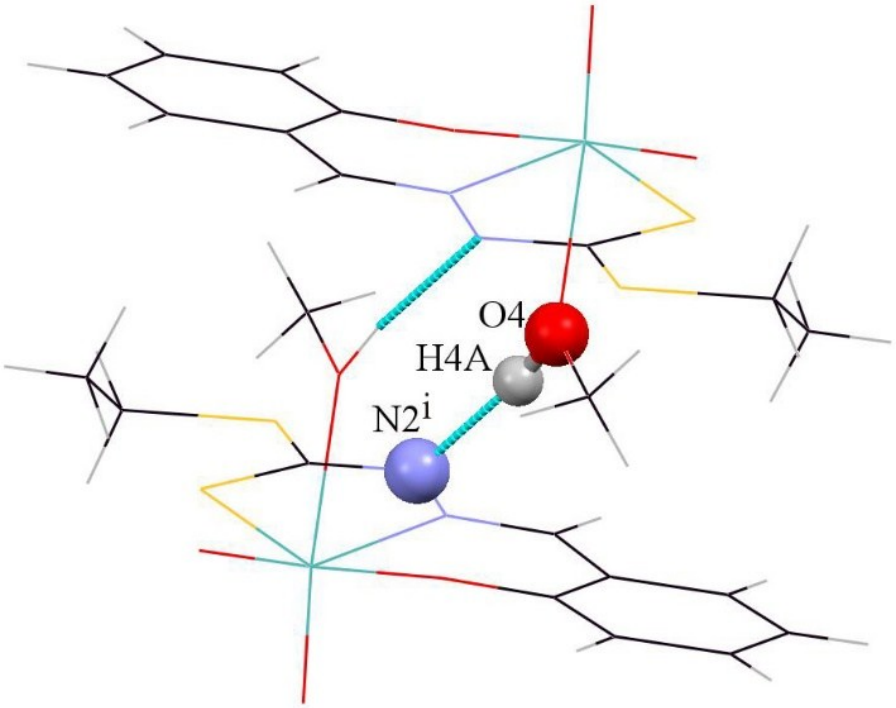

SI 5 c. Form a dimer through pairwise hydrogen bond of O4—H4A···N2^{i} (1.913(2) Å) (symm. code *i*: 1-*x*, 1-*y*, 1-*z*).

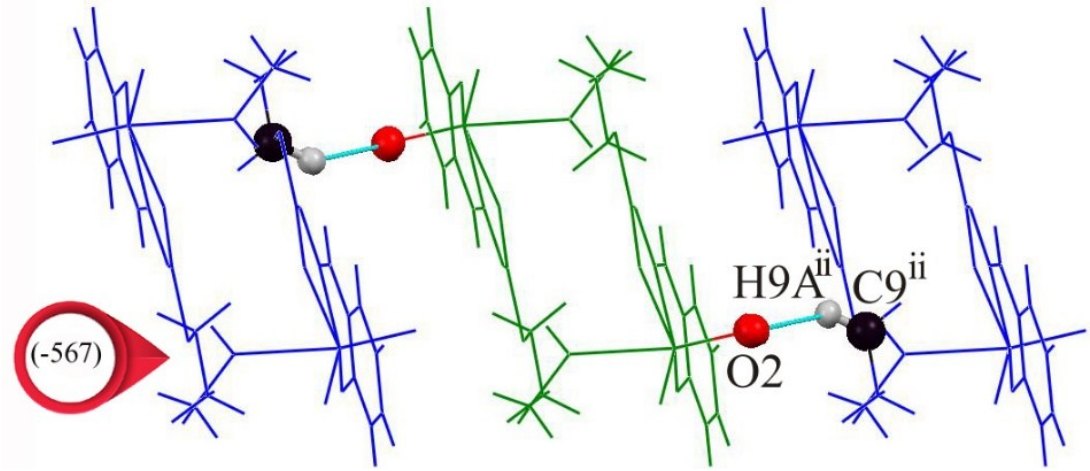

SI 5 d. Form a one-dimensional chain in the direction of the (-567) plane through the hydrogen bond C9^{ii}—H9A^{ii}···O2 (2.543 Å) (symm. code *ii*: *x*, 1.5 - *y*, 1/2 + z).

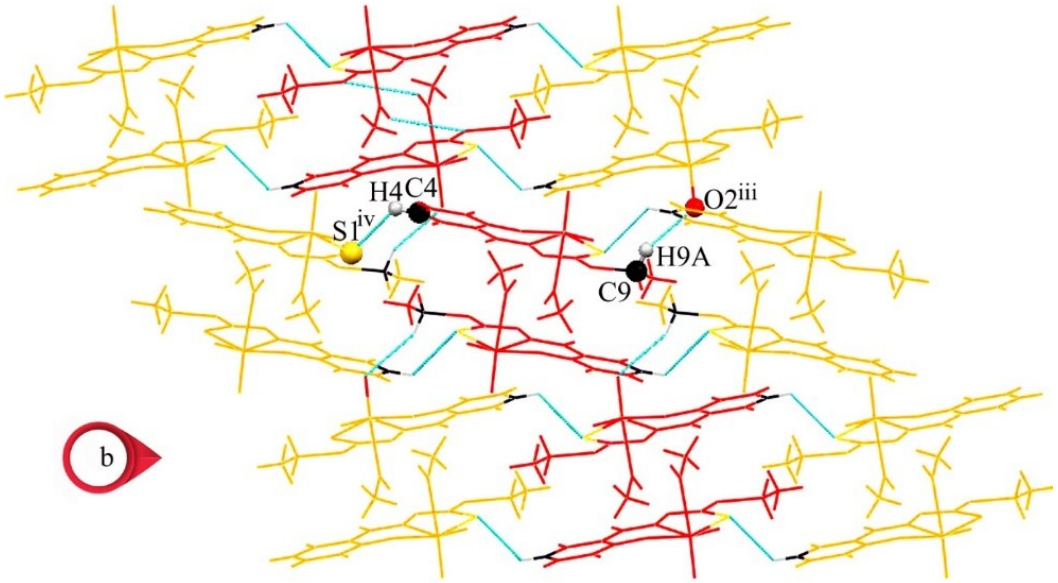

SI 5 e. Through C9—H9A···O2^{iii} and C4—H4A···S1^{iv} (2.961 Å) (symm. code *iii* and *iv*: 1 - *x*, 1/2 + *y*, 1/2 - *z* and *x*, -1 + *y*, *z*) hydrogen bonds the second dimension forms along the *b* axis.

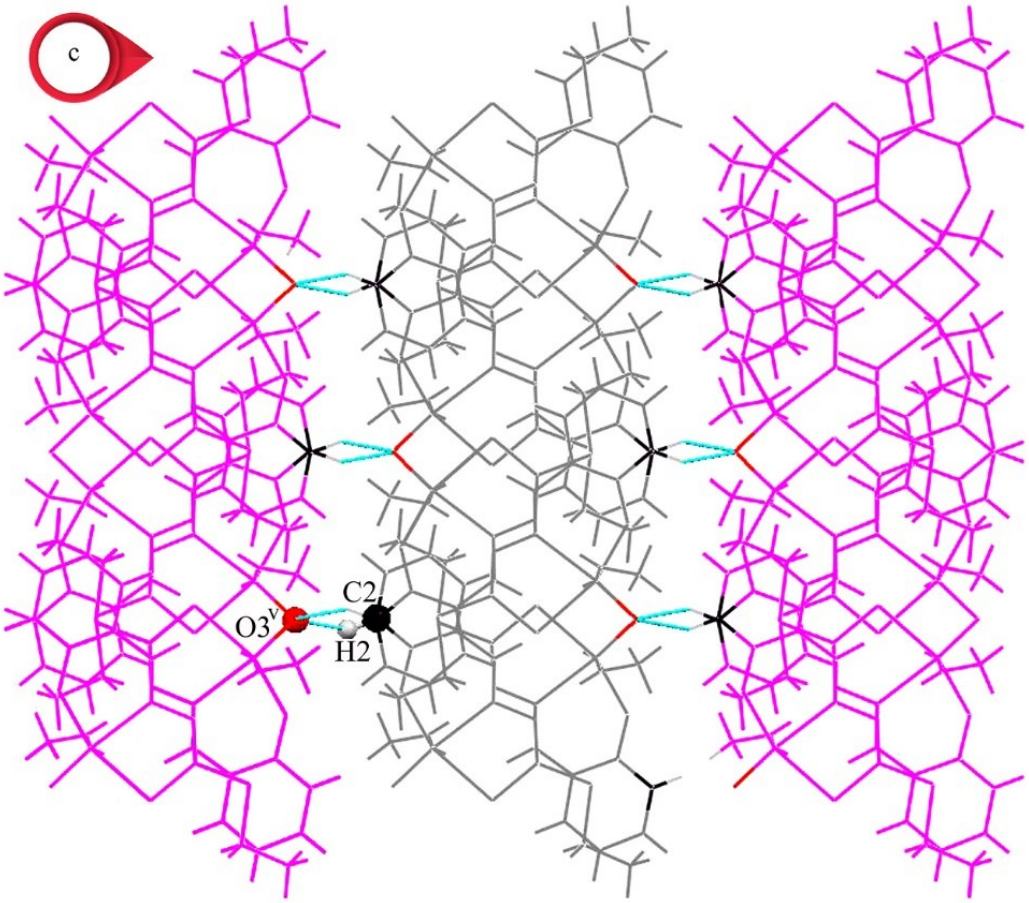

SI 5 f. Fulfill the three dimensional structure through C2—H2···O3^{v} (2.606 Å) (symm. code *v*: *x*, 1.5 - *y*, 1/2 + *z*) hydrogen bonds according to the *c* direction.

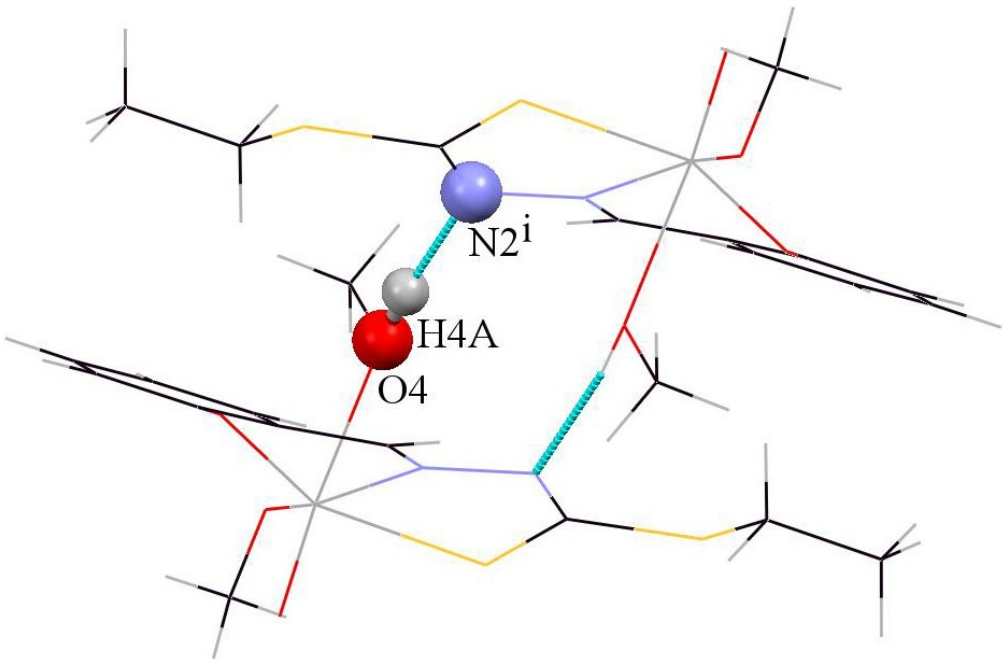

SI 5 g. Form dimer through pairwise hydrogen bonds O4—H4A···N2^{i} (1.963 Å) (symm. code *i*: 1 - *x*, 1 - *y*, 1 - *z*).

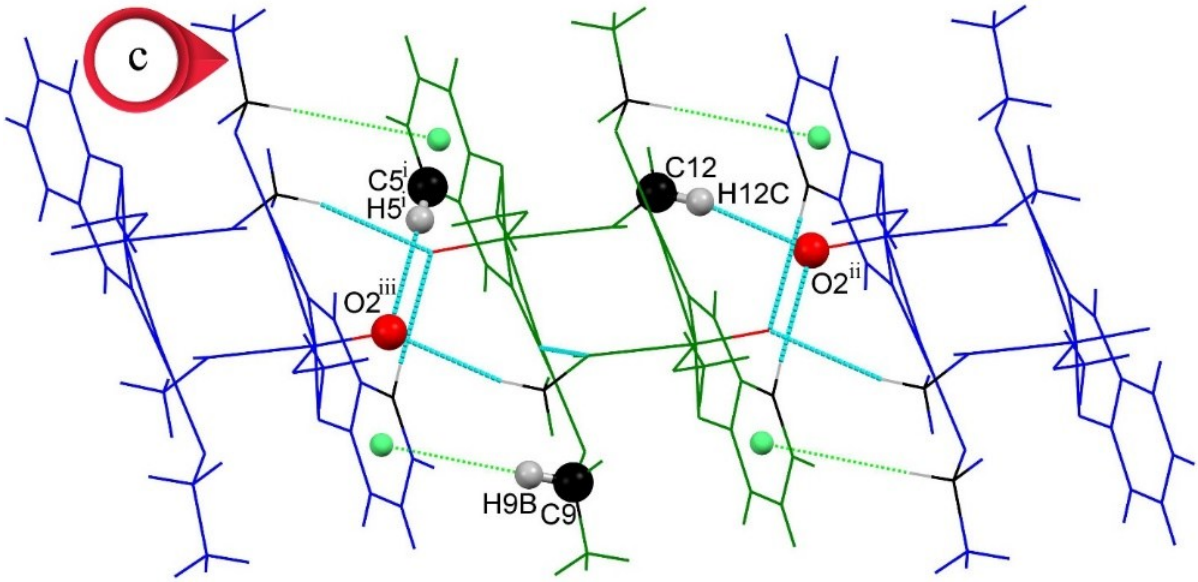

SI 5 h. Formation one-dimensional chain in the direction of the *c* axis through the hydrogen bondings C9—H9A···C_g, C12—H12C···O2^{ii} (2.681 Å) and C5^{i}—H5^{i}···O2^{iii} (2.665 Å) (symm. code *ii*: 2 - *x*, 1 - *y*, 1 - *z*, *iii*: -1 + *x*, *y*, *z*).

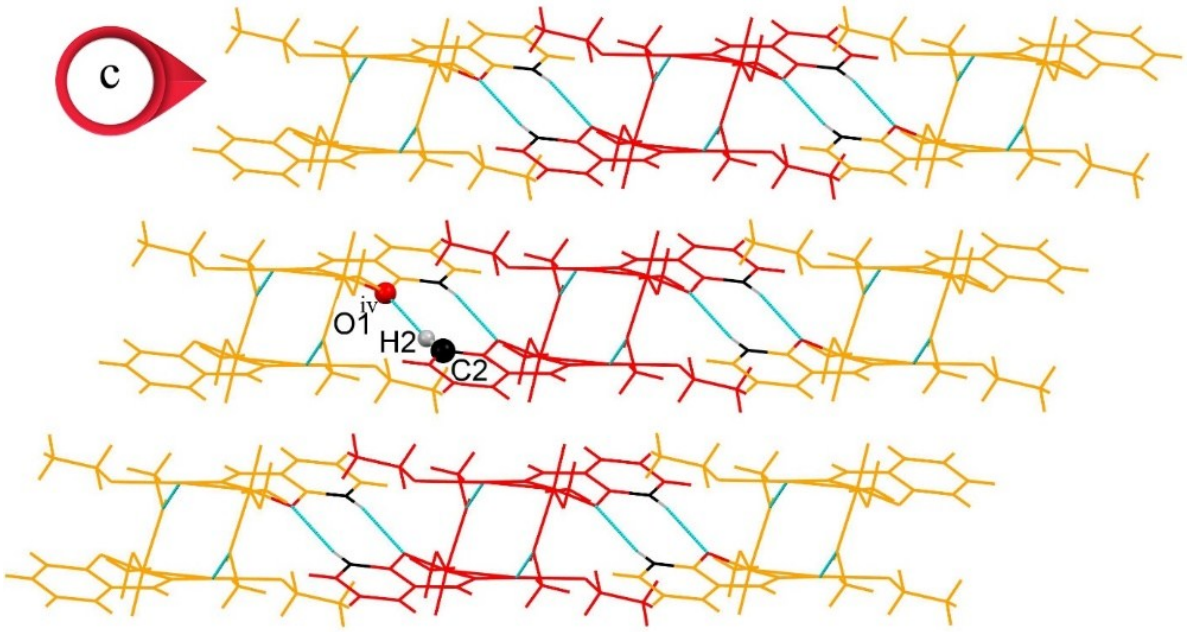

SI 5 i. Expanding of the second dimension along the *ac* plane C2—H2···O1^{iv} (symm. code *iv*: 1 - *x*, 1 - *y*, -*z*) hydrogen bond.

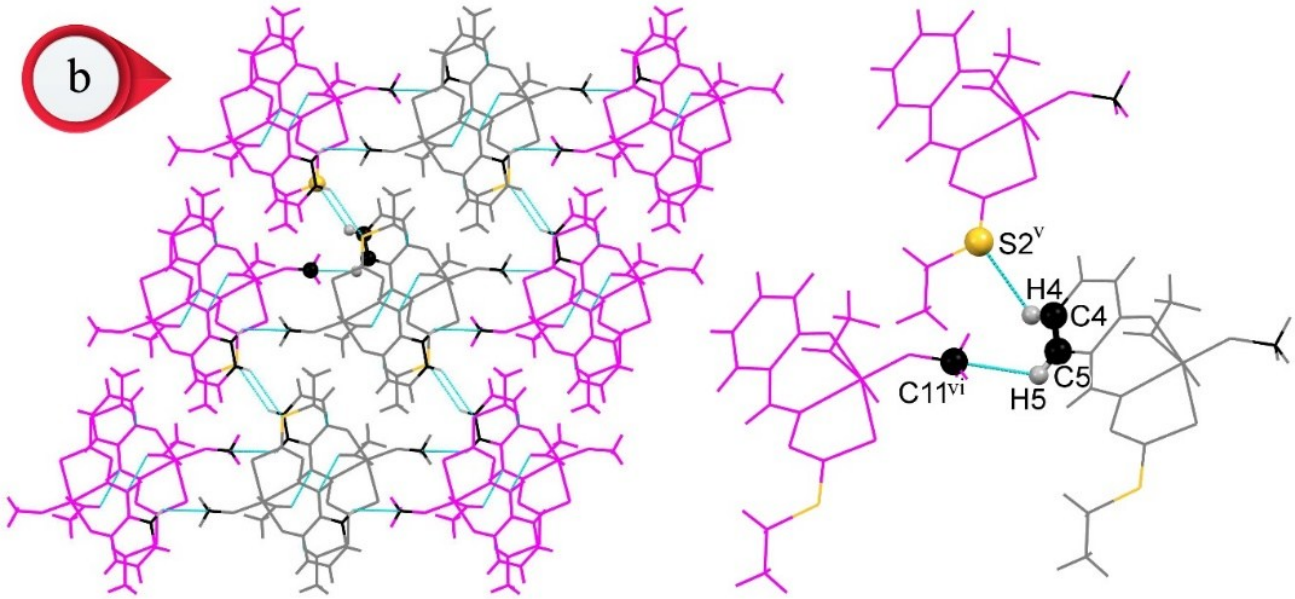

SI 5 j. The third dimension is formed through C4—H4···S^{v} and C5—H5···C11^{vi} (symm. code *v*: *x*, -1 + *y*, -1 + *z*, *vi*: *x*, -1 + *y*, *z*) interactions along the *b* axis.

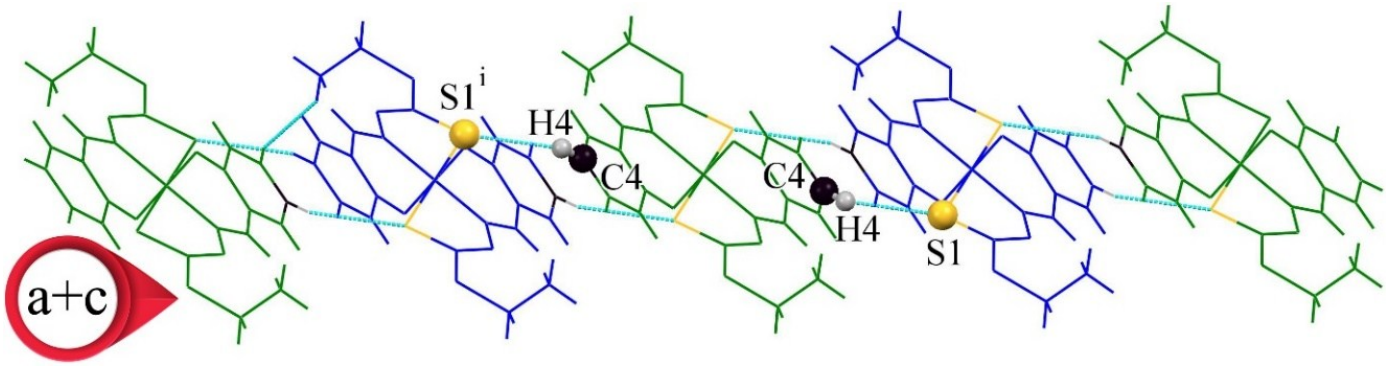

SI 5 k. C4—H4···S1^{i} (2.920 Å for **3** and 2.883 Å for **4**) (symm. code *i*: -1/2 + *x*, 1/2 + *y*, 1/2 + *z*) interaction leads to formation of one-dimensional chain through -*a*+*c* direction.

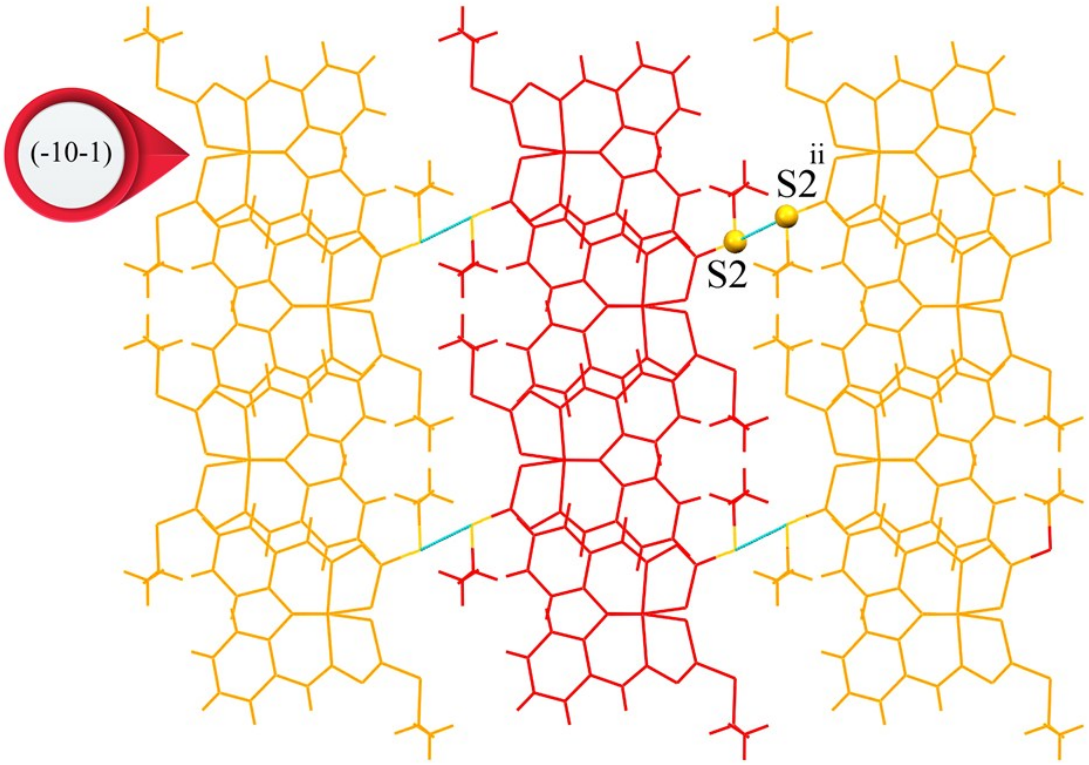

SI 5 l. Formation 2D sheets through chalcogen-chalcogen S2···S2^{ii} (*ii*: -1 + *x*, 1 - *y*, 1/2 + *z*) (3.403 Å) interactions.

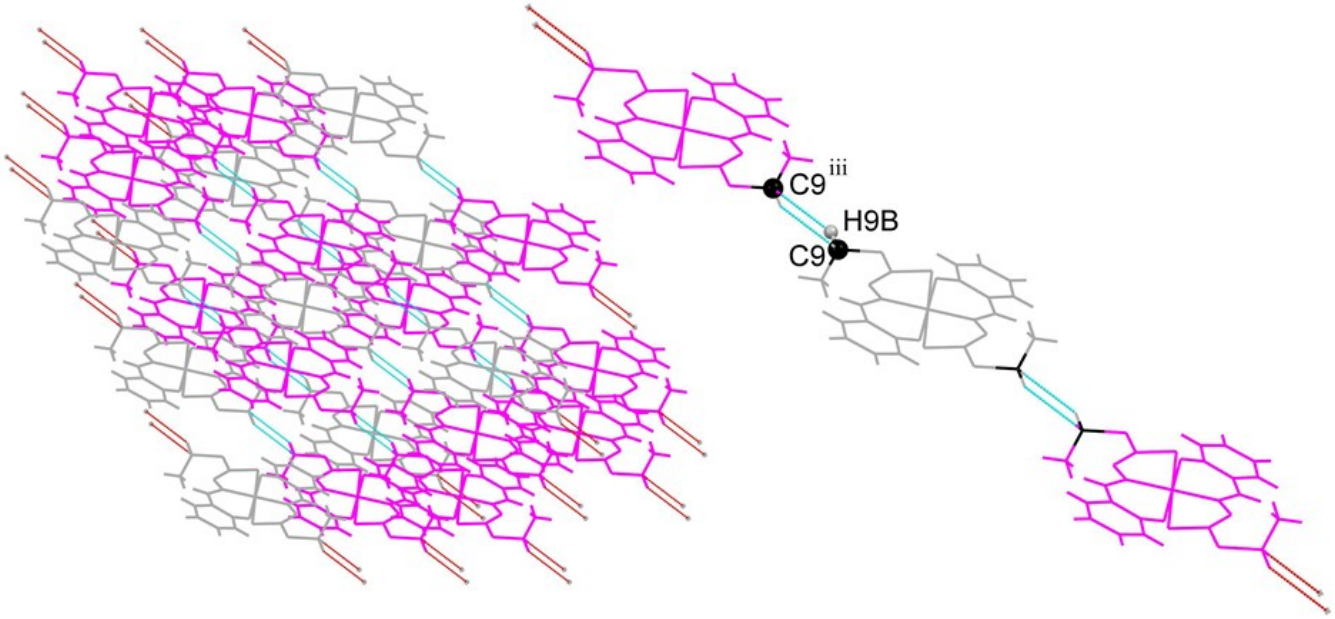

SI 5 m. Expanding the planes by C9—H9B···C9^{iii} (*iii*: -1 + *x*, *y*, -1 + *z*) interaction to construct the 3D supramolecular network.

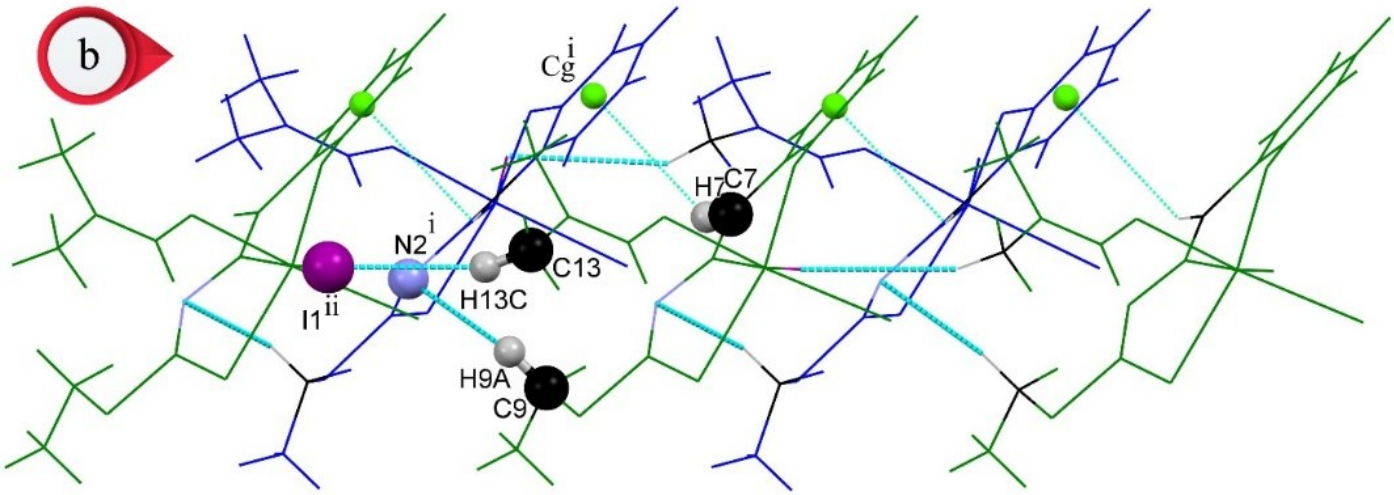

SI 5 n. Expanding the chains through C9—H9A···N2^{i}, C13—H13C···I1^{ii} (3.047 Å) and C7—H7···$C_g{}^{i}$ (symm. code *i*: 1.5 - *x*, -1/2 + *y*, 1- *z*, *ii*: *x*, -1 + *y*, *z*) interactions.

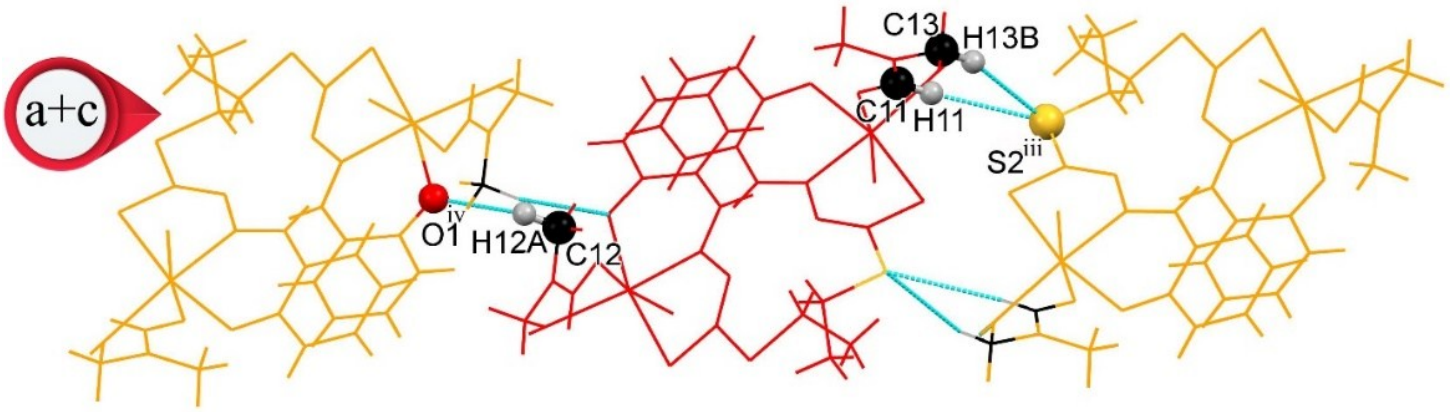

SI 5 o. Formation the second dimension along the $-a + c$ axis through the hydrogen bonding of C13—H13B···S2^{iii} (2.985 Å), C12—H12A···O1^{vi} (2.451 Å) and C11—H11···S2^{iii} (2.975 Å) (symm. code *iii*: 1 - *x*, -*y*, 1 - *z*, *vi*: 1/2 + *x*, -1 + *y*, 1/2 - *z*).

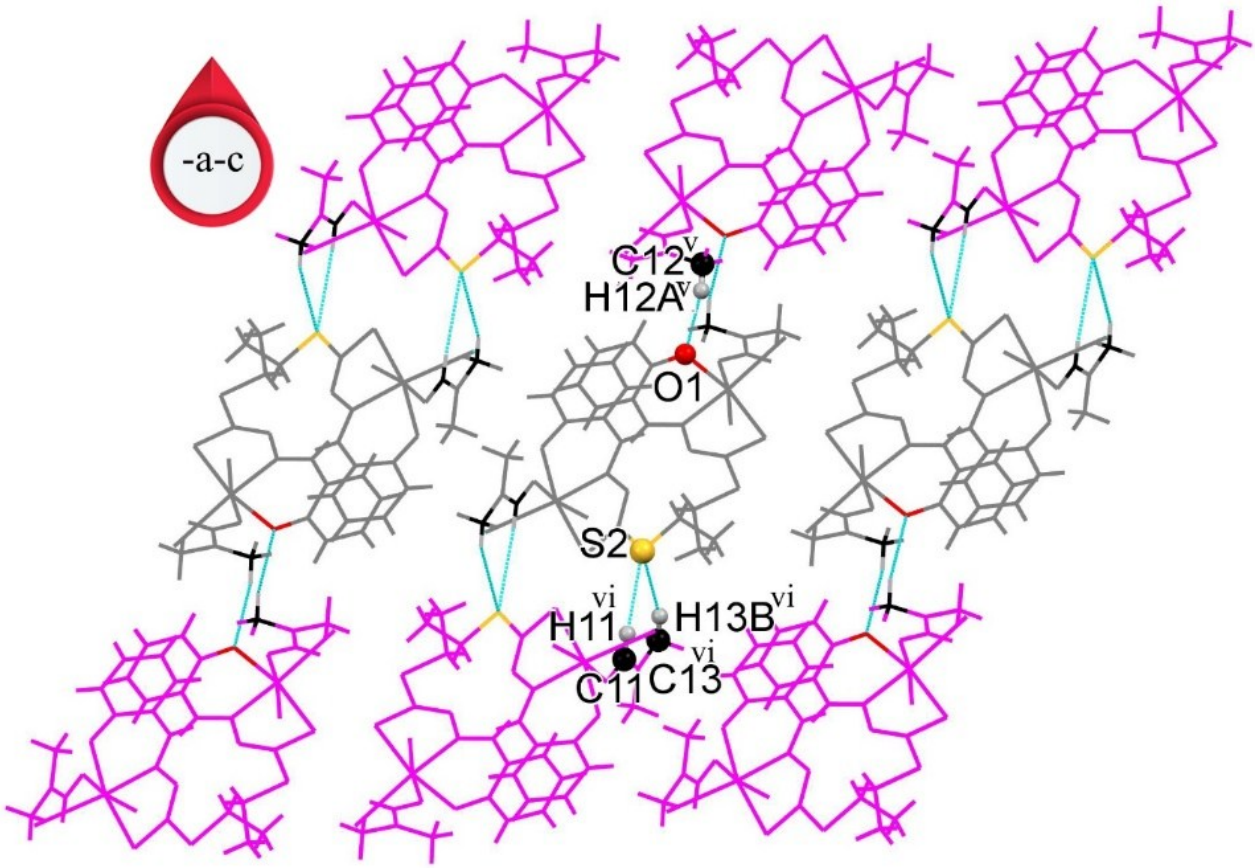

SI 5 p. The third dimension occurs along the *–a - c* axis through C12^{v}—H12A^{v}···O1, C11^{vi}—H11^{vi}···S2^{vi} and C13^{vi}—H13B^{vi}···S2^{vi} (symm. code *v*: 1 - *x*, -1.5 + *y*, 1/2 + *z*, *vi*: 1/2 + *x*, 1/2 - *y*, 1 - *z*) hydrogen bonds.

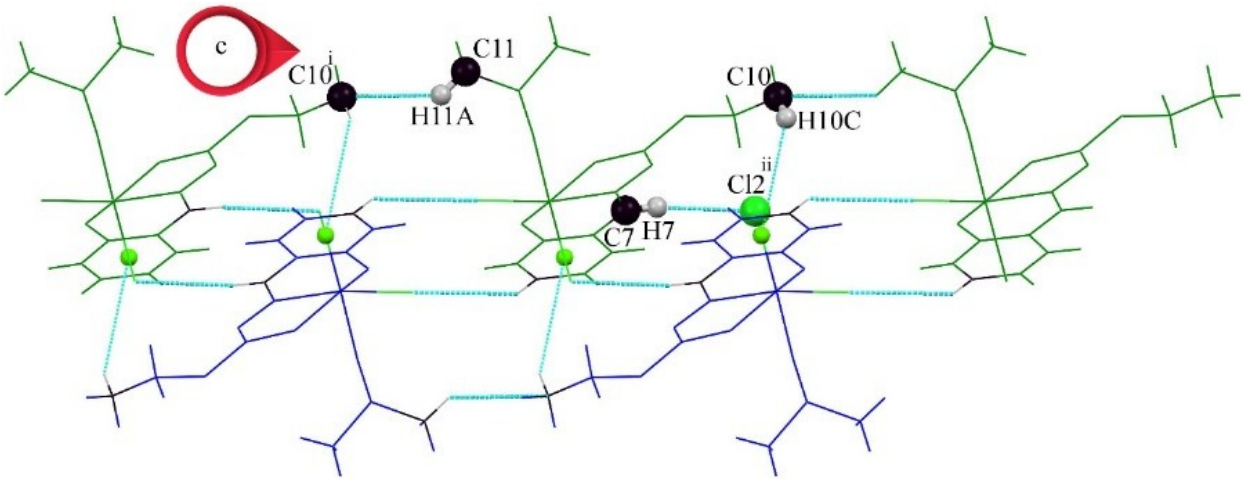

SI 5 q. Formation chains along the *c* axis according to the C11—H11A···C10^{i} (2.899 Å), C7—H7···Cl2^{ii} (2.819 Å), C10—H10C···Cl2^{ii} (3.397 Å) and H12B—C12···Cl2 (2.868 Å) interactions (symm. code *i*: *x*, *y*, -1+*z*, *ii*: 2 - *x*, 1 - *y*, 1 - *z*).

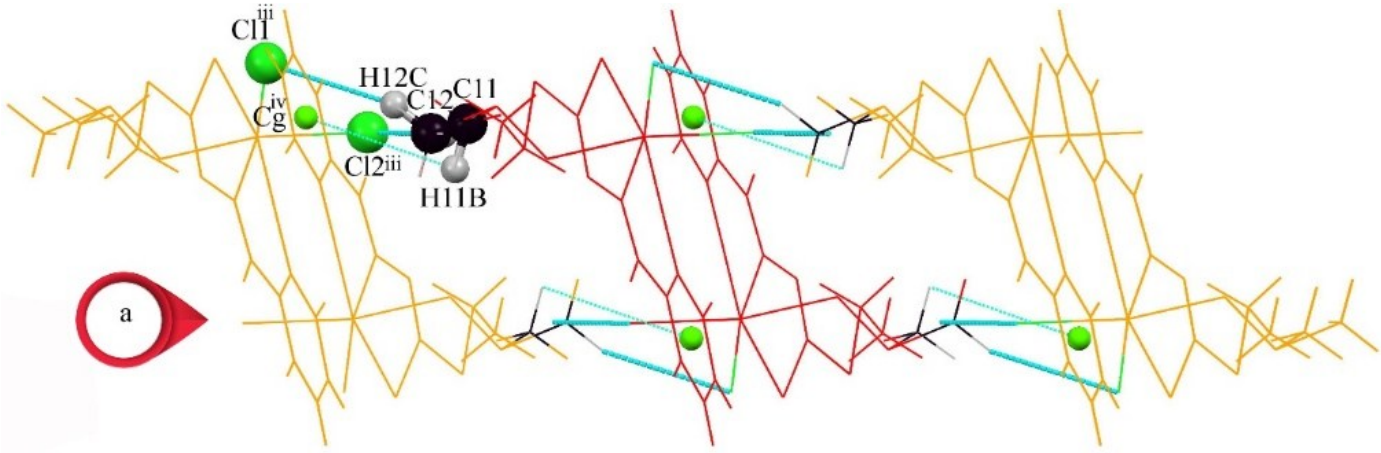

SI 5 r. formation the second dimension through the *a* axis *via* hydrogen bonds of C11—H11A···Cl2^{iii}, C12—H12C···Cl1^{iii} and C11—H11B···Cg^{iv} (symm. code *iii*: -1 - *x*, *y*, *z*, *iv*: 1 - *x*, 1 - *y*, -*z*).

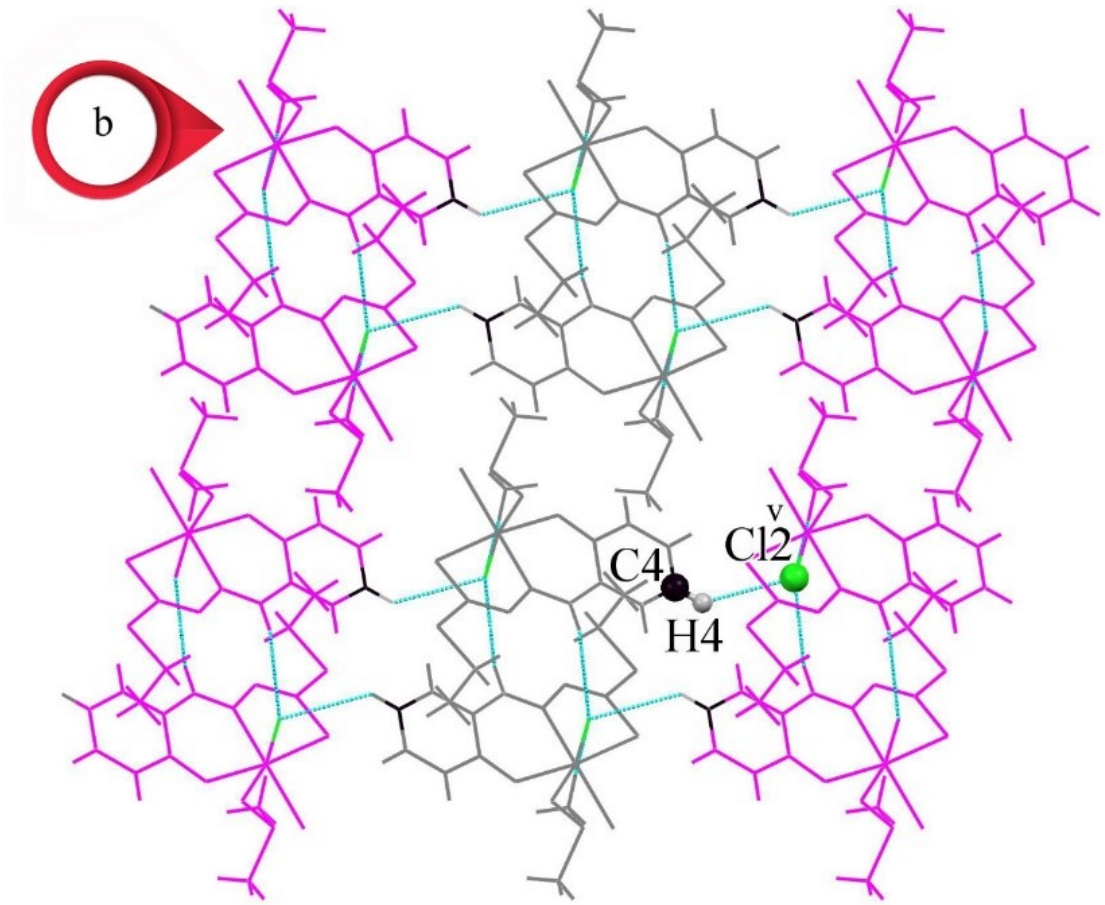

SI 5 s. Expanding of the third dimension along *b* axis via C4—H4C···Cl2^{v} (symm. code *v*: *x*, 1 + *y*, *z*) interaction.

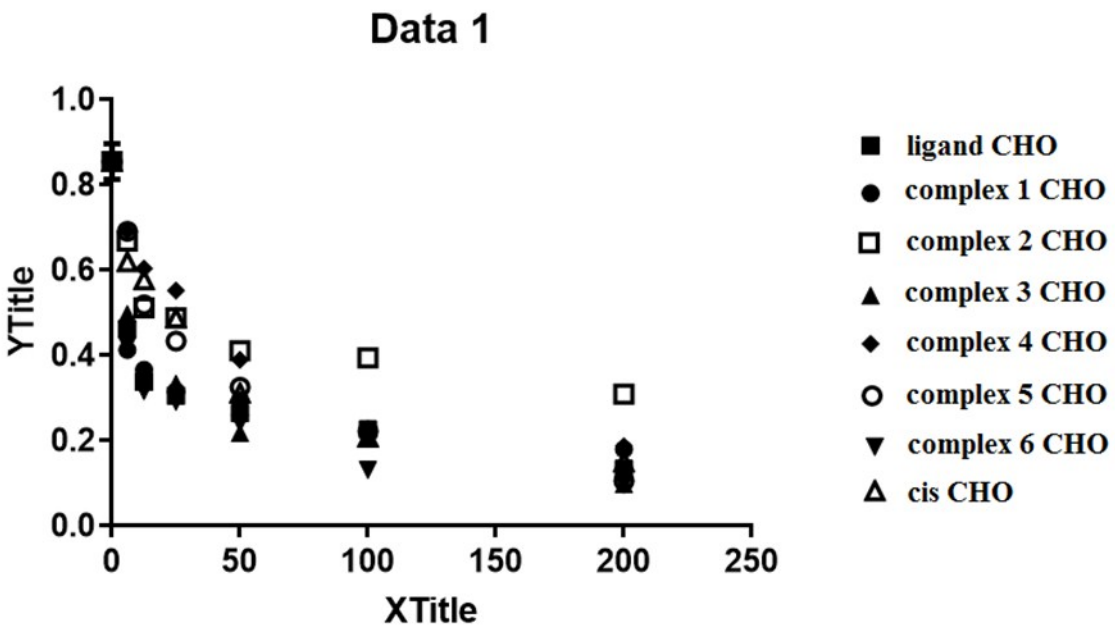

SI 6 a. Graph of cytotoxicity test against normal cell of CHO.

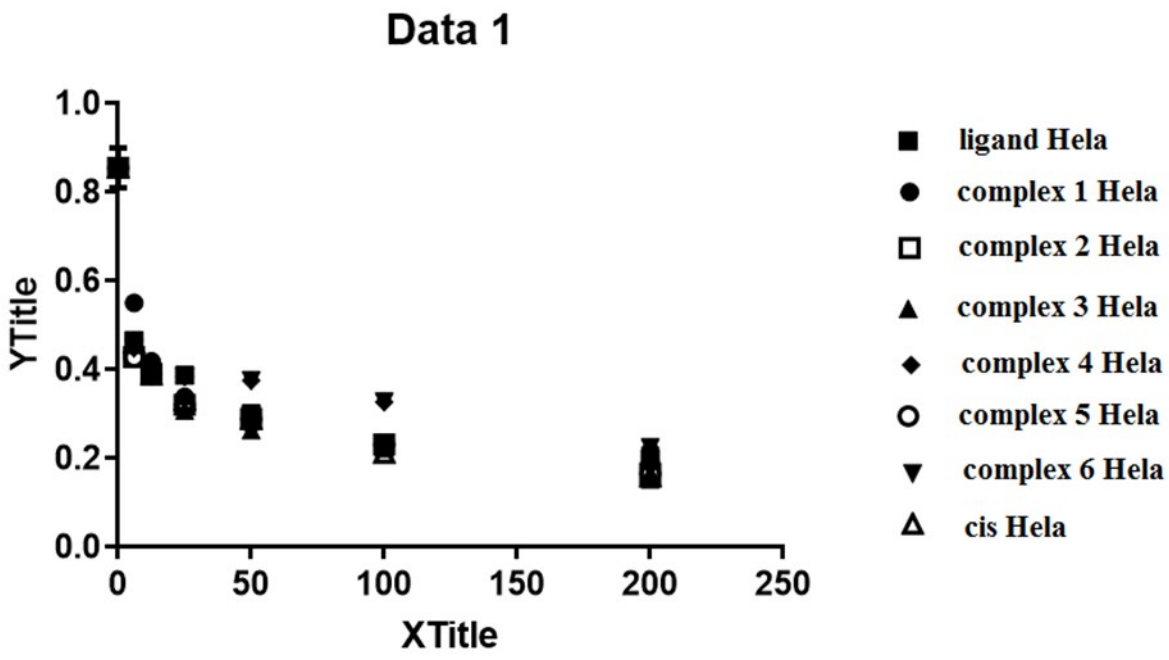

SI 6 b. Graph of cytotoxicity test against cancer cell of Hela.

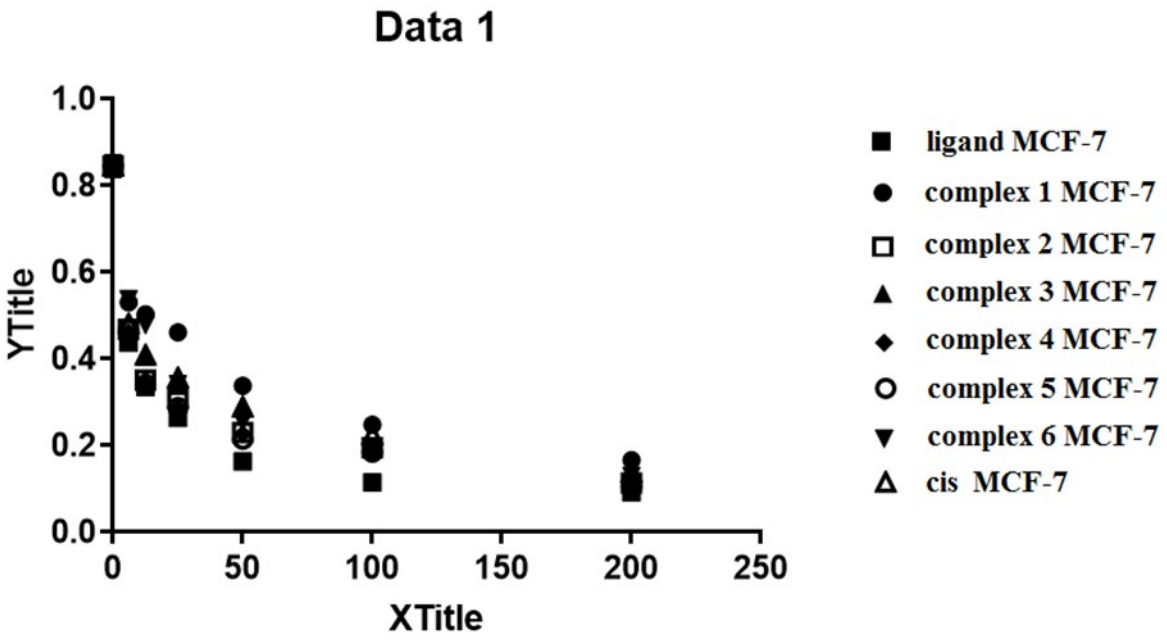

SI 6 c. Graph of cytotoxicity test against cancer cell of MCF-7.

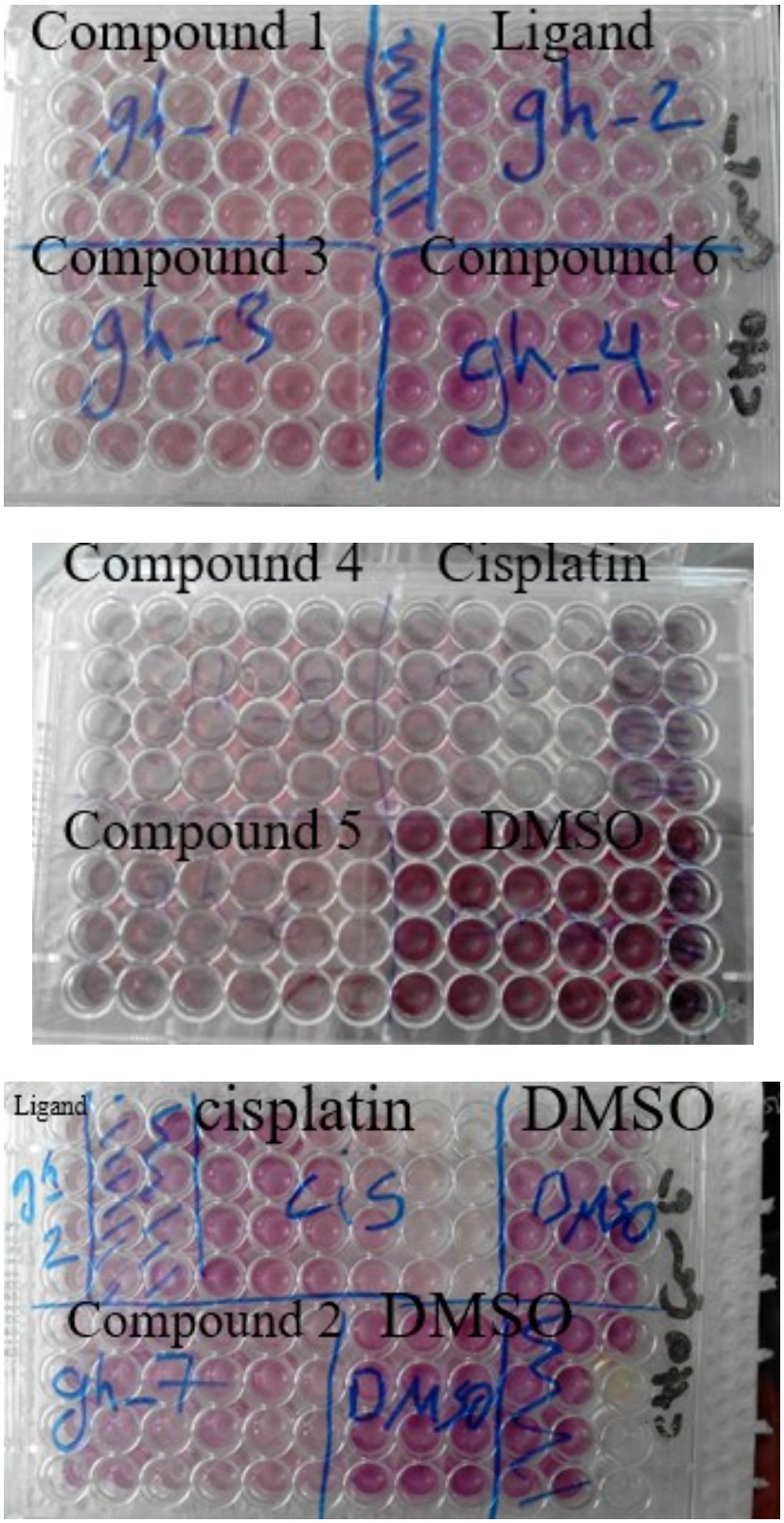

SI 6 d. The pictures of the color change of compounds during the MTT experiment against normal cell of CHO.

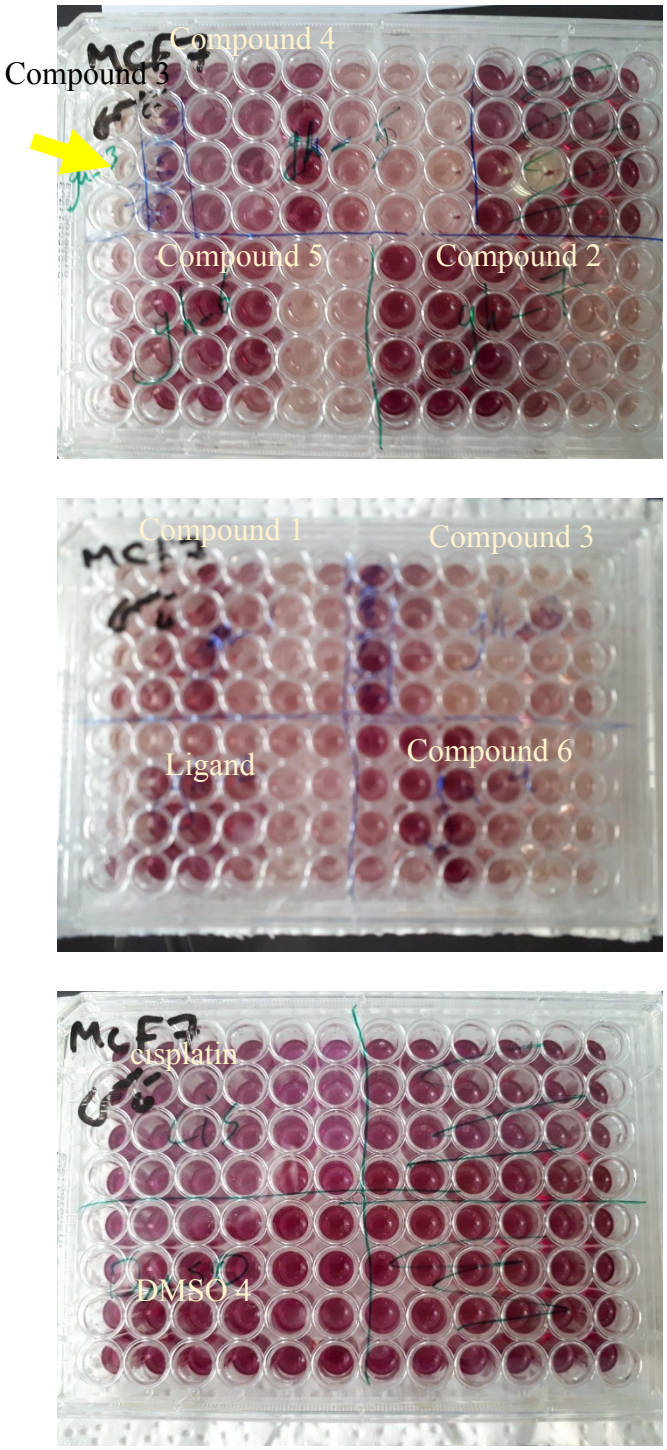

SI 6 e. The pictures of the color change of compounds during the MTT experiment against cancer cell of MCF-7.

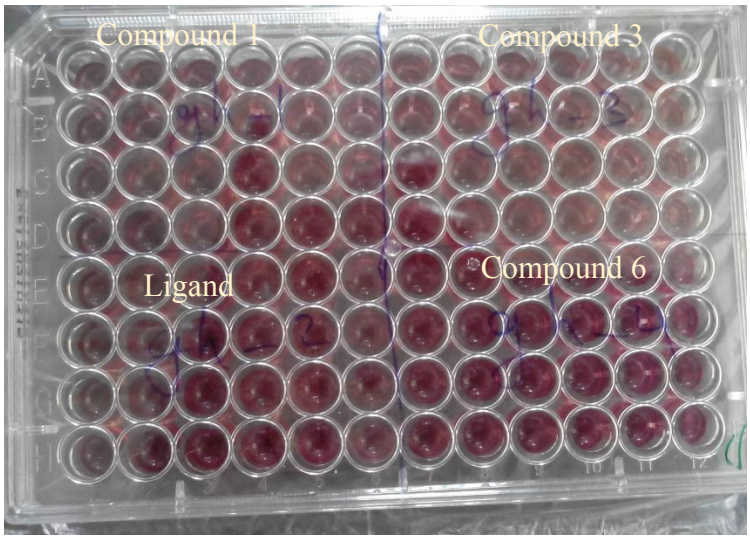
Compound 1
Compound 3
Ligand
Compound 6

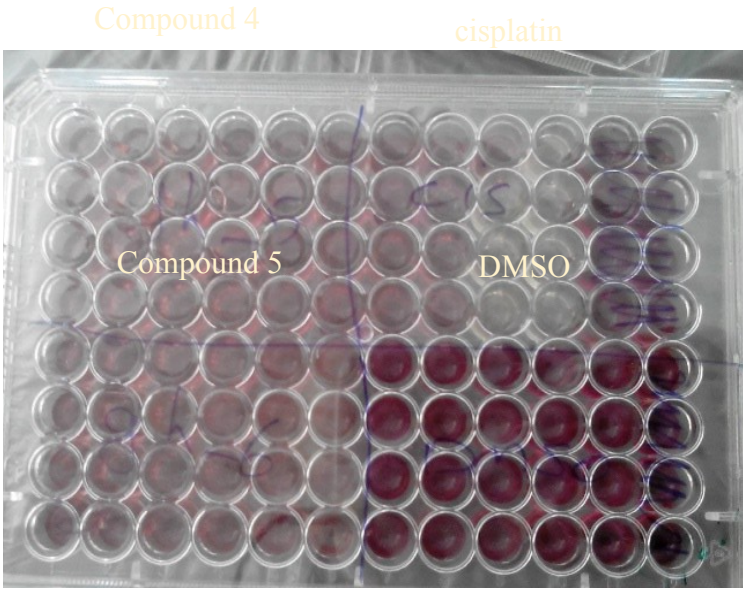
Compound 4
cisplatin
Compound 5
DMSO

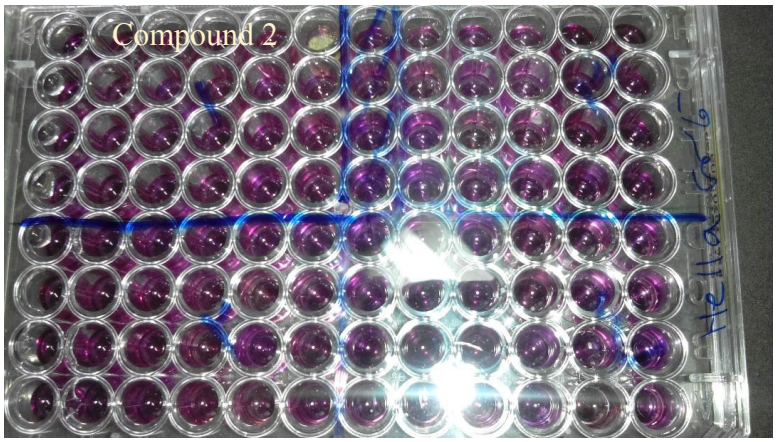

SI 6 f. The pictures of the color change of compounds during the MTT experiment against cancer cell of Hela.

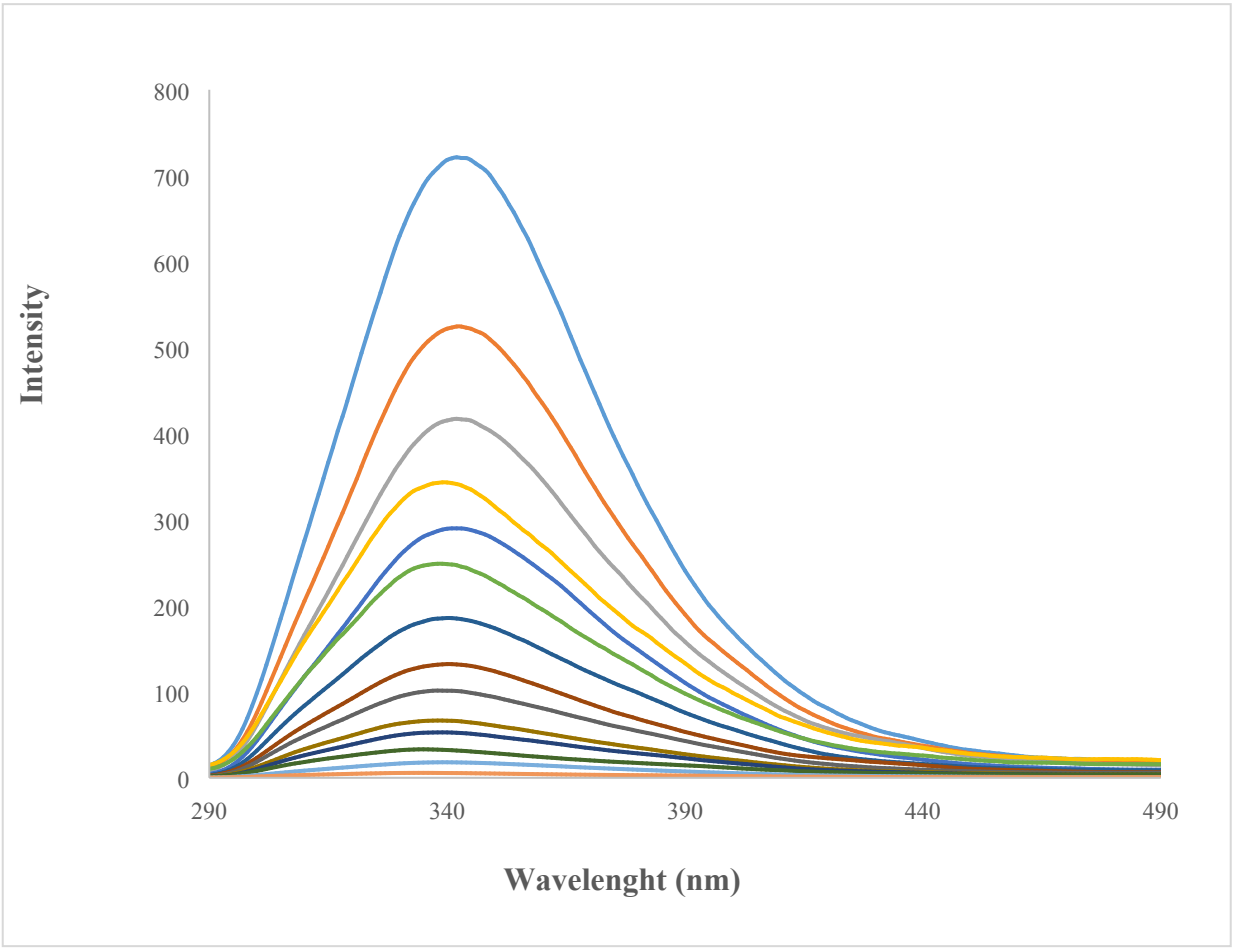

SI 7 a. Fluorescence quenching spectra of HSA in the presence of increasing concentration of **1**. [HSA] = 15 μM, [**1**] = 0-14 μM, λ_{ex} = 280 nm, T = 298 K.

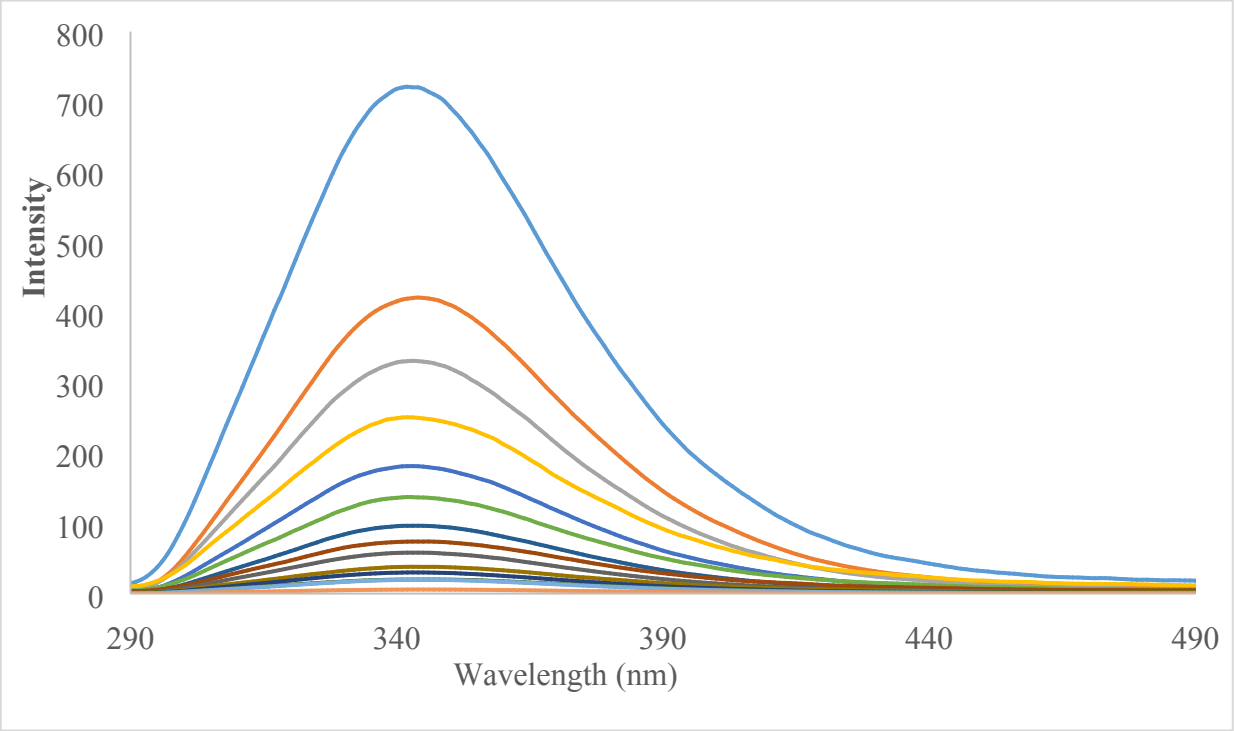

SI 7 b. Fluorescence quenching spectra of HSA in the presence of increasing concentration of **2**. [HSA] = 15 μM, [**2**] = 0-14 μM, λ_{ex} = 280 nm, T = 298 K.

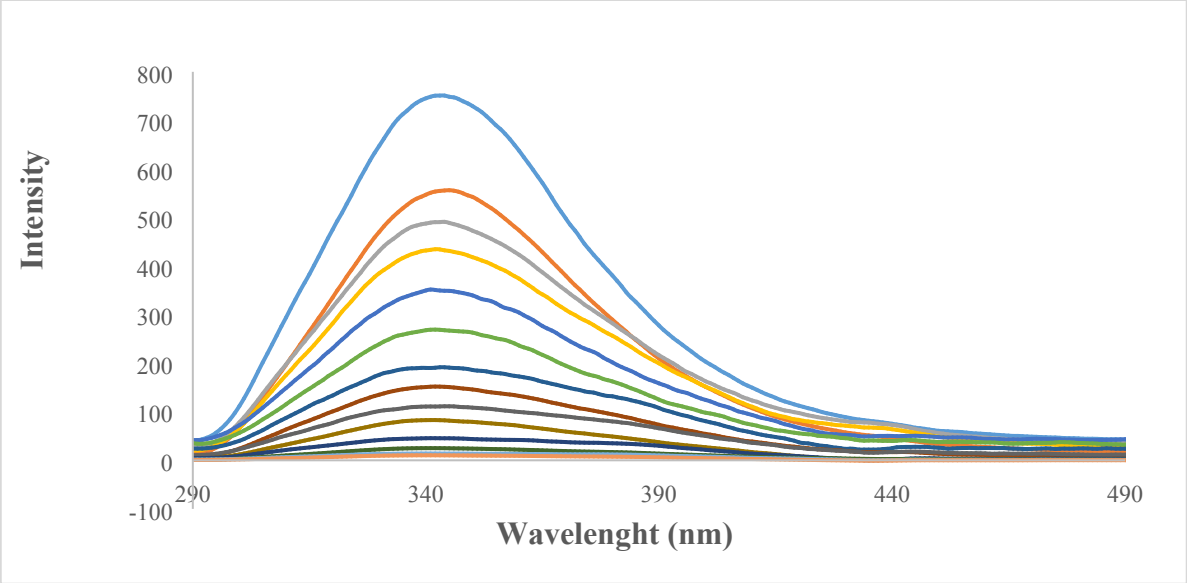

SI 7 c. Fluorescence quenching spectra of HSA in the presence of increasing concentration of **3**. [HSA] = 15 μM, [**3**] = 0-14 μM, λ_{ex} = 280 nm, T = 298 K.

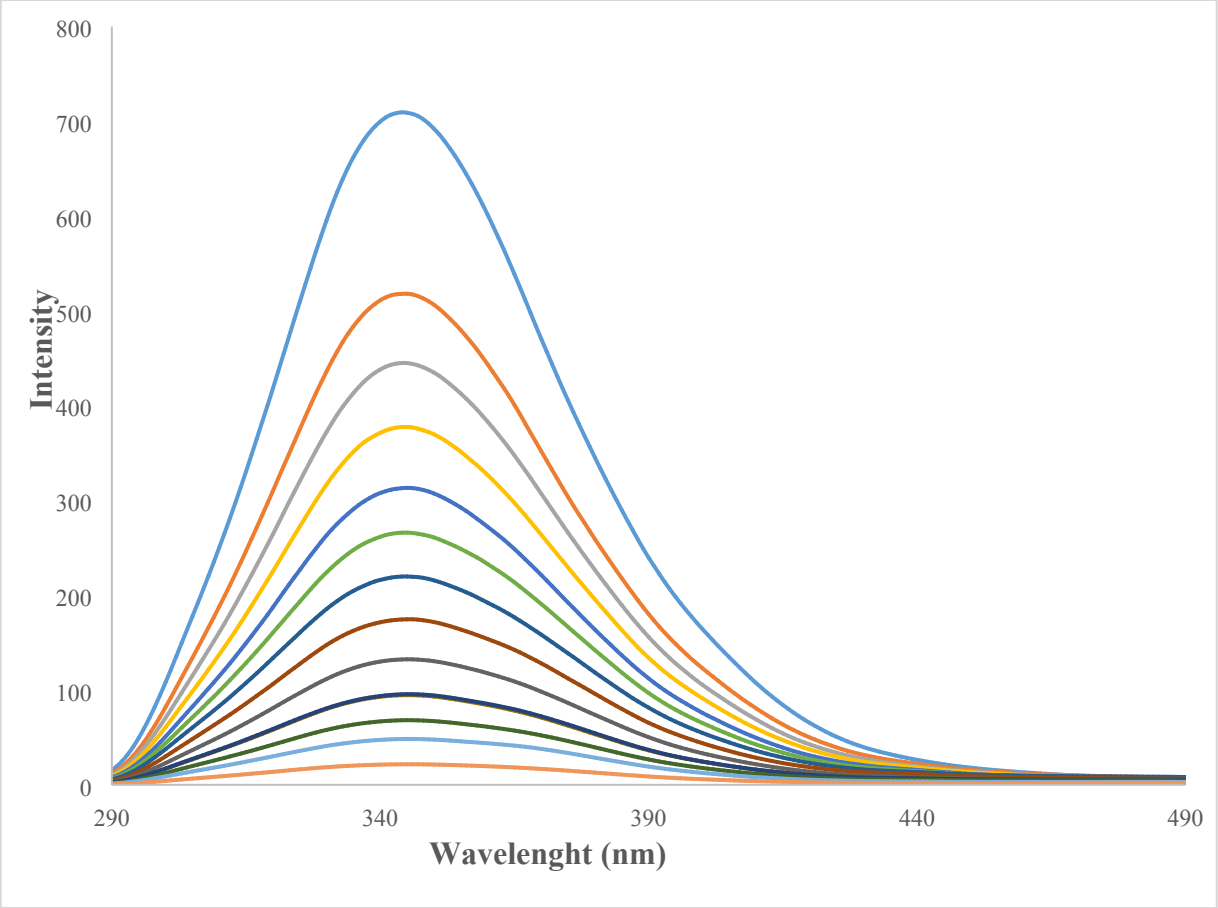

SI 7 d. Fluorescence quenching spectra of HSA in the presence of increasing concentration of **4**. [HSA] = 15 μM, [**4**] = 0-14 μM, λ_{ex} = 280 nm, T = 298 K.

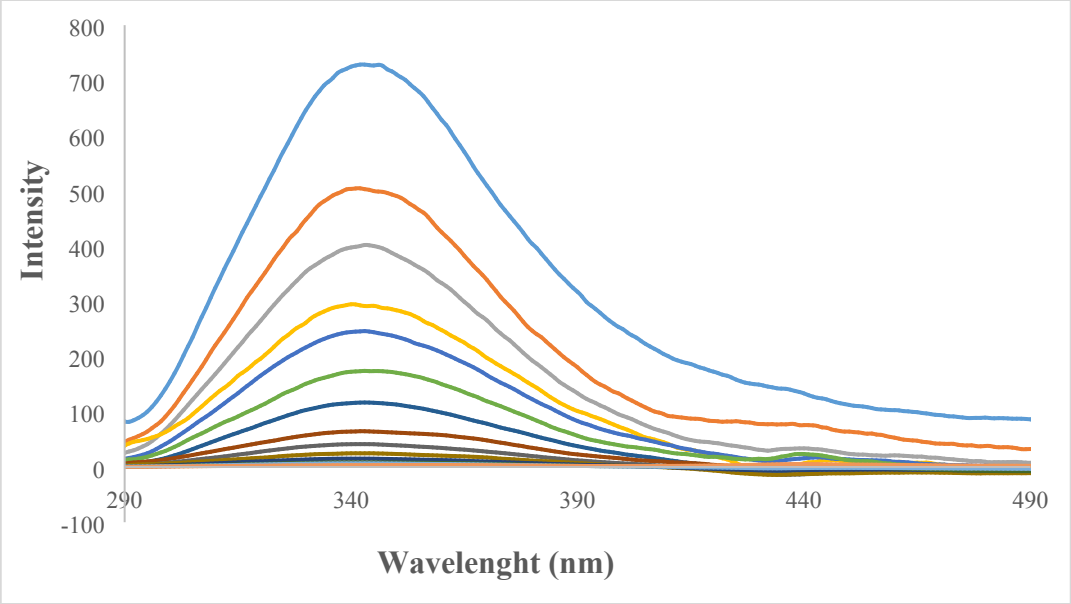

SI 7 e. Fluorescence quenching spectra of HSA in the presence of increasing concentration of **5**. [HSA] = 15 μM, [**5**] = 0-14 μM, λ_{ex} = 280 nm, T = 298 K.

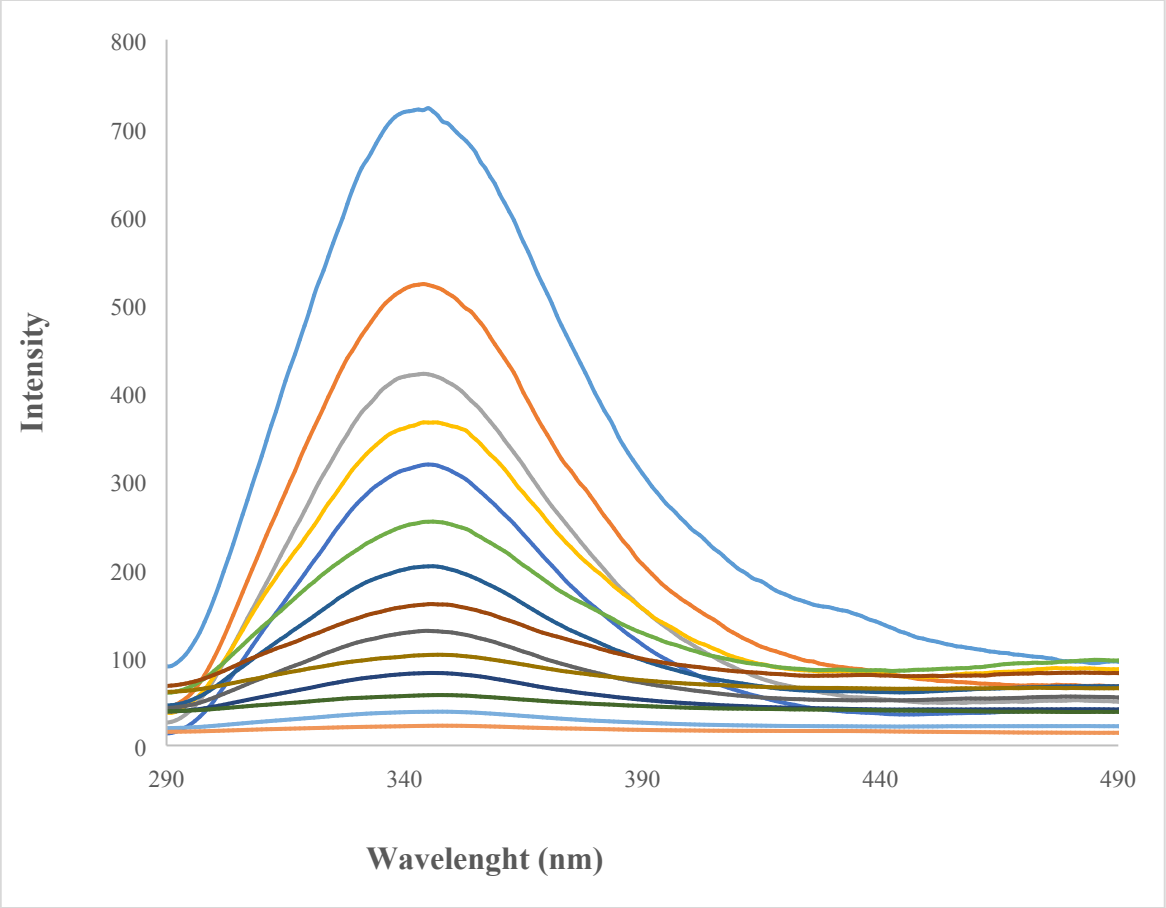

SI 7 f. Fluorescence quenching spectra of HSA in the presence of increasing concentration of **6**. [HSA] = 15 μM, [**6**] = 0-14 μM, λ_{ex} = 280 nm, T = 298 K.

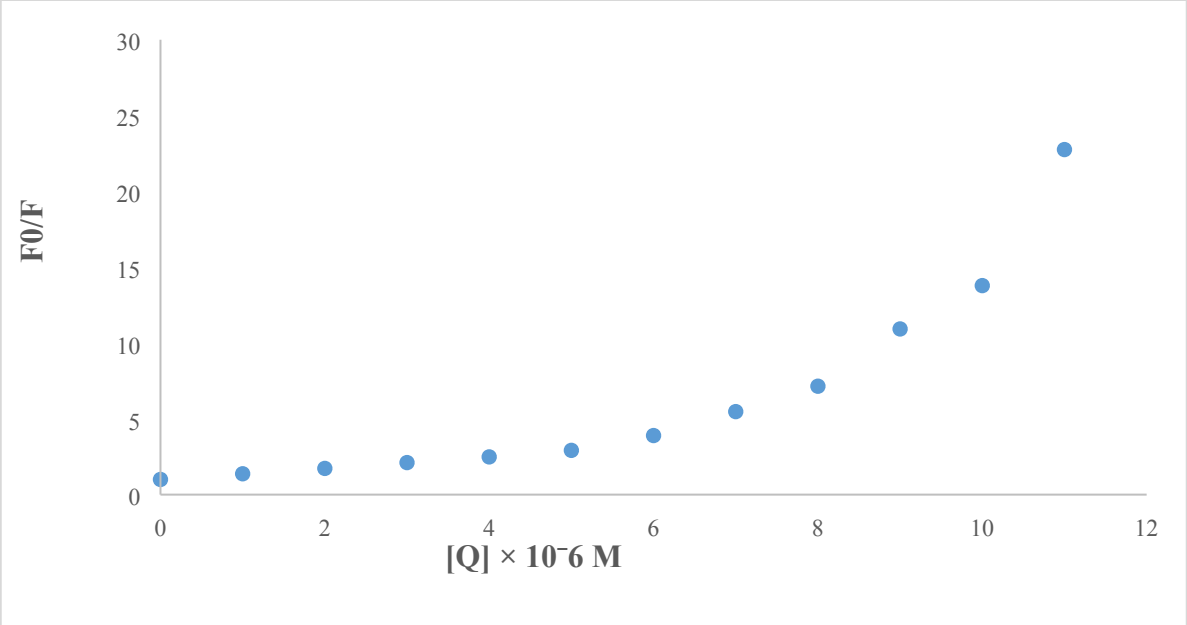

SI 7 g. Stern-Volmer plot for quenching of HSA (15 μM) fluorescence by **1** at different concentrations (λ_{ex} = 280 nm, λ_{em} = 342 nm).

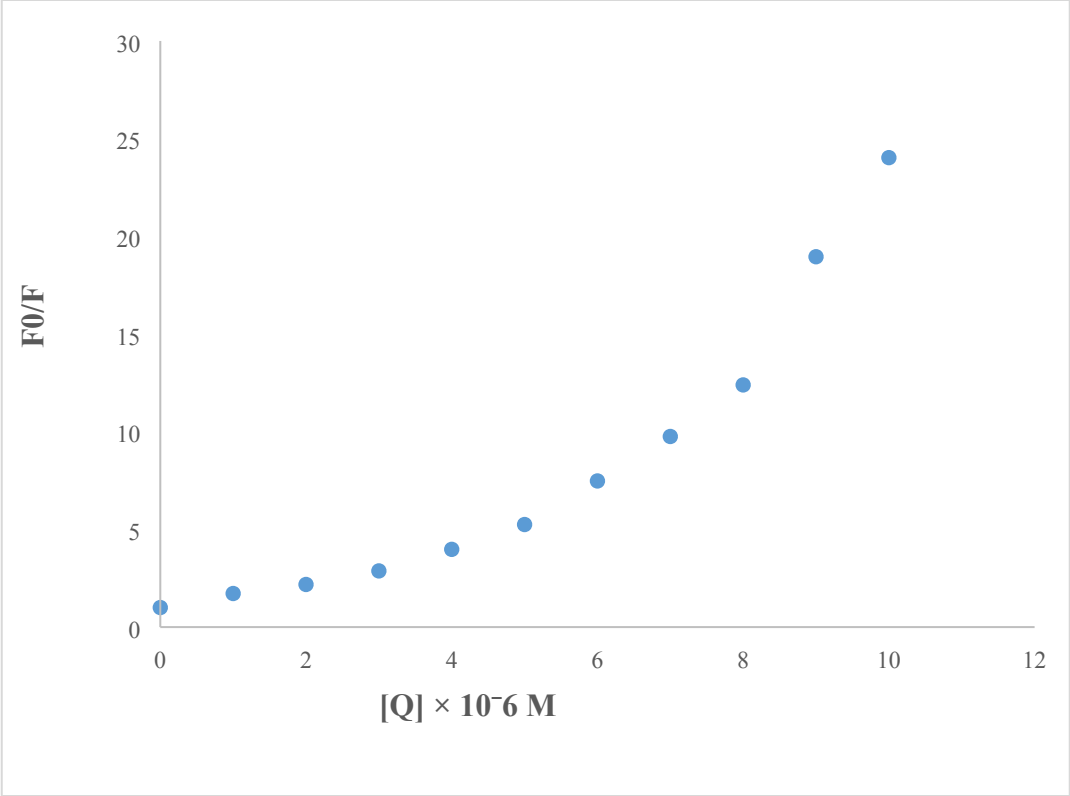

SI 7 h. Stern-Volmer plot for quenching of HSA (15 μM) fluorescence by **2** at different concentrations (λ_{ex} = 280 nm, λ_{em} = 342 nm).

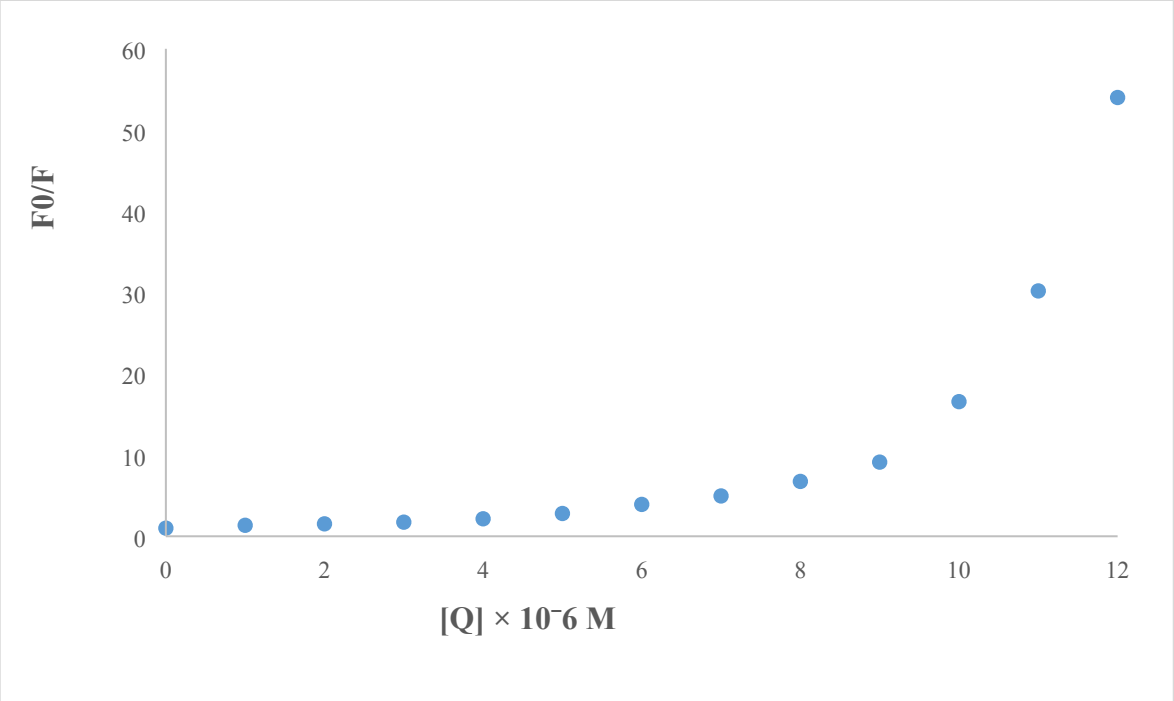

SI 7 i. Stern-Volmer plot for quenching of HSA (15 μM) fluorescence by **3** at different concentrations (λ_{ex} = 280 nm, λ_{em} = 344 nm).

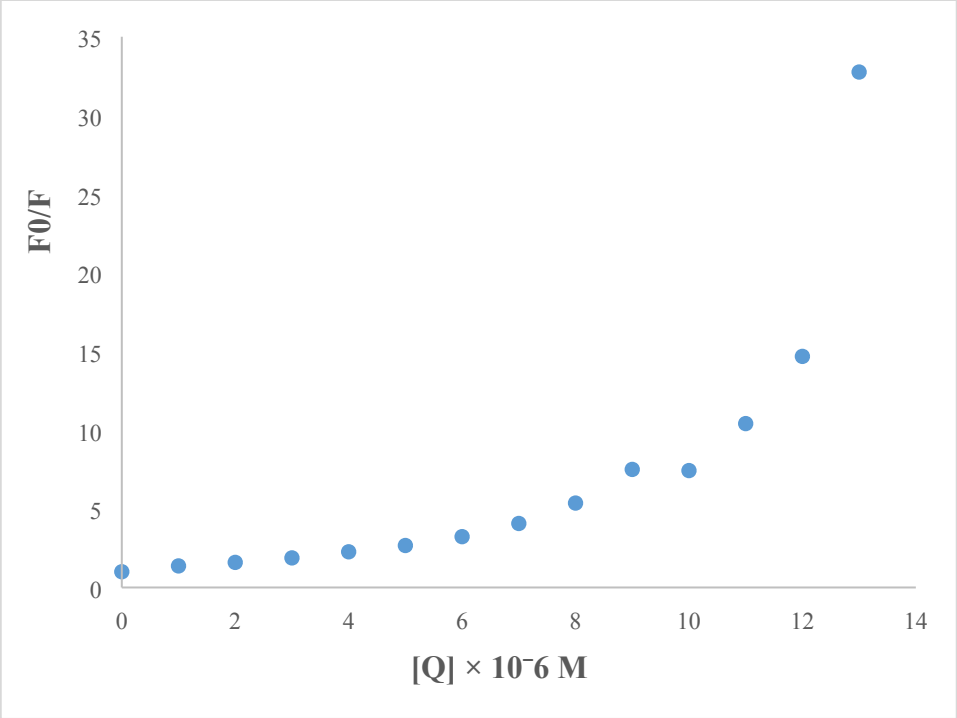

SI 7 j. Stern-Volmer plot for quenching of HSA (15 μM) fluorescence by **4** at different concentrations (λ_{ex} = 280 nm, λ_{em} = 344 nm).

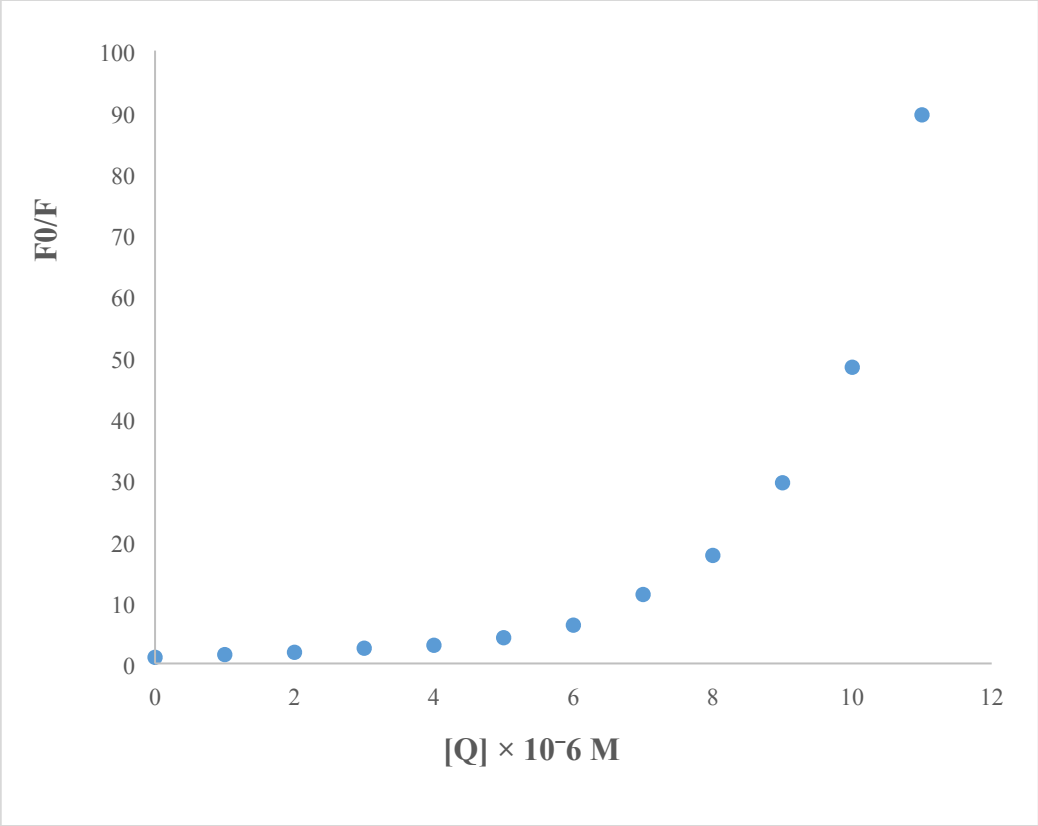

SI 7 k. Stern-Volmer plot for quenching of HSA (15 μM) fluorescence by **5** at different concentrations (λ_{ex} = 280 nm, λ_{em} = 342 nm).

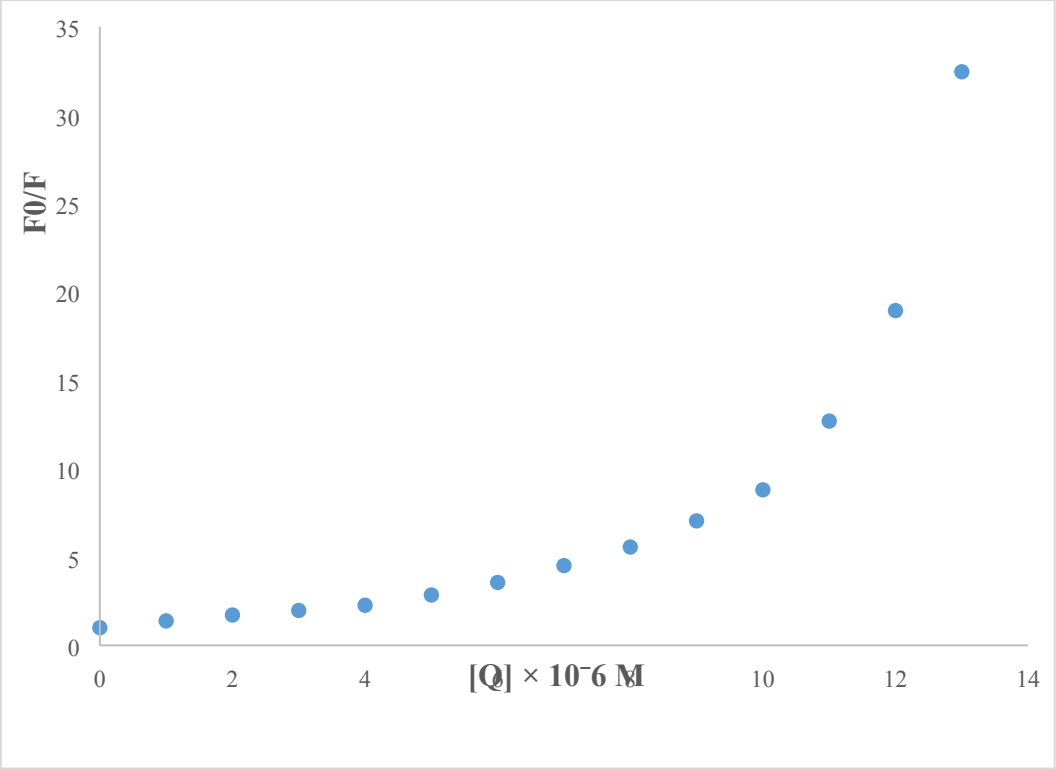

SI 7 l. Stern-Volmer plot for quenching of HSA (15 μM) fluorescence by **6** at different concentrations (λ_{ex} = 280 nm, λ_{em} = 345 nm).

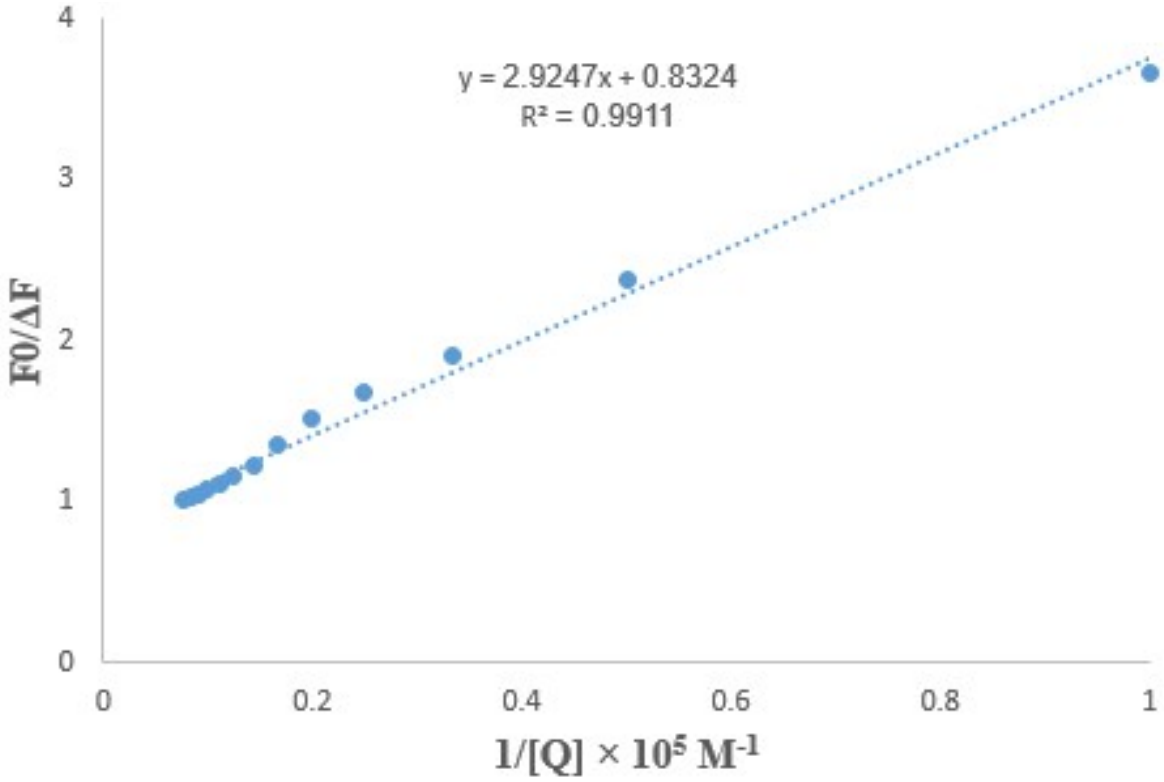

SI 7 m. Plot of $\frac{F_0}{F_0 - F}$ *vs* 1/[L^{2-}] for HSA in the presence of increasing concentrations of **1** at T = 298 K (λ_{ex} = 280 nm, λ_{em} = 342 nm).

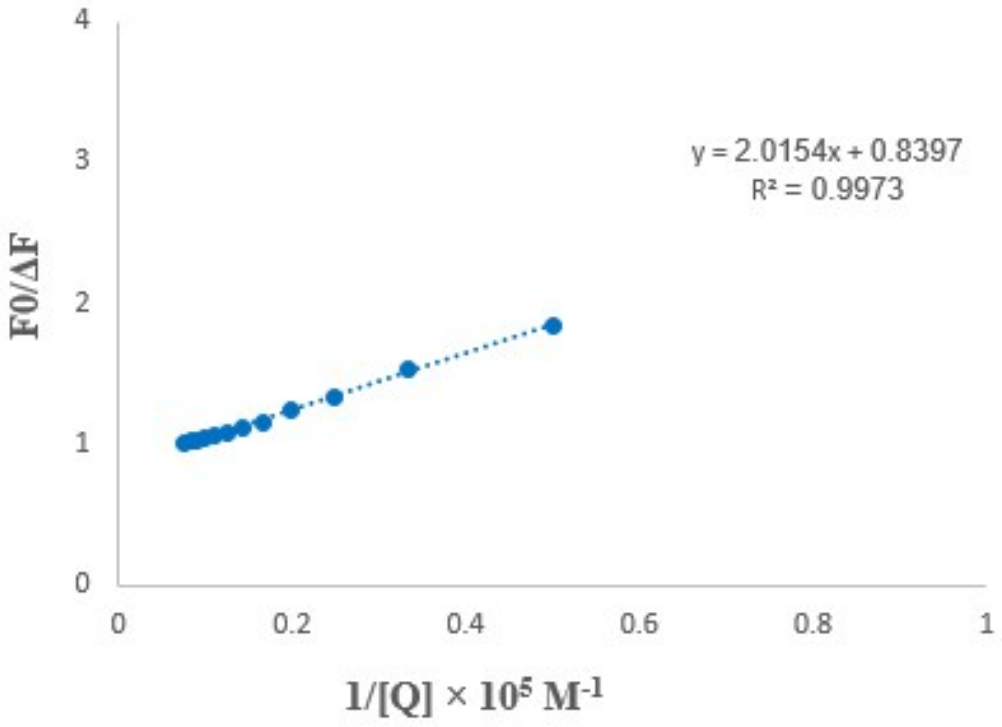

SI 7 n. Plot of $\frac{F_0}{F_0 - F}$ *vs* 1/[L^{2-}] for HSA in the presence of increasing concentrations of **2** at T = 298 K (λ_{ex} = 280 nm, λ_{em} = 342 nm).

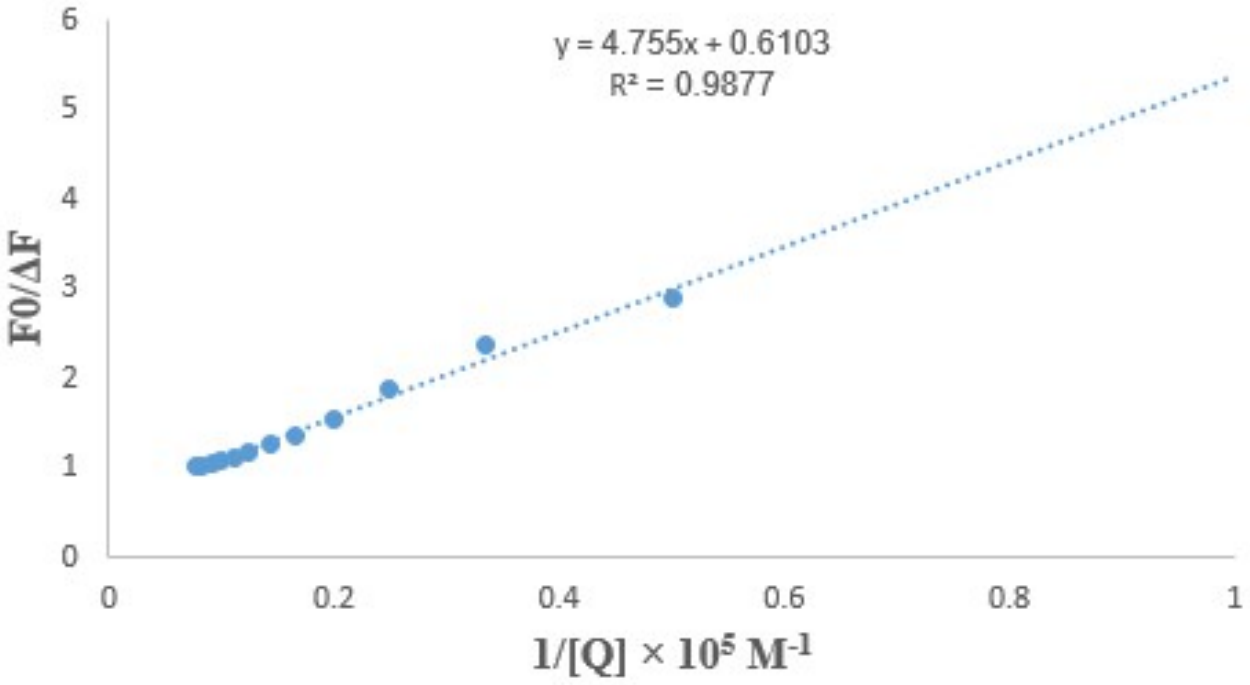

SI 7 o. Plot of $\frac{F_0}{F_0 - F}$ *vs* 1/[L^{2-}] for HSA in the presence of increasing concentrations of **3** at T = 298 K (λ_{ex} = 280 nm, λ_{em} = 344 nm).

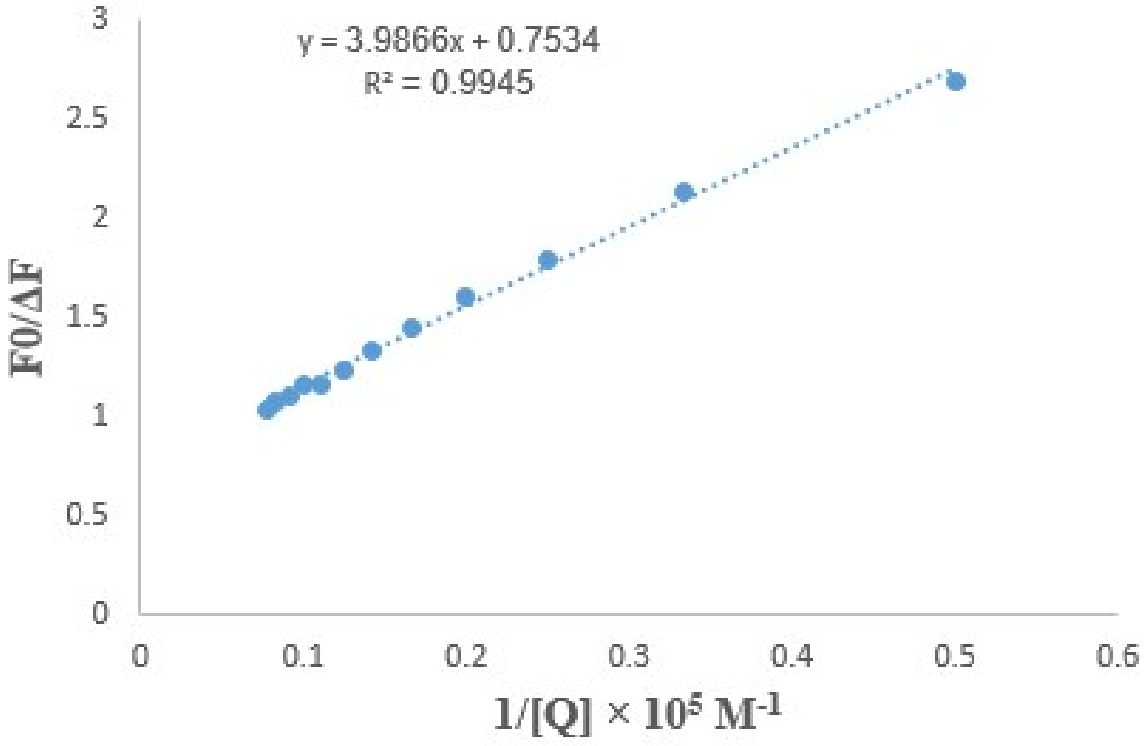

SI 7 p. Plot of $\frac{F_0}{F_0 - F}$ *vs* 1/[L^{2-}] for HSA in the presence of increasing concentrations of **4** at T = 298 K (λ_{ex} = 280 nm, λ_{em} = 344 nm).

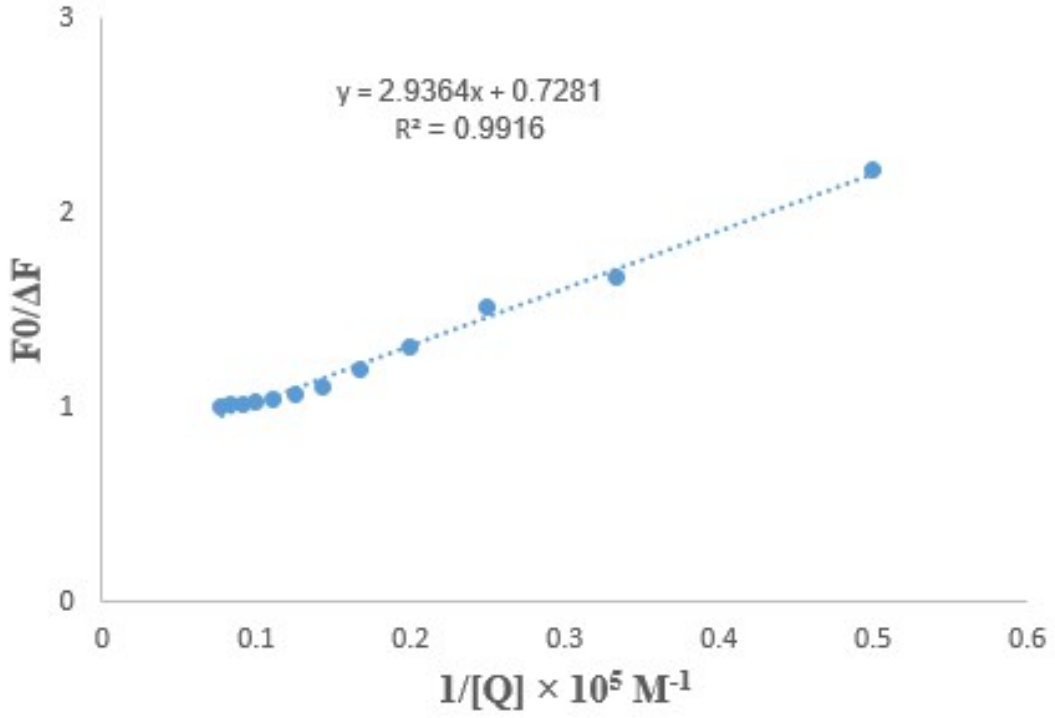

SI 7 q. Plot of $\frac{F_0}{F_0 - F}$ *vs* 1/[L^{2-}] for HSA in the presence of increasing concentrations of **5** at T = 298 K (λ_{ex} = 280 nm, λ_{em} = 342 nm).

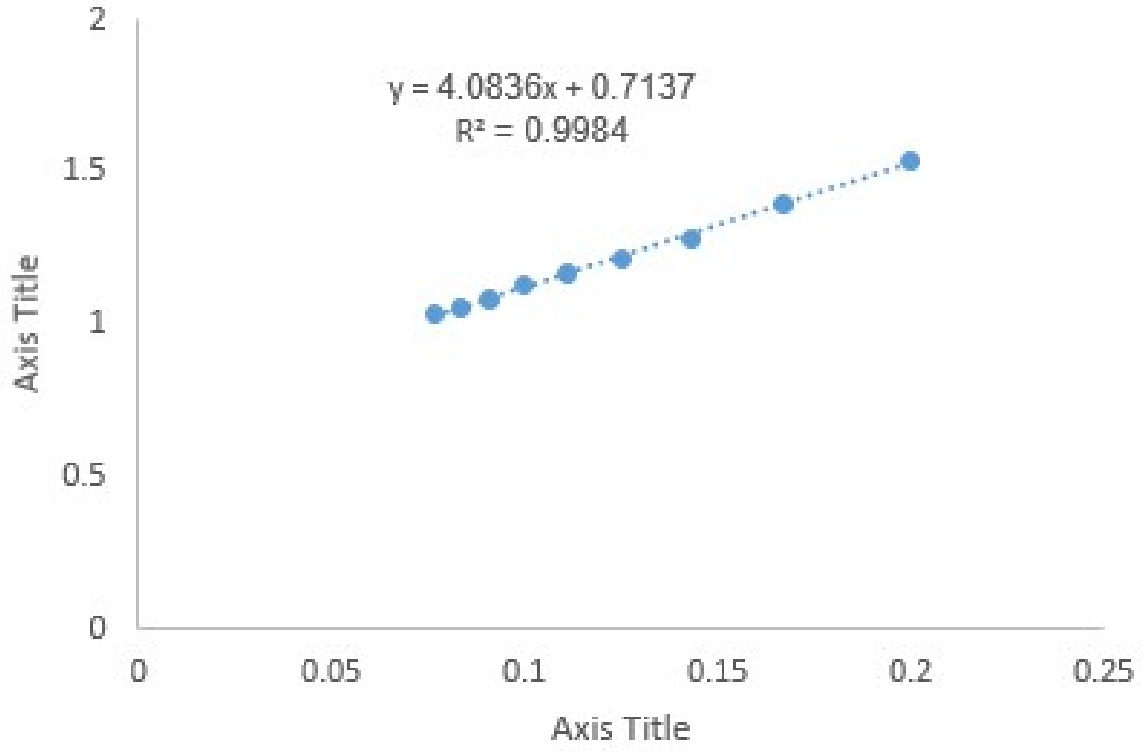

SI 7 r. Plot of $\frac{F_0}{F_0 - F}$ *vs* 1/[L^{2-}] for HSA in the presence of increasing concentrations of **6** at T = 298 K (λ_{ex} = 280 nm, λ_{em} = 345 nm).

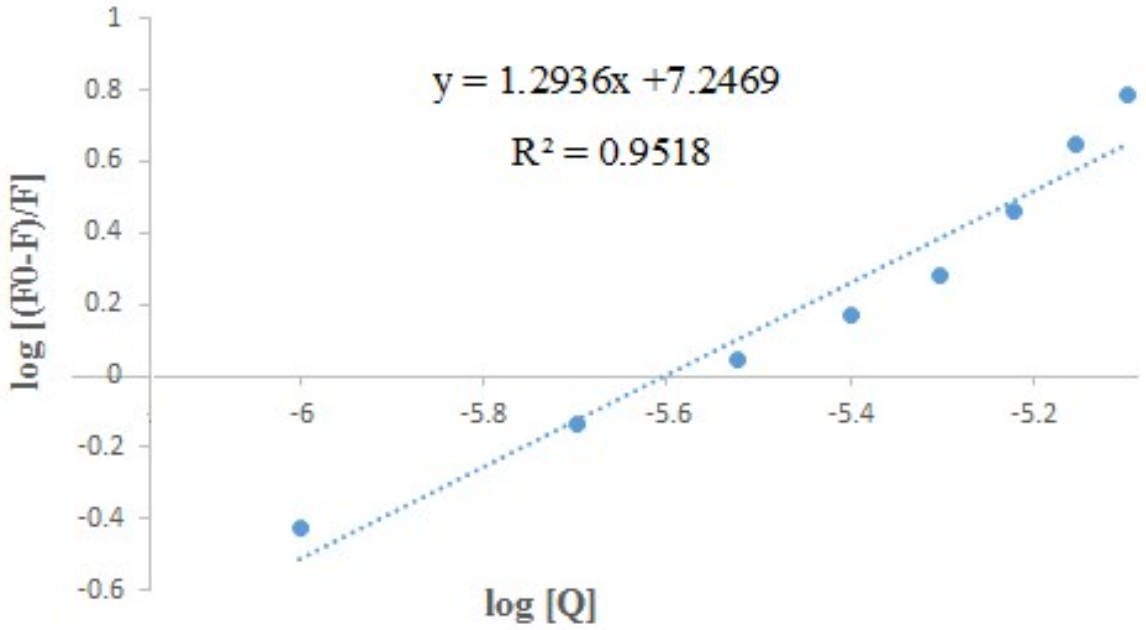

SI 7 s. Double-log plots for the fluorescence quenching of the HSA by **1**.

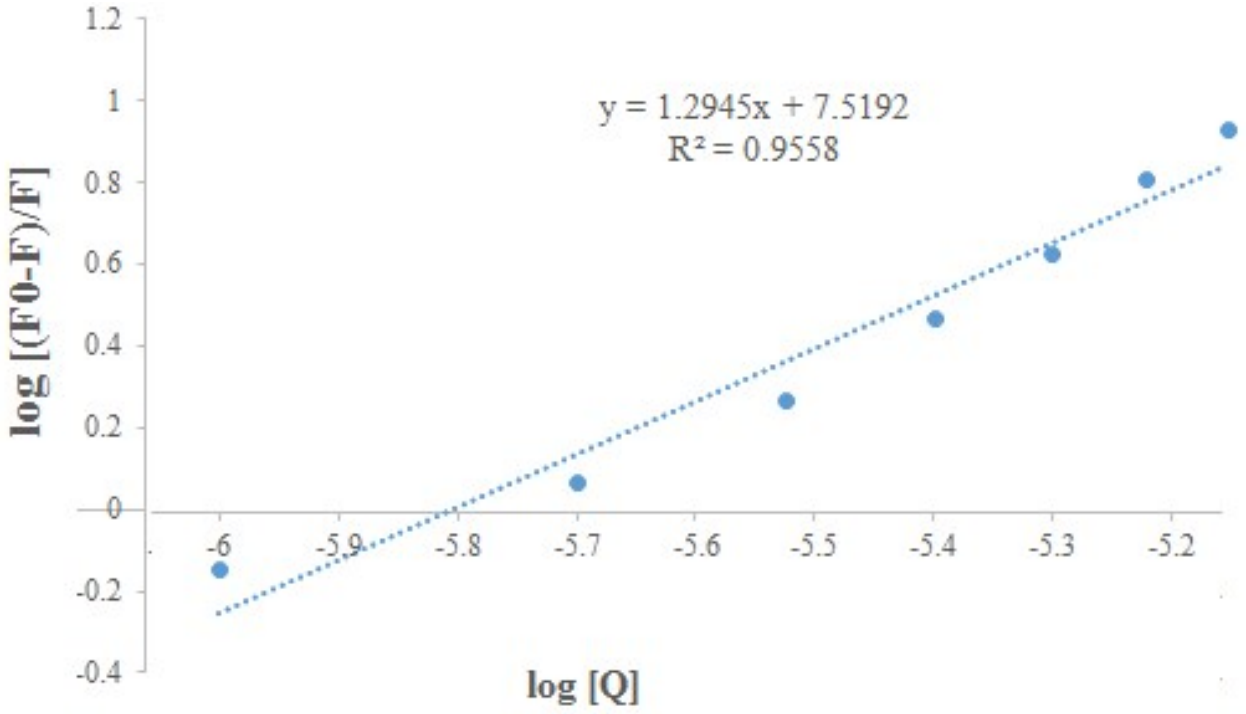

SI 7 t. Double-log plots for the fluorescence quenching of the HSA by **2**.

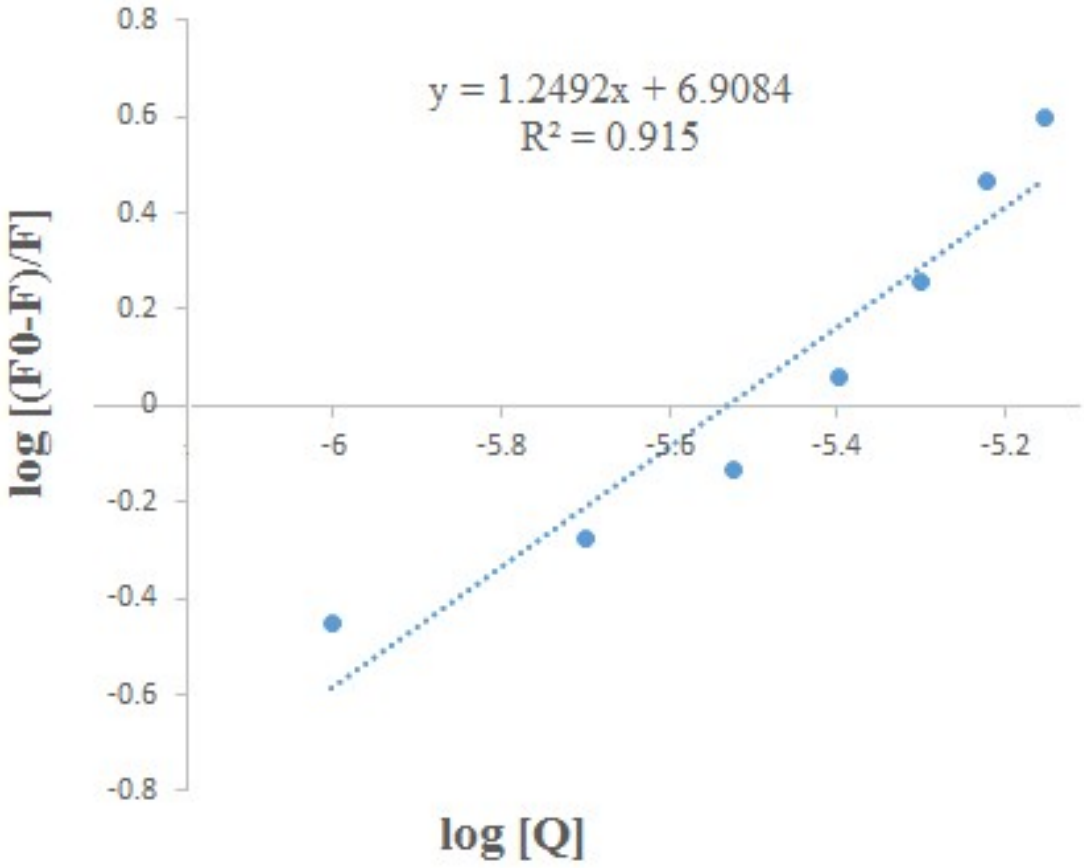

SI 7 u. Double-log plots for the fluorescence quenching of the HSA by **3**.

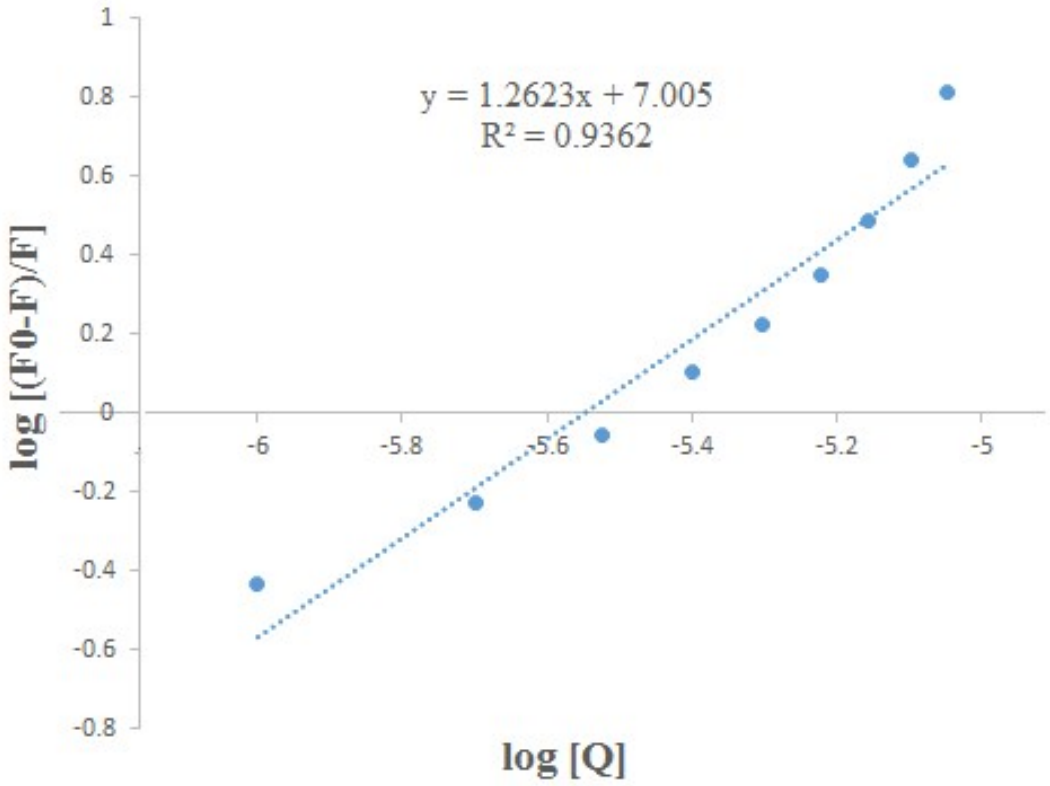

SI 7 v. Double-log plots for the fluorescence quenching of the HSA by **4**.

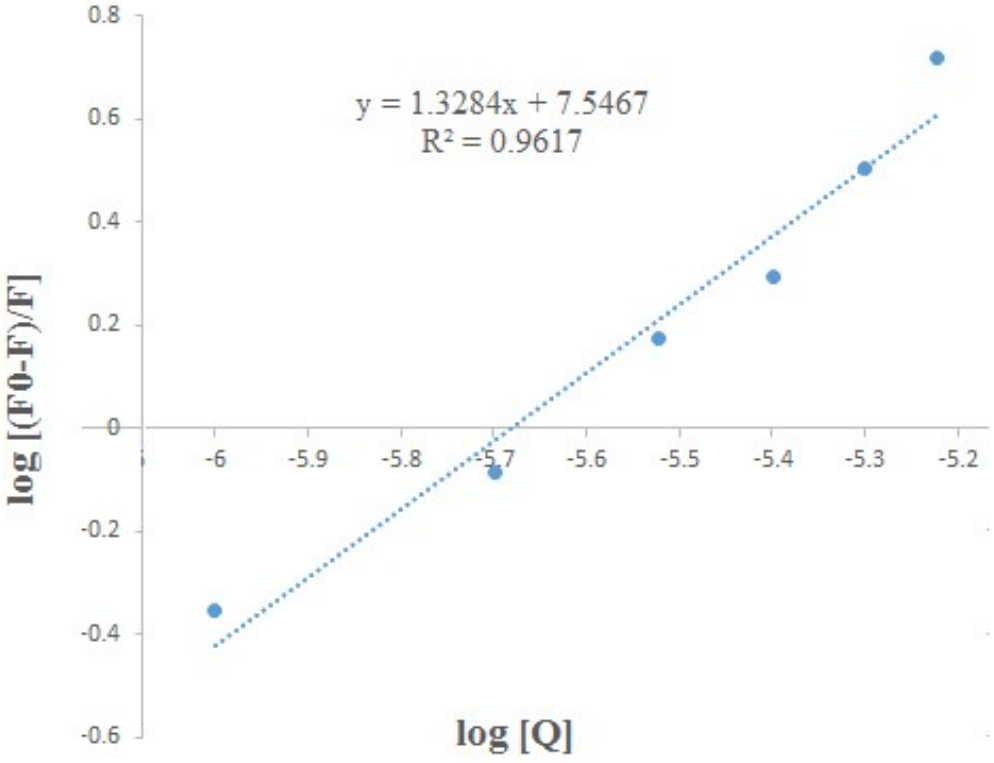

SI 7 w. Double-log plots for the fluorescence quenching of the HSA by **5**.

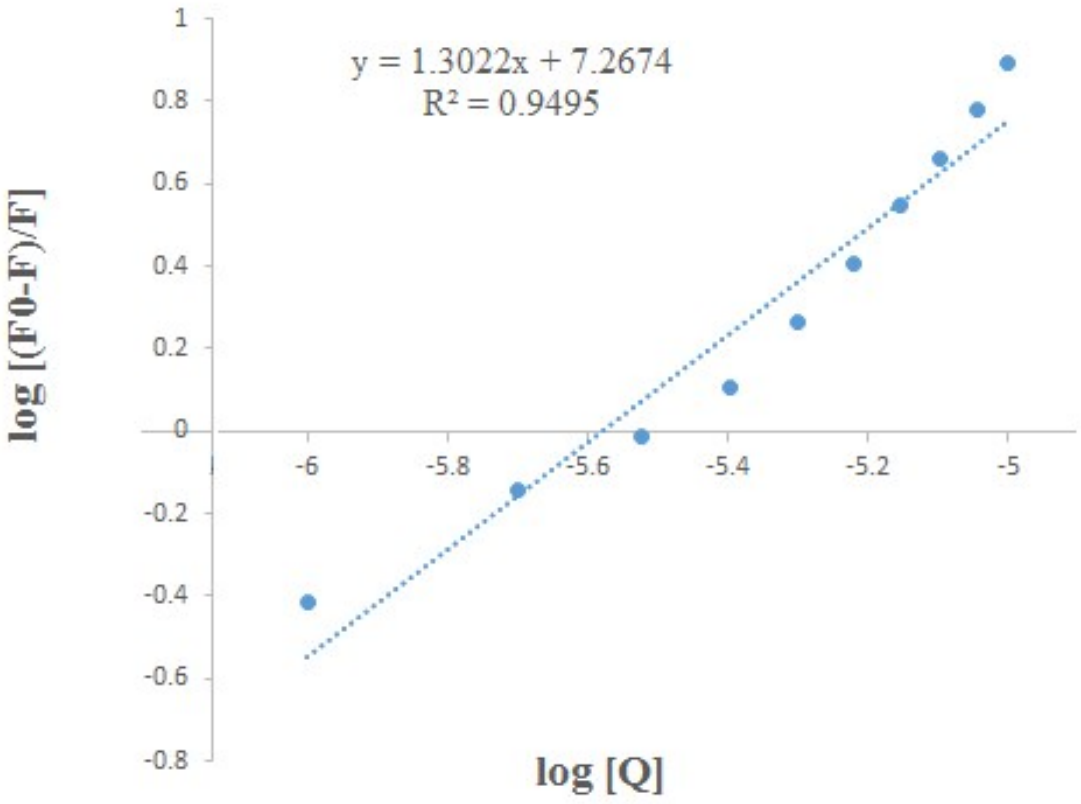

SI 7 x. Double-log plots for the fluorescence quenching of the HSA by **6**.

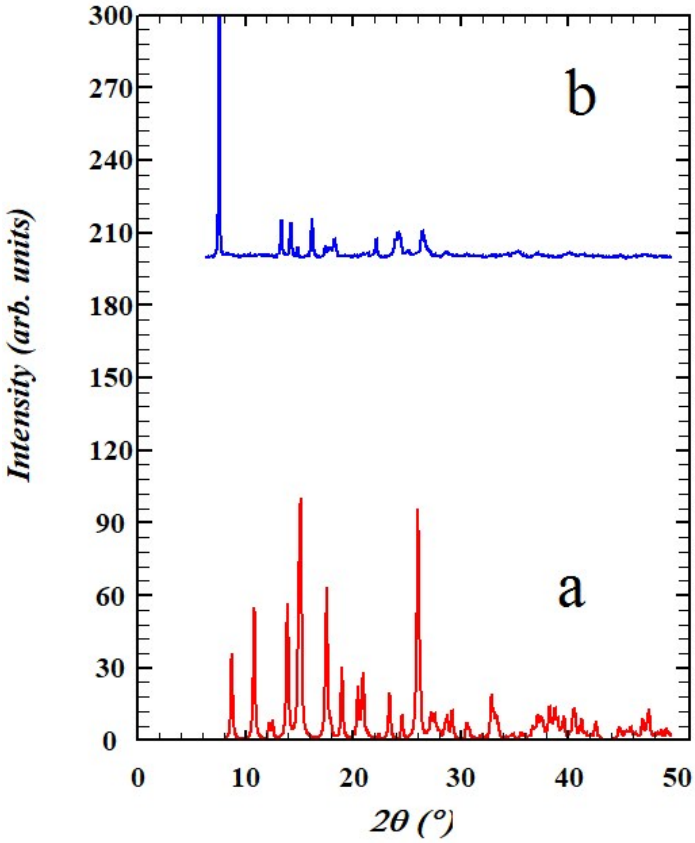

SI 8 a. The XRD patterns of *a*) computed from single-crystal X-ray data of **1** and *b*) Nanostructure of **1**.

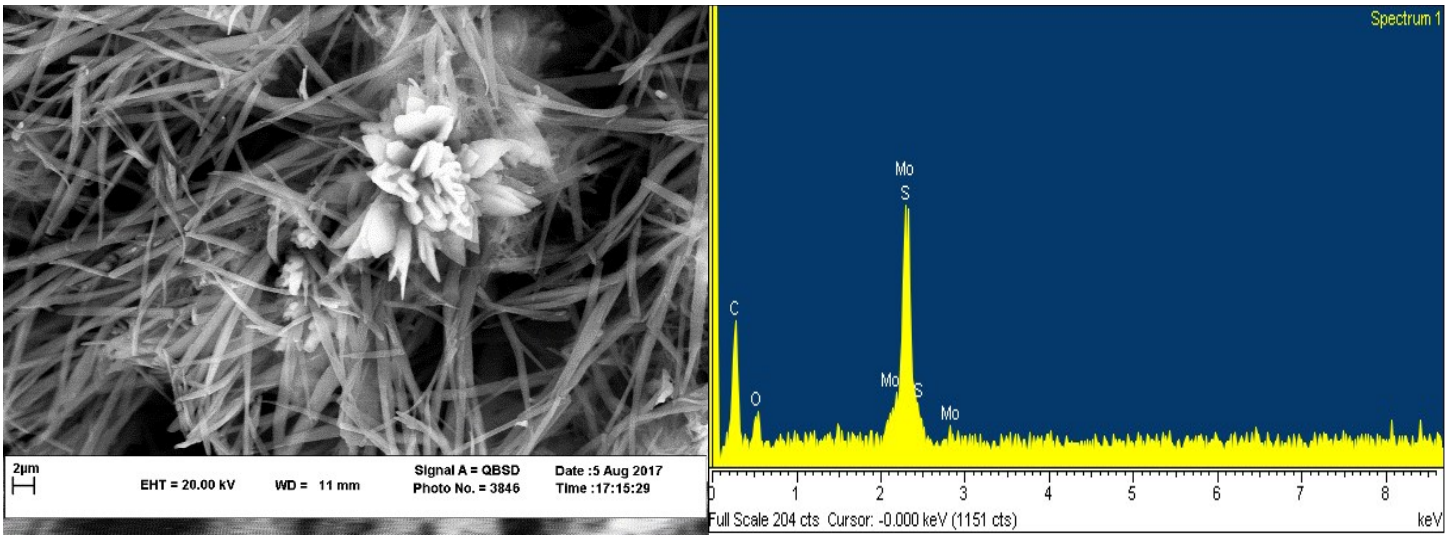

SI 8 b. **a)** SEM image of **1** complex, **b)** EDX spectrum analysis of **1** complex.

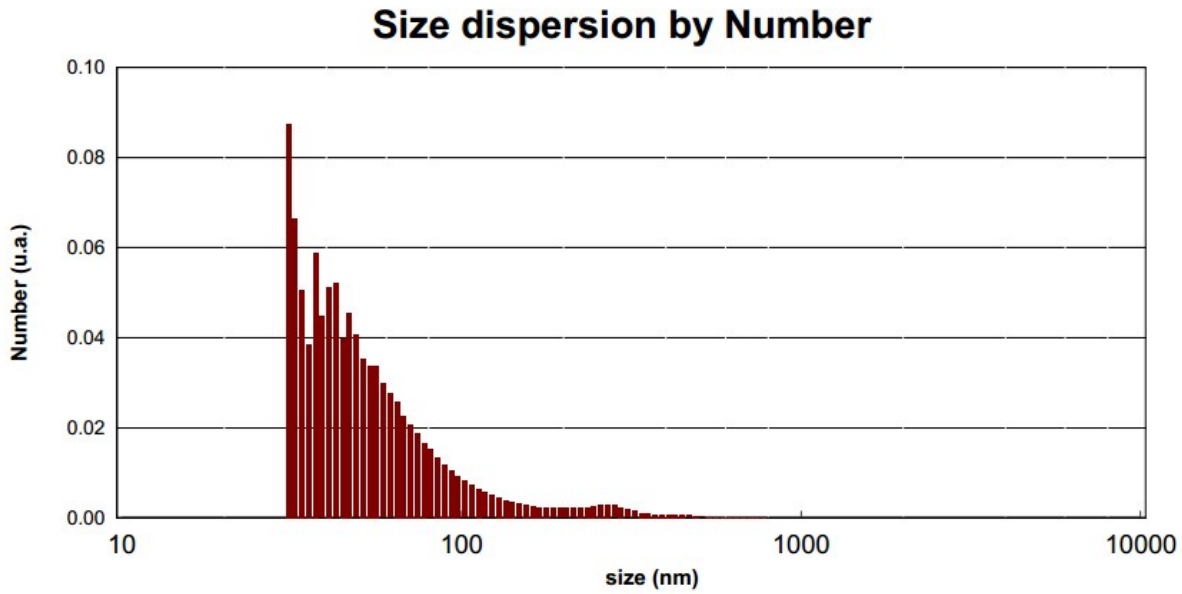

SI 8 c. The average nanoparticle size by PLS method of **1**.

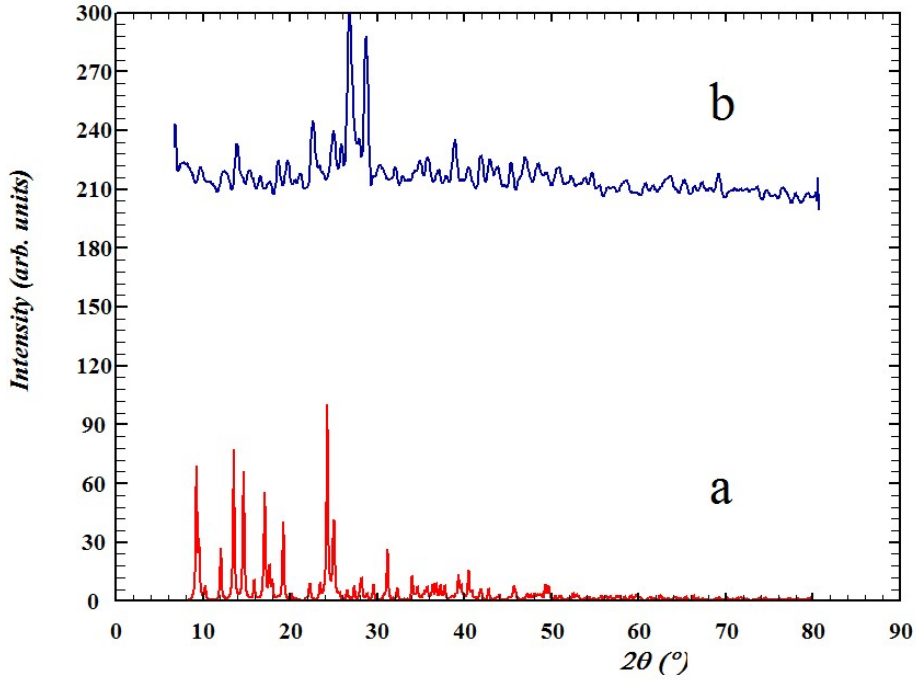

SI 8 d. The XRD patterns of *a*) computed from single-crystal X-ray data of **2** and *b*) Nanostructure of **2**.

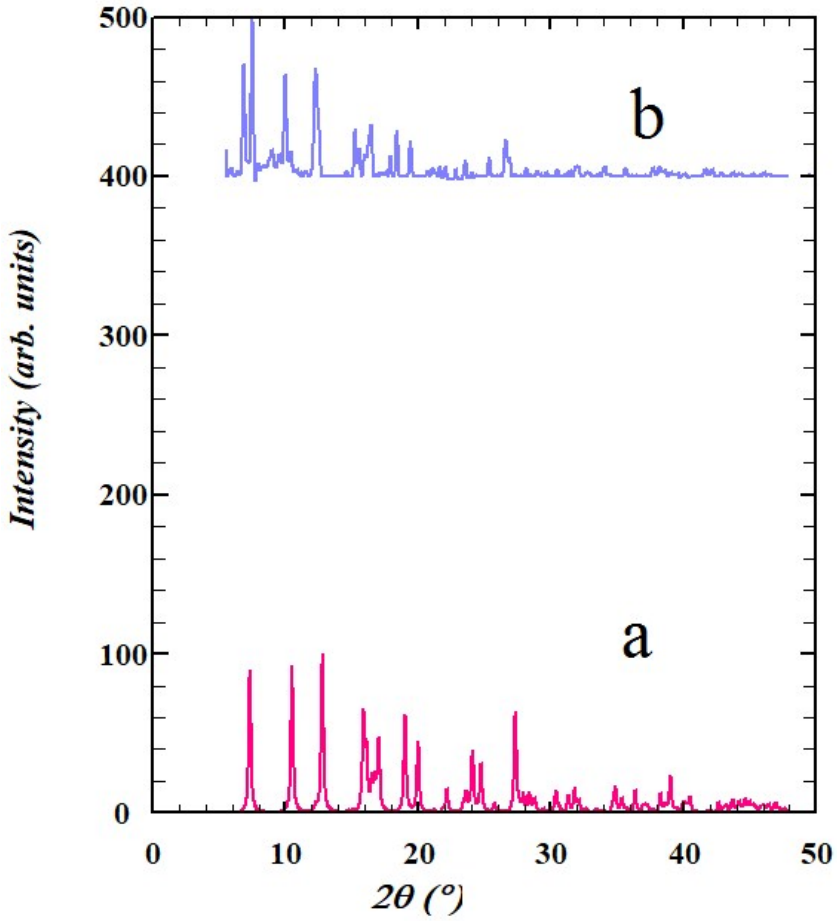

SI 8 e. The XRD patterns of *a*) computed from single-crystal X-ray data of **3** and *b*) Nanostructure of **3**.

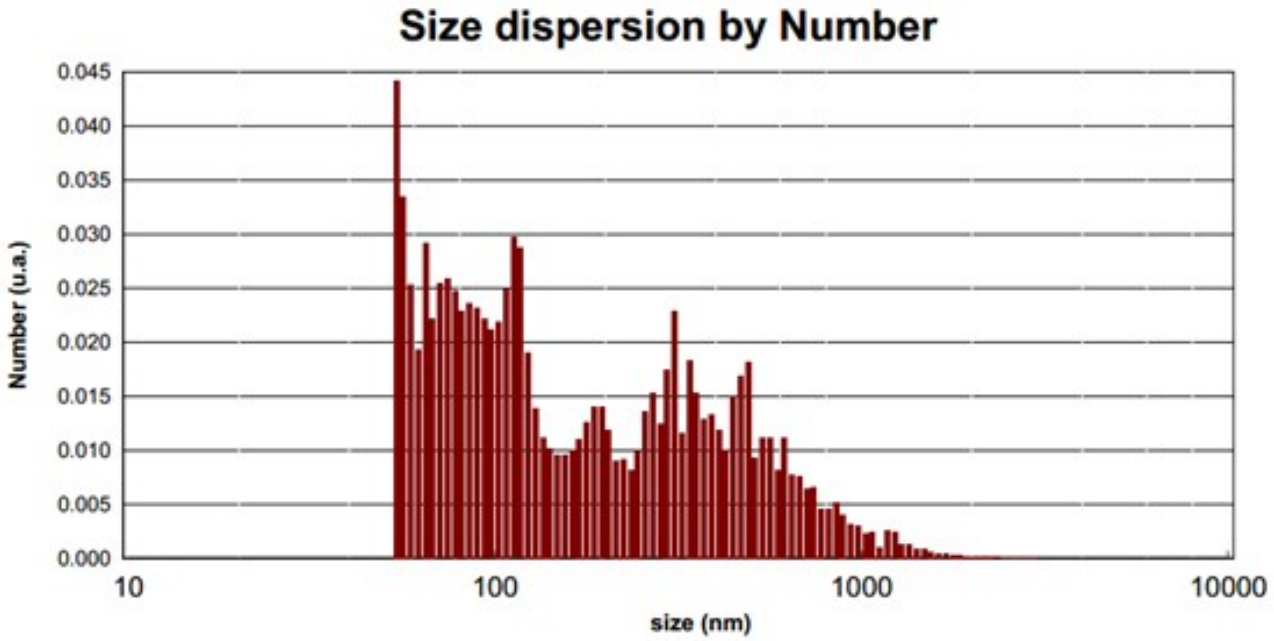

SI 8 g. The average nanoparticle size by PLS method of **3**.

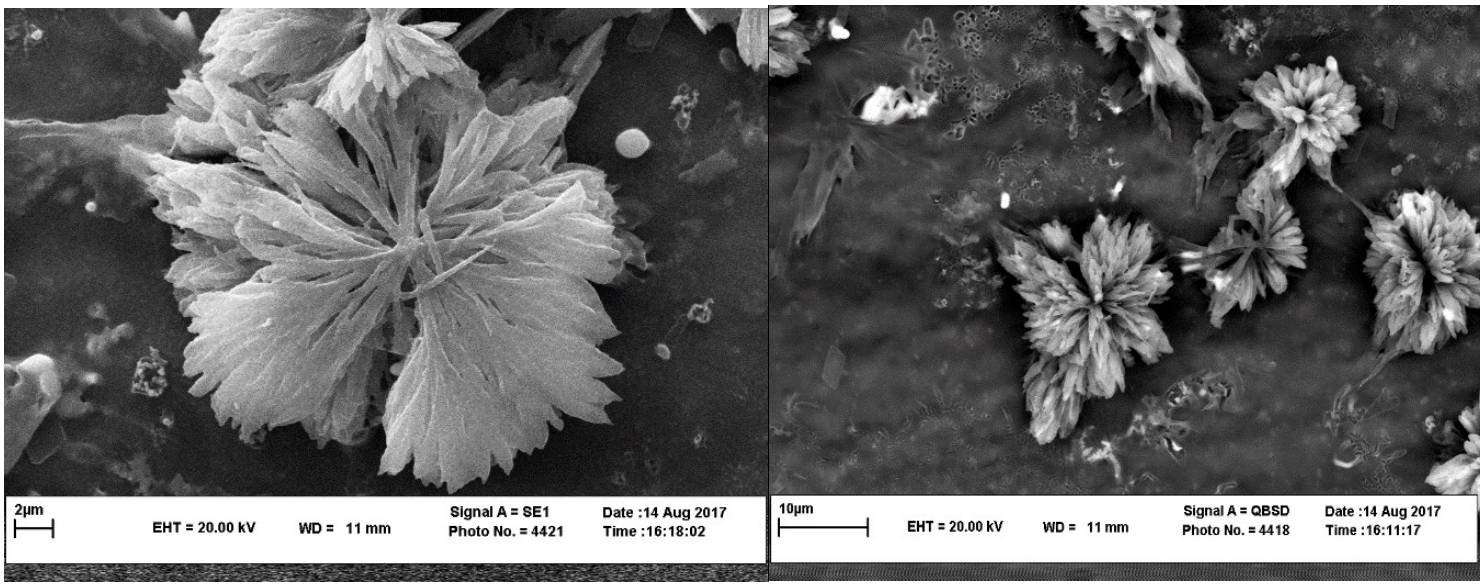

SI 8 h. SEM images of **4** complex.

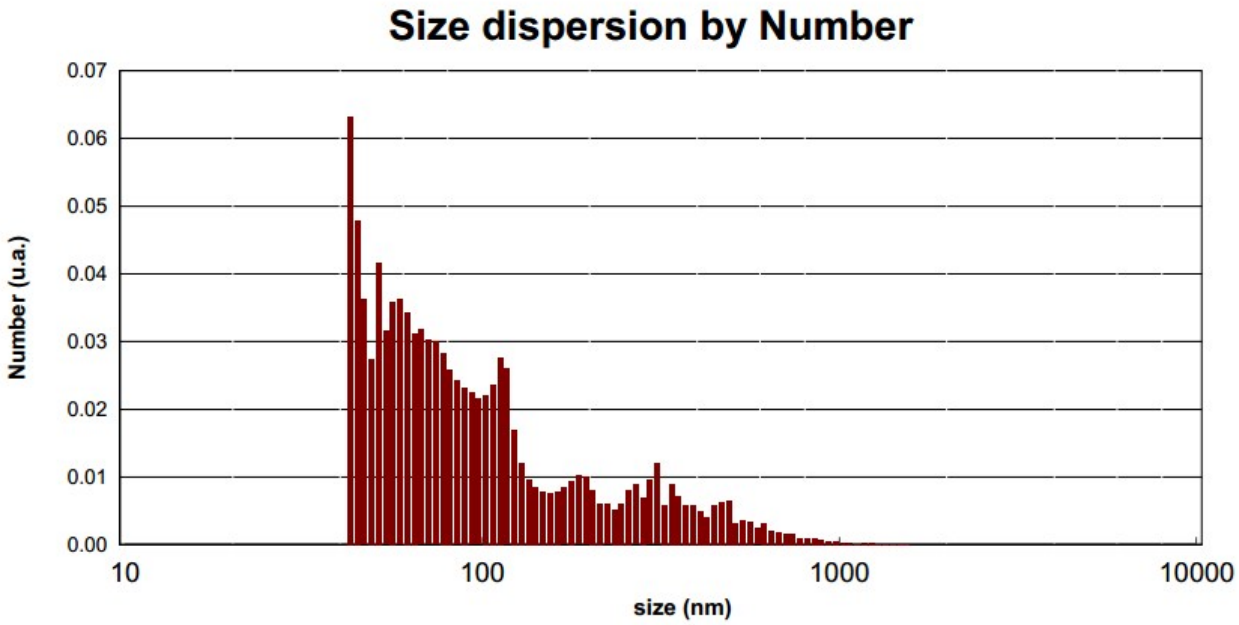

SI 8 i. The average nanoparticle size by PLS method of **4**.

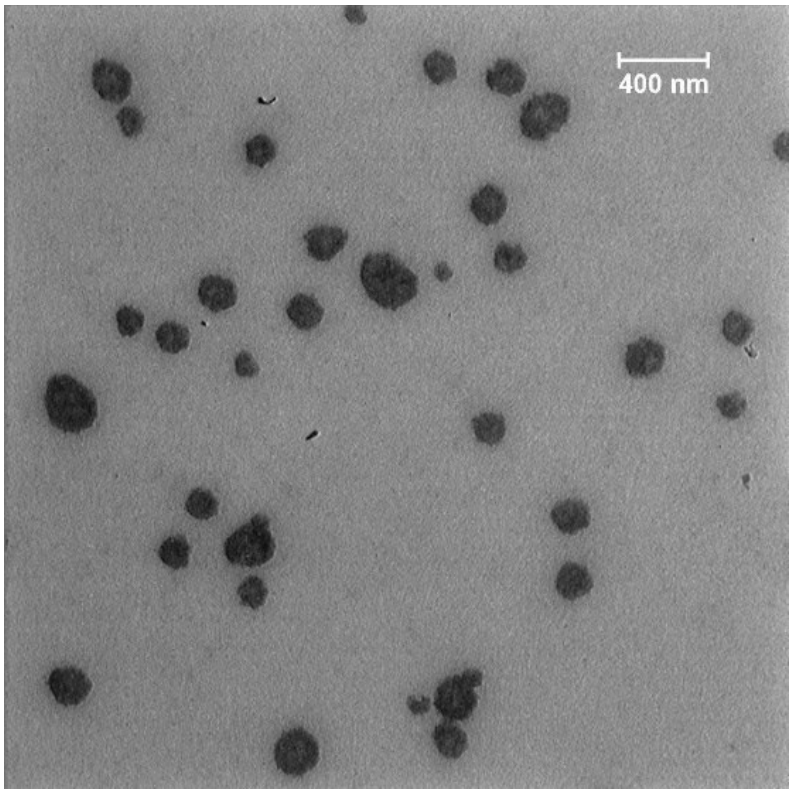

SI 8 j. TEM image of **5** complex.

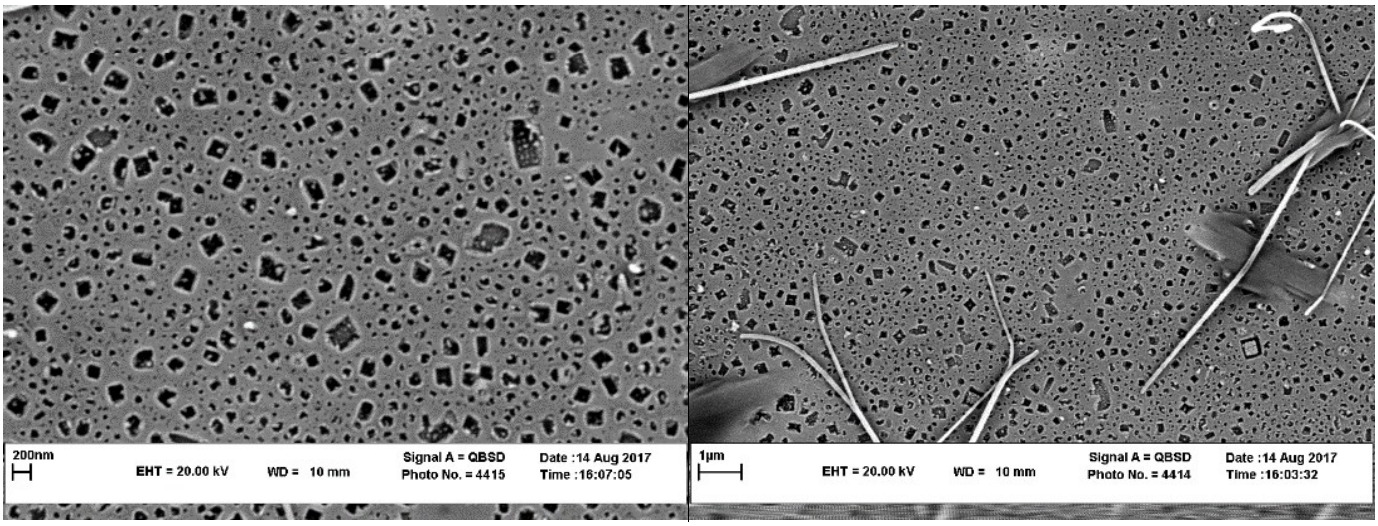

SI 8 k. SEM images of **5** complex.

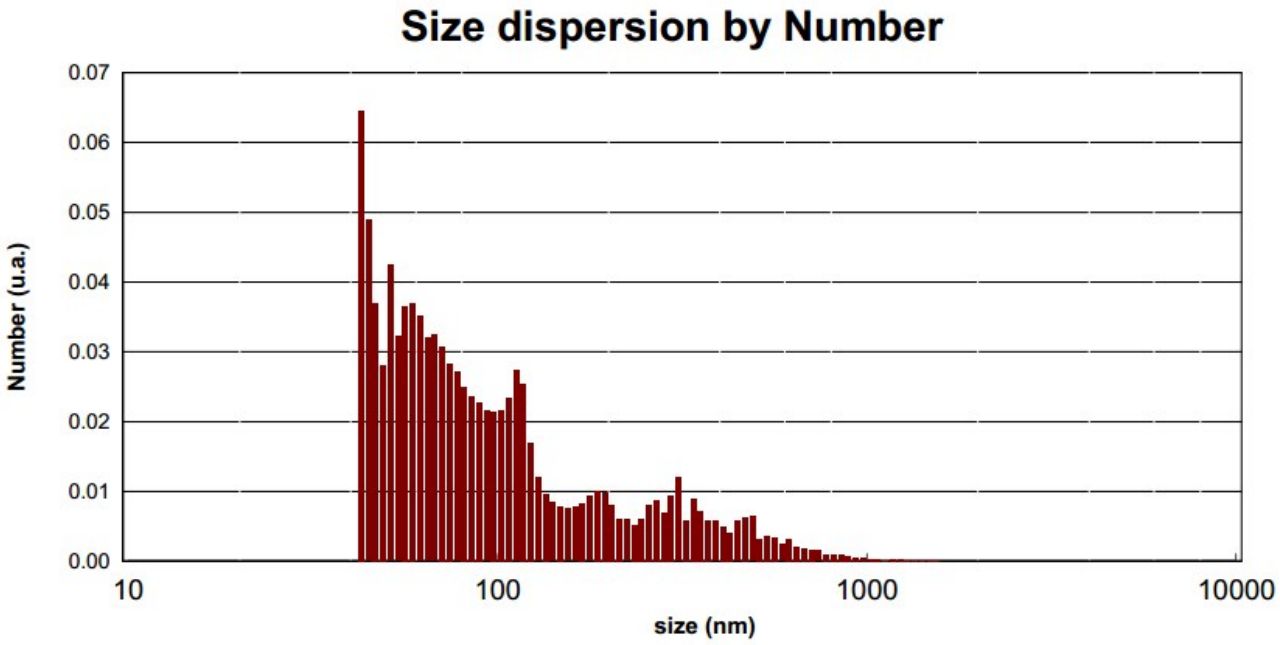

SI 8 l. The average nanoparticle size by PLS method of **5**.

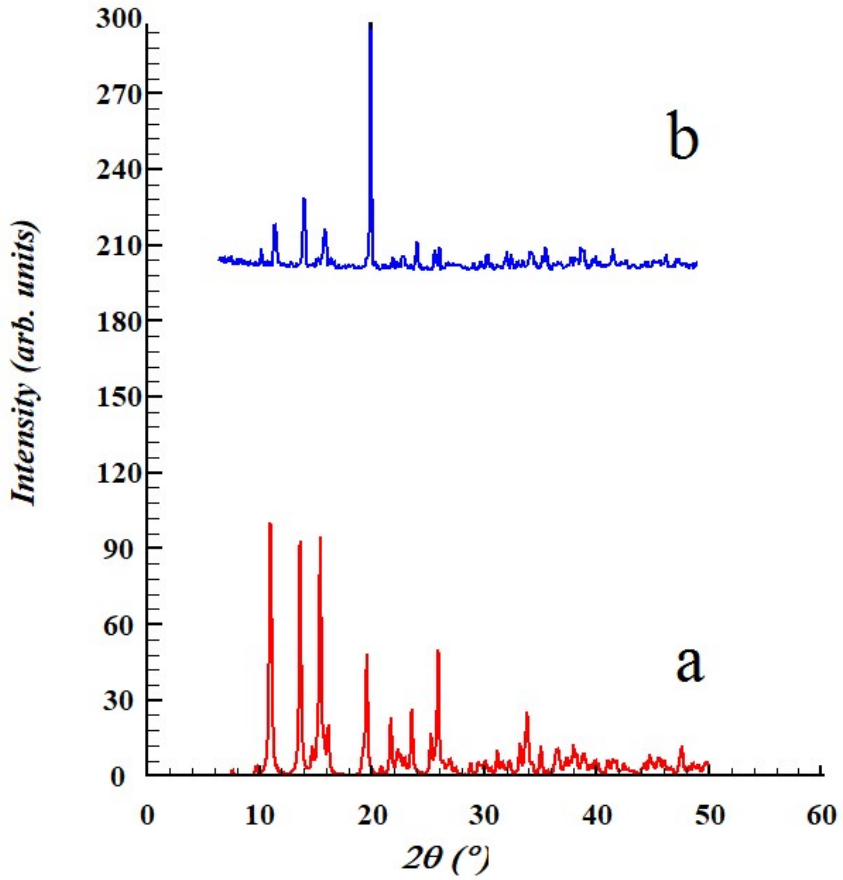

SI 8 m. The XRD patterns of *a*) computed from single-crystal X-ray data of **6** and *b*) Nanostructure of **6**.

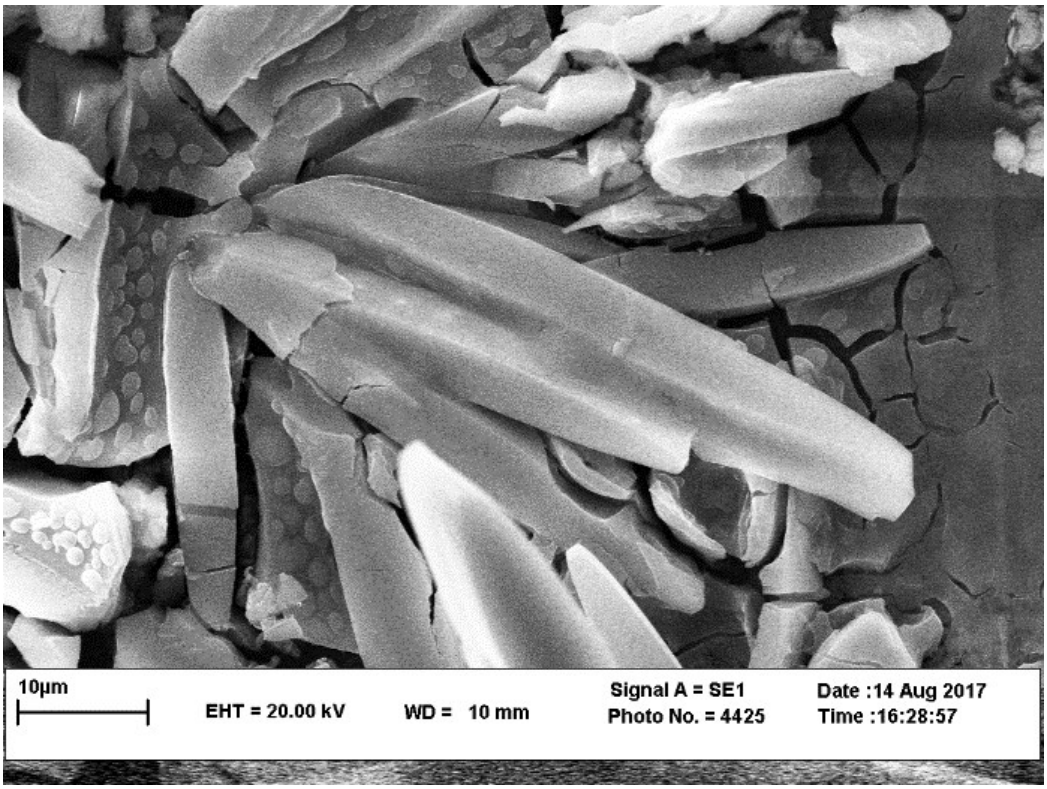

SI 8 n. SEM images of **6** complex.

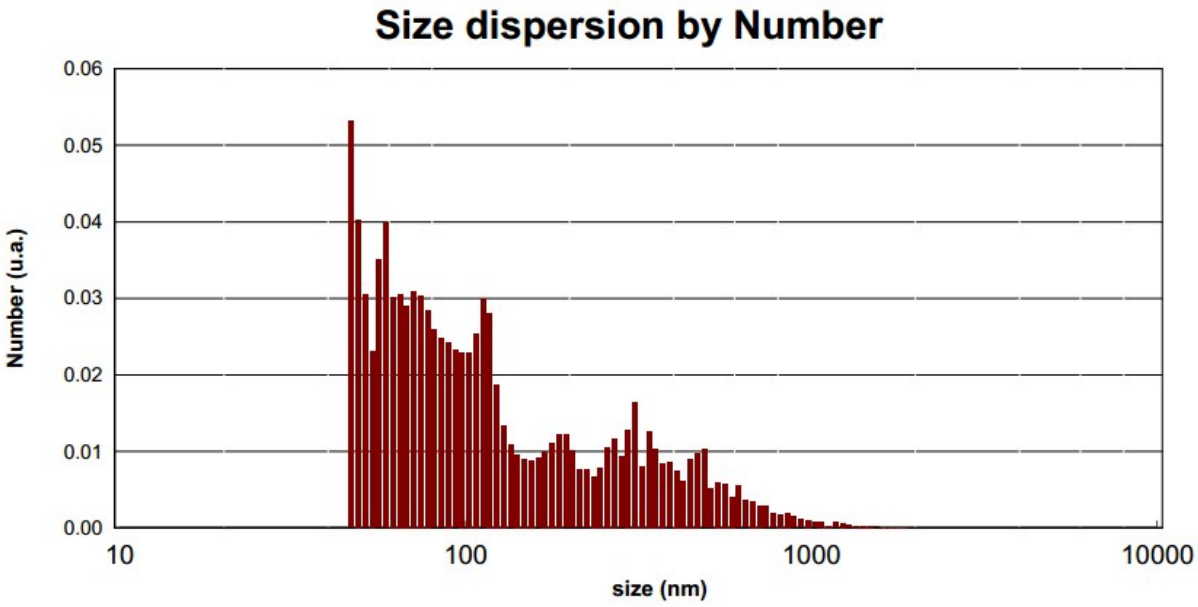

SI 8 o. The average nanoparticle size by PLS method of **6**.